For Reference

NOT TO BE TAKEN FROM THIS ROOM

Ex libris
universitatis
albertaensis

THE UNIVERSITY OF ALBERTA

KINETICS OF THE FORMATION OF HORSERADISH PEROXIDASE COMPOUND I AND ITS REACTION WITH *p*-CRESOL

by

© WILLIAM DONALD HEWSON

A THESIS

SUBMITTED TO THE FACULTY OF GRADUATE STUDIES AND RESEARCH

IN PARTIAL FULFILMENT OF THE REQUIREMENTS FOR THE DEGREE

OF DOCTOR OF PHILOSOPHY

DEPARTMENT OF CHEMISTRY

EDMONTON, ALBERTA

SPRING, 1977

ABSTRACT

An introductory chapter provides an explanation of the reasons for which this work was undertaken, and it provides a background discussion of the important physical and chemical properties of many other peroxidases as well as horseradish peroxidase. Laccase is also mentioned because of its phenol oxidase activity.

Rate constants for the reaction between horseradish peroxidase Compound I and *p*-cresol have been determined at several values of pH between 2.98 and 10.81. These rate constants were used to construct a log (rate) *vs.* pH profile. Base catalysis is evident. At the maximum rate, pH 8.74, the Arrhenius activation energy was determined to be 5.0±0.5 kcal/mole.

Over a wide range of pH horseradish peroxidase Compound I can be reduced quantitatively via Compound II to the native enzyme by only one molar equivalent of *p*-cresol. Since this requires two molar equivalents of electrons, *p*-cresol behaves as a two electron reductant. A possible explanation for *p*-cresol behaving as a two electron reductant involves the dimerization of two initially formed *p*-methylphenoxy radicals (from the reaction of Compound I with *p*-cresol) to form 2,2'-dihydroxy-5,5'-dimethylbiphenyl, and this dimer is then able to reduce Compound II to native horseradish peroxidase. The major steady state oxidation product of *p*-cresol is Pummer-

er's ketone. It is shown that Pummerer's ketone cannot be the main oxidation product of *p*-cresol when Compound I and *p*-cresol are present in a 1:1 molar ratio.

The rate of formation of Compound I from the reaction of native horseradish peroxidase with hydrogen peroxide was studied from 3.7 to 70.0°. The second-order rate constants were used to construct an Arrhenius plot from which the activation energy of this reaction was calculated to be 3.5±1.0 kcal/mole. The possibility is presented that the rate of this reaction is diffusion controlled.

Pseudo first-order kinetics was used to show that Compound I formation is second order from pH 3.19 to 9.76. This rate is pH independent from pH 5.96 to 9.76, and at pH 7.04 it is independent of ionic strength from I = 0.01 to 0.11. Near pH 7 and at 40° the rate is viscosity independent as tested in aqueous glycerol solutions, thus demonstrating that the rate is not diffusion controlled. The presence of ethanol decreases both the rate of Compound I formation and cyanide binding to the native enzyme. Since Compound I formation and cyanide binding involve ligation at the sixth coordination position of the heme moiety, the inhibition has been interpreted in terms of the binding of ethanol, probably to the sixth position of the heme iron.

Digitized by the Internet Archive
in 2023 with funding from
University of Alberta Library

https://archive.org/details/Hewson1977

ACKNOWLEDGEMENTS

Science is seldom a solo endeavor. Therefore, I would like to fully acknowledge those people who were especially helpful during the preparation of this thesis. Professor H.B. Dunford, my research director, provided benefical suggestions throughout all aspects of this work. Professor C.D. Hubbard, on sabbatical leave from the University of Hew Hampshire, furnished excellent tutelage in stopped-flow and several other laboratory techniques. Dr. Dominique Job, who had just completed his own thesis on peroxidase, was an extremely helpful discussant. Dr. Jennifer Stillman lent her assistance in many aspects of computing. The helpful suggestions of my graduate student colleagues and the competent technical staff in the Department of Chemistry deserve mention. Specific acknowledgements are made at the end of the appropriate chapters.

TABLE OF CONTENTS

CHAPTER		PAGE
I.	INTRODUCTION	1
1.1	General Background	1
1.2	Historical Background of Peroxidase	5
1.3	Physical and Chemical Properties of Some Native Peroxidases	6
	Horseradish Peroxidase	6
	Cytochrome c Peroxidase	15
	Turnip Peroxidase	18
	Japanese Radish Peroxidase	19
	Chloroperoxidase	21
	Lactoperoxidase	22
	Thyroid Peroxidase	25
	Myeloperoxidase	26
1.4	Oxidation-Reduction States of Peroxidase	28
	Ferroperoxidase and its Ligand Complexes	30
	Compound III or Oxyperoxidase	33
	Ligand Complexes of Ferriperoxidase	36
	Compound I and Compound II	41
1.5	Laccase	53
1.6	References	64
II.	THE OXIDATION OF *p*-CRESOL BY HORSERADISH PEROXIDASE COMPOUND I	91

2.1 Summary 91
2.2 Introduction 91
2.3 Experimental 93
Materials 93
Apparatus 95
Methods 96
2.4 Results 100
2.5 Discussion 112
2.6 References 125
2.7 Appendix 128
III. STOICHIOMETRY OF THE REACTION BETWEEN HORSERADISH PEROXIDASE AND *p*-CRESOL .. 129
3.1 Summary 129
3.2 Introduction 130
3.3 Experimental 131
3.4 Results and Discussion 136
Transient State Results for HRP-I and *p*-Cresol in a 1:1 Ratio 136
Transient State Results for HRP-I and *p*-Cresol in a 2:1 Ratio 141
Steady State Results 143
Equilibrium and Kinetic Studies on Pummerer's Ketone 147
Comparison of Transient State and Steady State Results 161
Acknowledgements 169
3.5 References 169

IV. ARRHENIUS ACTIVATION ENERGY FOR THE FORMATION OF HORSERADISH PEROXIDASE COMPOUND I 173
4.1 Summary 173
4.2 Introduction 173
4.3 Experimental 174
Materials 174
Apparatus 175
Methods 175
4.4 Results and Discussion 178
4.5 References 185
V. EFFECT OF GLYCEROL AND ETHANOL ON THE REACTIVITY OF HORSERADISH PEROXIDASE WITH HYDROGEN PEROXIDE AND CYANIDE ... 189
5.1 Summary 189
5.2 Introduction 190
5.3 Experimental 191
Materials 191
Methods 192
5.4 Results 195
Compound I Formation in H_2O 195
Compound I Formation in Glycerol ... 198
Compound I Formation in Ethanol 201
Cyanide Binding to HRP in Ethanol .. 203
Spectrophotometric Detection of the HRP-EtOH Complex 208

Spectrophotometric Detection of Interactions between HRP and Glycerol 211
Temperature Dependence of the CD Spectrum of HRP 211
CD Spectrum of Compound I 215
5.5 Discussion 215
5.6 References 221
VI. CONCLUSION 226
6.1 Concluding Remarks 226
6.2 References 229

LIST OF TABLES

TABLE		PAGE
2.1	The kinetic parameters for the nonlinear plots of k_{obs} *vs.* the concentration of *p*-cresol	107
2.2	Values of $k_{1,app}$ as a function of pH ..	108
2.3	The parameters for the $\log(k_{1,app})$ *vs.* pH profile	116
2.4	The second-order rate constants for the reaction of *p*-cresol with HRP-I at several temperatures at pH 8.74	122
3.1	Best fit values of the parameters obtained from a nonlinear least squares analysis of the data in curve A of Fig. 3.6	156
3.2	The calculated values of some equilibrium and rate constants from Fig. 3.7	160
4.1	Second-order rate constants for the formation of Compound I from native HRP at pH 7.10	180
5.1	Apparent second-order rate constants for the formation of Compound I as a function of pH at 25°	197

5.2 Apparent second-order rate constants for Compound I formation as a function of total ionic strength 199
5.3 Apparent second-order rate constants for the formation of Compound I as a function of the concentration of glycerol .. 200
5.4 Apparent second-order rate constants for the formation of Compond I as a function of the concentration of ethanol 202
5.5 Apparent second-order rate constants for the binding of cyanide as a function of the concentration of ethanol 205
5.6 Kinetic and equilibrium parameters for the reaction of HRP with hydrogen peroxide and cyanide in the presence of ethanol 207

LIST OF FIGURES

FIGURE		PAGE
1.1	The structure of ferriprotoporphyrin IX	2
1.2	Soret and visible absorption spectra of HRP	8
1.3	The oxidation-reduction and proton balance relationships among the various forms of HRP	29
1.4	Plots of the log of the second-order rate constant for the reaction of HRP Compound I with several substrates	51
1.5	Plots of the log of the second-order rate constant for the reaction of HRP Compound II with several substrates ...	52
1.6	Absorption spectra of laccase	56
2.1	A stopped-flow oscilloscope trace of the reaction of HRP-I with *p*-cresol	98
2.2	Examples of linear plots of k_{obs} *vs.* the concentration of *p*-cresol	101
2.3	Example of a nonlinear plot in citrate buffer at pH 3.70	102
2.4	Log ($k_{1,app}$) *vs.* pH profile for the reaction of HRP-I with *p*-cresol	103
2.5	Arrhenius plot for the reaction of HRP-I with *p*-cresol	104

2.6 Reaction scheme proposed to explain the log ($k_{1,app}$) *vs.* pH profile 114
3.1 Spectra obtained at different pH values by adding one half molar equivalent of *p*-cresol to HRP-I 144
3.2 The log (rate) *vs.* pH profiles for HRP-I and HRP-II with *p*-cresol as the substrate 145
3.3 Gas chromatogram of the volatile peroxidase steady state oxidation products of *p*-cresol 146
3.4 The reaction of Pummerer's ketone with HRP-I at pH 10.51 149
3.5 The unreactivity of Pummerer's ketone with HRP-I at pH 7.06 150
3.6 Spectrophotometric titration curves of Pummerer's ketone 152
3.7 A possible scheme for the ionization of Pummerer's ketone and enol formation .. 153
3.8 Logarithmic plot for the reaction of HRP-I with Pummerer's ketone 158
4.1 Arrhenius plot of ln k *vs.* T^{-1} 179
5.1 Linear plots of k_{obs} *vs.* $[H_2O_2]$ for Compound I formation at 25° and several pH values 196
5.2 Linear plot of the reciprocal of $k_{1,app}$ *vs.* the concentration of ethanol 204

5.3 Linear plot of the reciprocal of $k_{2,app}$ *vs.* the concentration of ethanol 206

5.4 The difference absorption spectra of HRP in ethanol relative to HRP in water ... 209

5.5 Double reciprocal plot of the absorbance change *vs.* the concentration of ethanol 210

5.6 Circular dichroic spectra of HRP and its ethanol complex 212

5.7 The difference absorption spectrum of HRP in glycerol relative to HRP in water 213

5.8 Circular dichroic spectra of HRP at several temperatures 214

5.9 Circular dichroic spectra of HRP and Compound I 216

CHAPTER I. INTRODUCTION

1.1 General Background

The combination of a metalloporphyrin with a protein (as found in the hemoprotein horseradish peroxidase) is extremely fundamental to the life processes of both plants and animals. Hemoproteins and chlorophylls (heme is an iron-containing porphyrin and chlorophyll is a magnesium-containing porphyrin) are found in most forms of life, from unicellular microorganisms to the higher animals (1). The only exceptions appear to be some of the anaerobic bacteria and lactobacilli which obtain energy by the fermentation of organic substrates (1).

The best known hemoproteins are probably hemoglobin which transports molecular oxygen to respiratory cells and myoglobin which provides a storage site for the oxygen. Horseradish peroxidase has the same heme prosthetic group (Fig. 1.1) as hemoglobin and myoglobin, except that in the latter hemoproteins the iron is normally in the ferrous oxidation state whereas in horseradish peroxidase the iron is normally in the ferric oxidation state.

The basic process of cell respiration involves a series of hemoproteins known as cytochromes. During cell respiration, electrons are transferred from nicotinamide adenine dinucleotide, NADH, to O_2 through a series of cytochromes. Cytochromes are ubiquitous to most forms of life, including some anaerobes (1). The cytochromes accomplish electron trans-

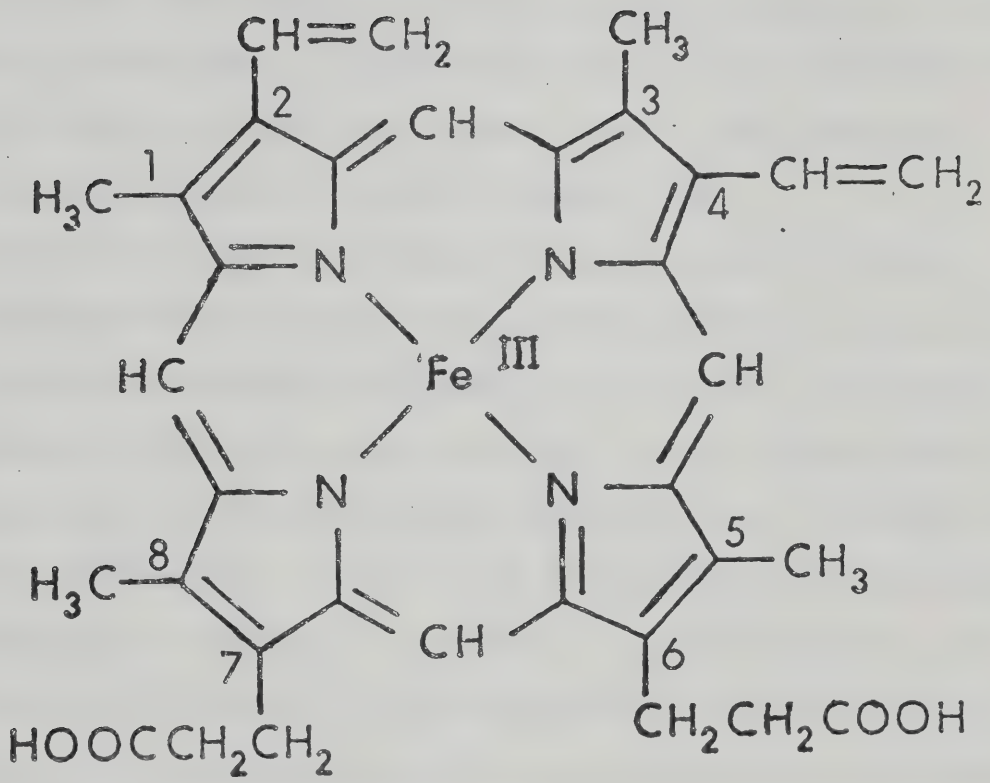

Fig. 1.1 The structure of ferriprotoporphyrin IX. The positions on the porphyrin are numbered 1 to 8.

port by varying the oxidation state of the heme iron (2). It is also via changes in the oxidation state of peroxidase that this enzyme is able to catalyze the oxidation of substrates by hydrogen peroxide.

Another hemoprotein, catalase, which is located in the cellular peroxisomes, appears to function as a catalyst to convert hydrogen peroxide to water and O_2 when hydrogen peroxide is formed by various oxidases (3).

Depending upon the nature of the protein to which ferriprotoporphyrin IX is bound, this prosthetic group can be involved in diverse biochemical functions. Therefore, the protein moiety has a large effect on the properties of heme and may directly determine the particular function of a certain hemoprotein. The central importance of hemoproteins in biological processes is difficult to overemphasize, and consequently, a study of the hemoprotein horseradish peroxidase can be related, in part, to a broad area of science dealing with life processes.

The enzymatic oxidation and subsequent coupling of phenolic compounds is a subject of great importance in biological chemistry. Horseradish peroxidase easily oxidizes a variety of phenolic compounds by hydrogen peroxide, and this may suggest a possible biological role for the enzyme. Biosynthetic pathways to a wide variety of natural products involve enzymatic oxidation and coupling of phenols as the key reactions (4). A considerable portion of the monomeric aromatic substances (i.e. flavonoids) and the aromatic poly-

mers (i.e. lignin, melanin) found in nature are derived from relatively simple phenolic precursors by oxidative processes (5). Further examples of natural products derived from relatively simple phenolic precursors are tannins, pigments, antibiotics, and alkaloids (5). Lignins and tannins are the most abundant and widely distributed phenolic polymers found in plants. Peroxidase and laccase have been frequently implicated in the biosynthesis of lignins and tannins because of the ability of these enzymes to oxidize phenolic compounds which yield lignin-like polymers as products (5,6). The mechanism through which damaged plants protect themselves from fungal and viral infection appears to involve enzymatic oxidation and polymerization of phenols (7). The polymeric products are believed to inhibit the enzymes of the invading microorganism.

The biosynthesis of natural products via phenolic oxidation is a complicated process, and in order to comprehend this process it is necessary to have a detailed knowledge of the mode of action of the enzymes which catalyze the reactions. Unfortunately, knowledge about enzymes that oxidize phenols is scarce. Since phenolic compounds are substrates for peroxidase, a detailed study of the reaction between peroxidase and phenolic compounds is an undertaking of biochemical significance.

These research efforts are presented in this thesis as follows: The introductory chapter describes the present state of knowledge of horseradish peroxidase and several

other peroxidases from both plant and animal sources. Since much of this thesis deals with the enzymatic phenolic oxidation of *p*-cresol by horseradish peroxidase and hydrogen peroxide, a report on laccase, which is also capable of enzymatic phenolic oxidation, concludes the introductory chapter. In Chapters II and III the results of the kinetic, equilibrium, and product analysis studies of the reaction between horseradish peroxidase and *p*-cresol are presented. A detailed knowledge of both reactants, Compound I and *p*-cresol, is necessary to achieve insights concerning their mode of reaction. More information about the nature of Compound I is presented in Chapters IV and V which present kinetic studies of Compound I formation from the reaction between native horseradish peroxidase and hydrogen peroxide.

1.2 Historical Background of Peroxidase

The occurrence of a substance found in plants and animals which catalyzed oxidations by hydrogen peroxide was reported in 1855 (8). A tincture of guaiacum was used as a peroxidase detecting agent. The name peroxidase was first introduced by Linossier who isolated the enzyme from pus (9). Bach and Chodat (10) noted the presence of peroxidase in several plants and found the horseradish root to be a good source of the enzyme because the peroxidase was abundant and relatively free of oxidases. Willstäter and Polinger (11) advanced the peroxidase purification techniques and introduced the oxidation of pyrogallol as an activity test. The

early history of peroxidase has been reviewed (12). Peroxidases are now known as enzymes which catalyze the oxidation of a variety of organic and inorganic compounds by hydrogen peroxide.

1.3 Physical and Chemical Properties of Some Native Peroxidases

Horseradish Peroxidase

Horseradish peroxidase, HRP, is a glycohemoprotein isolated from the root of the horseradish plant. Its physiological role has remained uncertain due to the large number of reactions it catalyzes (13). The enzyme contains one mole of ferriprotoporphyrin IX, or heme, as a prosthetic group, and the enzyme has a molecular weight of about 40,000 g/mole based on heme content and hydrodynamic measurements (14,15). Approximately 18% of this weight is due to the covalently bound carbohydrate moiety (16,17). The existence of a second component called paraperoxidase was reported by Theorell (18), who also first crystallized HRP in thin needles and reported their optical spectrum (19). Seven isozymes have been isolated and characterized by their chromatographic behavior, electrophoretic behavior, spectrophotometric properties, amino acid analysis, and carbohydrate composition (16). The two most abundant isozymes, designated B and C, were crystallized. Thin layer isoelectric focusing has revealed more than 20 distinct isozymes differing in

their isoelectric points (20). Paul and Stigbrand (13) isolated four isozymes, and their properties agree with the previous work (16).

There are two enzymatic intermediates in the usual peroxidase steady state cycle, known as Compound I and Compound II, where the Roman numerals indicated their order of appearance when starting with HRP and hydrogen peroxide.

[1] $HRP + H_2O_2 \longrightarrow$ Compound I

[2] Compound I + AH $\longrightarrow$ Compound II + A·

[3] Compound II + AH $\longrightarrow$ HRP + A·

Hydrogen peroxide, or alkyl hydroperoxides, convert HRP to Compound I which is two oxidation equivalents above HRP (21). An oxidizable substrate, AH, reduces Compound I to Compound II, which is one oxidation equivalent above HRP (22,23). More AH reduces Compound II to HRP so that another cycle can begin. Fig. 1.2 shows the optical spectra of HRP isozyme C and the two intermediate Compounds. The physical and chemical properties of the intermediates are discussed in section 1.4.

The electronic structure of the heme iron can be investigated by magnetic susceptibility because the paramagnetic susceptibility of hemoprotein is principally controlled by the state of the 3d electrons of the iron. Since the iron is in the ferric state in the native enzyme, there are five 3d electrons. Depending on the degree of spin pairing, the electronic structure may vary between 5 and 1 unpaired electrons

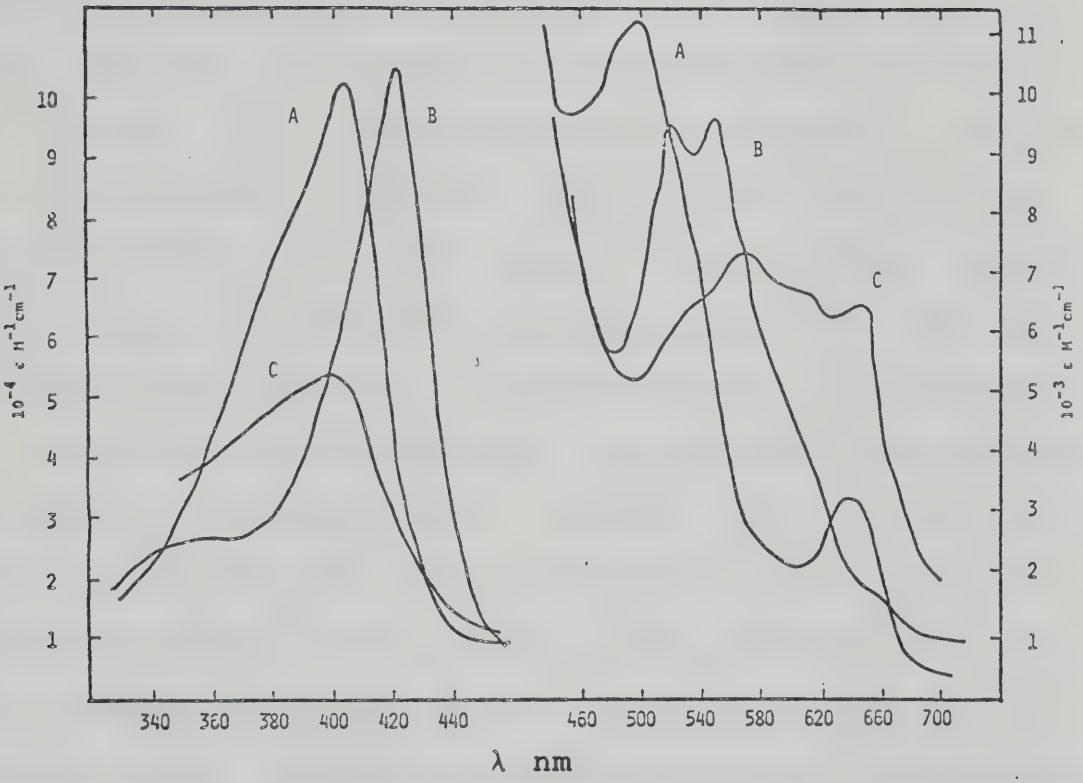

Fig. 1.2 Soret and visible absorption spectra of HRP (A), Compound I (B), and Compound II (C). Soret maximum molar absorptivities $\varepsilon^{403}_{HRP} = 1.02 \times 10^5$ $M^{-1}cm^{-1}$, $\varepsilon^{400}_{\text{Compound I}} = 5.31 \times 10^4$ $M^{-1}cm^{-1}$, and $\varepsilon^{420}_{\text{Compound II}} = 1.05 \times 10^5$ $M^{-1}cm^{-1}$ (261). Visible spectra are unpublished results of J.S. Stillman and H.B. Dunford.

which are termed the high and low spin states, respectively.

Theorell measured the paramagnetic susceptibility of HRP at 20° from pH 4 to 9 and found a spin only value corresponding to about 5 unpaired electrons (19,24). Since the fluoride complex of HRP has a larger paramagnetic susceptibility than HRP, the latter is considered to be only about 80% high spin (25). The paramagnetic susceptibility of HRP has been measured at pH 4 and 4.8 from liquid-nitrogen to room temperature (26). The square of the effective magnetic moment, μ^2_{eff}, is independent of temperature from -196° to -90° but upon going from -90° to room temperature μ^2_{eff} decreases.

Optical rotatory dispersion and circular dichroism have been used to investigate HRP. The ORD curve for HRP shows a Cotton effect with the inflection point occurring near the absorption maximum at 640 nm (27). From the reduced mean residue rotation at 233 nm, HRP was estimated to have 43% α-helical content, whereas the apoenzyme formed by acid-splitting of the heme and protein had only 33% α-helical content (28). The conformations of two HRP isozymes, A1 and C, and their apoenzymes were investigated using CD (29). In the visible region the two isozymes were identical in five of seven optically active bands suggesting that the heme sites are only slightly different in the two isozymes. The ultraviolet CD showed that both isozymes have appreciable α-helicity, and when the heme was removed both isozymes displayed significant decreases in α-helicity.

The electron paramagnetic resonance spectrum of HRP

from pH 7 to 8.4 at liquid-helium temperature showed a single paramagnetic species, high spin iron (30). The EPR signal was easily power-saturated at liquid-helium temperature, and near saturation the details of the spectrum near g=6 were lost. High spin heme systems usually have axial symmetry, however HRP has an EPR spectrum of lower than axial symmetry. This asymmetry was ascribed to a distortion of the π electrons of the heme. Asymmetry may be induced by the binding of another species to the π electrons or by nonplanarity of the heme. The EPR spectrum of HRP has been recorded at -65° in a fluid solution of dimethylformamide (31) and gave the same spectrum as at -196° (30) in frozen aqueous solution except that the signal amplitude at -65° was considerably weaker than that of the sample at -196°.

Determination of the amino acid sequence of HRP has been undertaken by Welinder *et al.* (32-34). A commercial preparation of HRP was shown to be highly homologous except by gel isoelectric focusing over the pH range 8 to 10 which resolved several very close bands. This heterogeniety was assumed to be due to differences in carbohydrate composition rather than amino acid composition or sequence. Amino acid analysis after performic acid oxidation yielded eight cysteic acid residues, all of which are involved in disulfide bridges as implied by the absence of S-carboxymethylcyteine after iodoacetic acid treatment. The sequences of many tryptic digest peptides were determined which account for 203 of the approximately 300 amino acid residues of HRP.

About 120 thermolytic peptides were isolated which account for all the tryptic sequences except a dipeptide, a tripeptide and a unique thermolytic sequence. The sequences around all four disulfide bridges, three histidine residues, and the single tryptophan residue were elucidated. Eight sites of carbohydrate attachment were identified. A pyrrolidone carboxyl N-terminal residue was tentatively suggested. A tryptic peptide containing two histidine residues appears to be related to the distal histidine sequence of the globin family. The similarities and differences of the trypsin digested HRP has been compared using peptide maps with four peroxidase isozymes from turnip (35).

The Mössbauer spectrum of HRP isozyme C has been measured at -196° (36). Mössbauer spectroscopy is sensitive to the electronic configuration immediately surrounding the nucleus of the heme iron atom. The Mössbauer spectrum of HRP shares the following distinctive features with many high spin ferrihemoproteins: similar quadrupole splitting, 1.96 mm/s; similar isomer shift, +0.25 mm/s; and a similar temperature dependent line broadening (37).

Four of the six coordination positions of the ferric iron in heme are occupied by the four pyrrole nitrogen atoms of the porphyrin. In an early paper by Theorell (38) it was concluded from protein acid-base titration data that the fifth position was occupied by a carboxylate anion of an amino acid side chain. Based on diagnostic rules derived from the relationships among the properties of heme groups with known

groups in the fifth and sixth positions, Brill and Williams (39) proposed amino and carboxylate or amino and water ligands at the fifth and sixth positions respectively. However, recent experiments indicate that the fifth position is occupied by the imidazole group of histidine. This was indicated by difference absorption spectroscopy below 250 nm (40, 41). The cyanide complex of HRP exhibits an absorption band at 235 nm which is characteristic of a heme-histidine bond (40). Difference absorption spectra of Compounds I and II relative to HRP have been explained in part as due to a transition involving histidine in the fifth position (41). Photooxidation of the apoenzyme of HRP isozyme C showed the loss of one histidine residue (42). When the modified apoenzyme was recombined with ferriprotoporphyrin IX, the resulting holoenzyme was much less reactive than the native holoenzyme. The results suggested that the selectively photooxidized histidine is located in the heme binding site of peroxidase. The EPR spectrum of the nitric oxide complex of reduced HRP (ferroperoxidase) can be used to deduce the nature of the ligand in the fifth position (43). A triplet hyperfine splitting was ascribed to the superhyperfine interaction with another axially bound ^{14}N nucleus. Thus, the fifth ligand was identified as unprotonated nitrogen, and since the coupling constants are near those reported for hemoglobin, the imidazole group of histidine was proposed. Nuclear magnetic resonance has provided additional support for histidine as the proximal ligand (44). If the coordinated

nitrogen atom was derived form lysine or arginine the resonances of their side chain aliphatic protons would be anticipated at very high field in the NMR spectrum of the cyanide complex as has been observed for the resonances of the methionine ligand in cytochrome c (45). No such high field resonances were observed for the cyanide complex of HRP (44).

The question of whether the sixth coordination position of the iron in HRP is occupied by a water molecule as a ligand is not yet conclusively resolved. High spin ferric iron at neutral pH suggests that the sixth position is empty or is occupied by a ligand such as water. By analogy with ferrimyoglobin and ferrihemoglobin, it has often been assumed that water occupies the sixth position (14, 46-50). Attempts have been made using NMR spectroscopy to determine the presence of a coordinated water molecule. Lanir and Schejter (51) studied the nuclear magnetic longitudinal relaxation of water protons in solutions of HRP over a wide range of pH. The molar relaxivity was constant from pH 3 to 12, and it was concluded that a water molecule does not occupy the sixth position. If there were a coordinated water molecule a decrease in relaxivity should have been observed upon forming alkaline HRP above about pH 11 (49). The structure in the immediate vicinity of the heme was studied by Vuk-Pavlović and Benko (52) using NMR in conjunction with a marker technique in which only the relaxation of the aliphatic protons of certain low molecular weight alcohols is measured in an

otherwise deuterated solution. They concluded that the ethanediol marker molecule was too large to enter into the heme pocket, and it was not possible to draw conclusions concerning the presence of coordinated water. However, two recent papers, based on NMR claim that the sixth ligand is a water molecule (44,53).

It is possible to separate HRP into ferriprotoporphyrin IX and apoenzyme, and these constituents can be recombined without loss of activity (54). The apoenzyme of HRP has been combined with proto-, meso-, deutero-, protoheme monomethyl ester, and protoheme dimethyl ester (55). Excepting the protoheme dimethyl ester, all these so-called synthetic peroxidases were able to form Compounds I, II, and III; and all reacted with fluoride, cyanide, and carbon monoxide. The peroxidases which contained meso- or deuteroheme had an activity similar to the native enzyme. The protoheme monomethyl ester derivative showed only 20% of the activity of native HRP. The porphyrin substituents at positions 2 and 4 were not essential for catalytic activity, but the free carboxyl groups at positions 6 and 7 were essential.

Only recently has resonance Raman spectroscopy been applied to hemoproteins (56). Raman spectra were first reported for hemoglobin (57) and cytochrome c (58). The main Raman bands are attributable to porphyrin vibrations, and several frequencies are sensitive to changes in the spin and oxidation state of the iron. Anomalous Raman frequencies for HRP at pH 7 suggest doming of the porphyrin ring, which is

characteristic of high spin ferriheme (59). This doming appears to be less pronounced in HRP than it is in aquo-ferrihemoglobin. Heme nonplanarity in HRP was also suggested as a cause for the axial asymmetry in the EPR spectrum of the native enzyme (30).

Cytochrome c Peroxidase

Cytochrome c peroxidase, CcP, is a hemoprotein isolated from baker's yeast and was first discovered in 1940 (60). In contrast to most other heme-containing peroxidases, CcP is not a glycoprotein (61). The enzyme has a molecular weight of 34,100 g/mole based on hydrodynamic measurements (62). CcP contains one mole of ferriprotoporphyrin IX (60). The EPR spectrum of the nitric oxide complex of ferrocytochrome c peroxidase indicates that the fifth position of the heme iron is occupied by the imidazole group of histidine as in HRP (43). CcP can be obtained in a highly purified state (63) free of isozymes and can be crystallized by dialysis against distilled water (61,64). The apoenzyme has an isoelectric point of 5.0 and consists of 272 amino acid residues (65,66). Much of the work on CcP up to 1970 has been reviewed by Yonetani (67).

One mole of CcP catalyzes the oxidation of two moles of ferrocytochrome c to ferricytochrome c by one mole of hydrogen peroxide. CcP also catalyzes the oxidation of a number of other reducing agents (63,68). The specificity of CcP is high toward ferrocytochrome c compared to ascorbate, pyrogallol, guaiacol, and ferrocyanide. Ferricytochrome c

was shown to act as an inhibitor of the peroxidation of ferrocytochrome c by CcP and hydrogen peroxide (69). From a kinetic study (69), it was postulated that CcP and ferricytochrome c form a complex. A complex between CcP and ferricytochrome c was detected by analytical centrifugation and by column chromatography (70). A complex of ferrocytochrome c and CcP was also detected in the absence of hydrogen peroxide (70). Cytochrome c from many different sources forms complexes with CcP (71). NMR has been used to investigate the complexation between ferricytochrome c and CcP (72). The hyperfine shifted resonances of ferricytochrome c broaden upon the addition of CcP in a manner which indicates a 1:1 stoichiometry of complexation, and complex formation was reversible (72). The redox potential of horse heart cytochrome c is unchanged in the presence of CcP, but the EPR spectrum of spin-labeled cytochrome c did change upon the binding of CcP (73).

As is observed for HRP, there are two intermediates in the steady state cycle of CcP, Compounds I and II. These Compounds of CcP are also analogous to HRP with regard to their oxidation states (23,74,75).

The paramagnetic susceptibility (76) and the optical spectrum (77) of CcP at 20° and pH 7 indicate that the heme iron is predominately high spin. The paramagnetic susceptibility at pH 5 and 7 was measured from -196° to room temperature (78). The susceptibilities deviate from the Curie law above -100°, and the deviations were explained on the basis

that the samples are pH dependent mixtures of two species. In one species the water molecule assumed to be bound to the heme iron is ionized, and in the second species the water molecule is un-ionized. Both species are thought to have high and low spin states populated in thermal equilibrium. The Mössbauer spectrum of CcP (79) at pH 7 also suggests these presence of both a high and low spin species.

The EPR spectra of CcP in the dissolved or crystalline state show well defined signals (79) with g-values typical of those due to the presence of a thermal mixture of high and low spin states of heme iron (80). This agrees with optical and paramagnetic susceptibility data (77,78). EPR spectra of CcP near pH 5 in frozen solutions at liquid-helium temperature (81) exhibited signals typical of high spin heme iron. Samples prepared at higher pH showed some formation of low spin heme iron, thereby indicating a pH dependent mixture of spin states.

CcP is resolvable into its heme and apoenzyme moieties, and the apoenzyme can be combined with modified porphyrins and metalloporphyrins to form unnatural holoenzymes (65). As with HRP (55), side chain modifications on the porphyrin at positions 2 and 4 had little effect on activity (82), but esterification at position 6 and 7 induces a considerable decrease in activity (83). CcP containing only porphyrins are inactive (84), but manganese prophyrins do show activity (85).

Turnip Peroxidase

Turnip peroxidase, TP, is a glycohemoprotein isolated from the root of the turnip plant. It was crystallized in 1956 (86). Three TP isozymes were isolated by Hosoya (87). Mazza *et al.* (88) found seven isozymes, five of which were sufficiently abundant for characterization. The isozymes all contain one mole of ferriprotoporphyrin IX and have molecular weights from 34,000 to 51,500 g/mole. Their isoelectric points vary from 3.3 to 11.6, and in the order of increasing isoelectric points the isozymes are called P_1 to P_7. The most basic isozyme, P_7, has the lowest molecular weight, the lowest carbohydrate content, 9.6%, and a distinct amino acid composition relative to the other isozymes (89). The optical spectra of the isozymes (88) indicate that the heme iron is predominately high spin (90). EPR studies of the nitric oxide complex (43) of the isozymes of the ferroperoxidases P_1, P_2, P_3, and P_7 have shown that the fifth coordination position of the heme iron is occupied by a nitrogen atom, perhaps derived from the imidazole group of histidine (91). P_1 and P_7 have also been characterized with repect to their redox potentials as a function of pH (50). P_7 is more easily reduced to the ferrous state than is P_1 , and this suggested a significant difference in the iron environment between these two isozymes.

Peptide maps of four TP isozymes and HRP were prepared by high-voltage electrophoresis of their tryptic digests (35). A comparison of these maps showed that all detected half-

cysteine residues in TP apparently occur as part of disulfide bridges. P_1 and P_2 differ significantly in only one peptide. P_3 is quite distinct from P_1 and P_2 , but these three isozymes appear to be related to each other and to HRP in their amino acid sequences around the four disulfide bridges. The basic isozyme P_7 differs from P_1 to P_3 and HRP in its amino acid sequence in the region of two of its disulfide bridges. Two highly homologous sequences which contain histidine were present in all five enzymes that were examined.

Proton NMR studies of amino acids near the heme have been used to evaluate the variations in the structure of the heme crevice among P_1, P_2, P_3, P_7, and HRP (44). The electronic structure of the heme and the tertiary structure of the heme crevice are essentially the same for P_1 and P_2 and to a lesser extent P_3, but they differ markedly in P_7.

Japanese Radish Peroxidase

Japanese radish peroxidase, JRP, is a glycohemoprotein isolated from the root of the Japanese radish plant (92). The three abundant isozymes, labeled a, b, and c (93), all contain ferriprotoporphyrin IX as a prosthetic group (92). Up to 18 isozymes of JRP have been detected using polyacrylamide gel electrophoresis (94). The molecular weights of JRPa and JRPc are 54,500 and 41,500 g/mole (95,96), respectively. JRPa and JRPc have been crystallized (95,96). Many properties of JRPa and JRPc have been compared (97). The amino acid composition (98) and the acid-base titrimetric

behavior (99) of JRPa have been determined. JRPa is 28% carbohydrate by weight (100). The amino acid composition was determined for seven peptides isolated from the peptic hydrosylate of performic acid oxidized JRPa (101). The aromatic amino acid residues in JRPa change their titrimetric (102) and spectrophotometric (103) behavior upon the removal of the heme. Tyrosine appears to be relatively masked or buried in the holoenzyme compared to the apoenzyme.

The EPR spectra of JRPa and JRPc have been obtained in the crystalline state and in frozen solutions between -193° and -93° (104). Both isozymes exhibited absorptions in the regions g=6 and g=2, and the temperature dependencies were explained in terms of a thermal equilibrium between high and low spin forms of the heme iron. At neutral pH the iron in JRPa is essentially high spin, whereas JRPc is essentially low spin. The equilibrium between spin states agrees with the temperature dependence of the optical spectra.

The Mössbauer spectra of JRPa have been determined at four temperatures (105,106). The temperature dependence of the quadrupole splitting was consistent with a thermal equilibrium between spin states.

The circular dichroic spectrum of JRPa in the ultraviolet region indicated the presence of about 35% α-helical structure (107). The ultraviolet CD spectrum of JRPa showed that removal of the heme caused the α-helical structure to disappear and be replaced by a β- or pleated-sheet structure.

Chloroperoxidase

Chloroperoxidase, ClP, is a glycohemoprotein isolated from the mold *Caldariomyces fumago*, and it has been obtained in the crystalline form (108,109). ClP has the unusual ability to oxidize the chloride ion (110,111), but it can also oxidize the usual peroxidase substrates such as guaiacol and pyrogallol (112), and exhibits catalase activity (113). Since ClP catalyzes halogenation, except fluorination, it has been used in a diversity of halogenation applications (110,114-117). The enzyme contains one mole of ferriprotoporphyrin IX as a prosthetic group and has a molecular weight of 42,000 g/mole, 25 to 30% of which is carbohydrate (109). The amino acid composition of ClP reveals a high amount of aspartic and glutamic acid, serine, and proline (109).

By means of Mössbauer spectroscopy the existence of a thermal equilibrium between spin states of the heme iron in ClP was demonstrated (118). Below about -70° the iron is in the low spin ferric state, whereas above this temperature the iron is in the high spin ferric state. This agrees with the optical spectra of ClP, which, at room temperature, is typical of a high spin ferrihemoprotein; but at -196° the spectrum is typical of the low spin state (118).

ClP has been extensively compared with cytochrome P-450. The cytochromes of the P-450 type derive their name, in part, from the absorption maximum they exhibit near 450 nm when reduced and ligated with carbon monoxide (119). The carbon monoxide complex of ferro-ClP is of the P-450 type (120).

It is thought on the basis of model studies that thiolate ligands (121-123) may be responsible for the P-450 type absorption, and the P-420 type may be ligated by the imidazole group of histidine. For ClP, however, sulfhydryl reagents and amperometric titrations indicated that this enzyme does not contain a sulfhydryl group (124). The Mössbauer and magnetic Mössbauer spectra of ferrous cytochrome P-450 (125), in which the heme group may have a thiolate ligand (119), are very similar to the Mössbauer and magnetic Mössbauer spectra of ferro-ClP (126). This was taken as evidence that cytochrome P-450 and ClP have closely related, if not identical, ligand structures of the heme iron. Cytochrome P-450 and ClP in their ferric and ferrous states and in their ferrous carbon monoxide complex have similar magnetic circular dichroic spectra (127). This provided further evidence for the similarity of their heme environments.

Lactoperoxidase

Lactoperoxidase, LP, a glycohemoprotein, was originally isolated from cow's milk (128). It has been obtained in crystalline form (128). LP has also been identified, using highly sensitive immunological techniques, in bovine tissues other than mammary glands. The salivary glands of both male and female cattle, the cow submaxillary and the steer sublingual glands (129), and the bovine harderian and lacrimal glands (130) contain LP. The enzyme has a molecular weight of 78,000 g/mole, 10% of which is carbohydrate (131). Peptide

maps of the soluble tryptic peptides suggest that LP may consist of two nearly identical subunits, but the single mole of heme per mole of LP is of unknown structure (131). LP was estimated to have 17% α-helical content based on the ORD trough at 233 nm (132).

Treatment of LP with acidified acetone failed to extract the heme indicating that the heme could be covalently bound to the protein (133). The thioether bond, as found in cytochrome c, was unlikely to be present because reagents known to cleave this bond did not cleave the heme from LP (133). A number of chemical procedures were developed in order to cleave the heme from the protein, and the spectral and chromatographic properties of the heme led to the conclusion that the prosthetic group of LP is a derivative of mesoprophyrin IX (134). On the basis of its reactivity, the covalent linkage between the heme and the protein was identified as an ester bond (134). It was also suggested that the linkage could be an amide bond (135). In a later study (136), proteolytic digestion of LP with pronase released a heme which could be extracted into an organic solvent. This extracted heme gave the pyridine hemochromogen of ferriprotoporphyrin IX. The nature of the prosthetic group of LP has not yet been resolved completely.

The EPR spectrum of the nitric oxide complex of ferro-LP did not show the superhyperfine splitting which was found for HRP and CcP, and was assigned to the nitrogen atom in the fifth coordination position of the heme iron (43). It could

not be determined if the absence of superhyperfine splitting in ferro-LP was due to fast relaxation of electron spin or due to the absence of coordinated nitrogen in the proximal site. However, histidine has been implicated in the catalytic mechanism of LP (137). Chemical modification of two histidine residues by 3-amino-1:2:4-triazole caused LP to lose enzymatic activity. The oxidation of iodide catalyzed by LP is an especially facile reaction, and this may suggest a biological role for the enzyme (138). All of the glands in which LP has been shown to exist are also efficient in their ability to concentrate iodide (139,140). This provides presumptive evidence that LP may have a role in halogenation reactions which occur in mammalian tissue. This led to studies of the rates of LP catalyzed reactions of tyrosine derivatives and tyrosine-containing peptides (141). Tyrosine residues have been implicated in the biosynthesis of thyroxine, an iodinated hormone of the thyroid gland. The iodination capabilities of LP have been used with $^{125}I^-$ to label proteins (142,143) and chloroplasts (144), and platlet (145,146) and erythrocyte (147,148) membranes.

LP, via the catalyzed oxidation of tyrosine (149,150), has been implicated in the formation of melanin, an aggregate of quinonoid pigment in a protein matrix found in dark skin and hair. LP may also be involved in controlling bacterial flora (130,151) since LP can inhibit bacterial growth under aerobic conditions.

Most recent reports on LP concern the use of this en-

zyme as a means of labeling with radioactive iodine. In particular, this technique has been used to determine whether membrane-bound proteins are on the inside or outside of a cell wall (152).

Thyroid Peroxidase

Thyroid peroxidase, ThP, is a glycohemoprotein isolated from rat (153), cattle (153,154), sheep (155), and pig (139, 156) thyroid glands. The porcine enzyme is the most extensively characterized. ThP contains ferriprotoporphyrin IX as a prosthetic group (157-159), and the molecular weight has been determined to be about 60,000 g/mole (157,160). A molecular weight of 104,000 g/mole (156), which was later revised to 200,000 g/mole(158), has been reported. Disc gel electrophoresis of these high molecular weight samples in sodium dodecyl sulfate revealed monomeric subunits of about 70,000 g/mole (158). This could account for the discrepancy in reported molecular weights. The presence of a ThP carbohydrate moiety has been verified (161).

ThP is a tightly bound membrane enzyme believed to be located principally on the rough-surfaced endoplasmic reticulum (162,163), and it is only released in soluble form after digestion of the membrane system with proteolytic enzymes (156). Trypsin treatment of thyroid membranes causes a drastic change in the molecular size of all detectable thyroid membrane proteins (164). Hence, ThP obtained by proteolytic digestion may not represent the intact enzyme.

Recently ThP has been won from the membrane system with non-ionic detergents (165). The molecular weight of ThP obtained by detergent solubilization could be as high as 500,000 g/mole. Difficulties obtaining pure preparations of ThP have hampered the characterization of this enzme.

There is considerable evidence that ThP has an essential role in the biosynthesis of thyroxine. Iodination of tyrosine residues in thyroglobulin, the major iodoprotein in the thyroid gland, is an essential step in thyroxine formation. It is believed that the iodide ion, which is the form in which iodide enters the thyroid gland, must be oxidized before it can act as an iodinating agent (161,166). Free 3,5-diiodotyrosine at micromolar concentrations can inhibit the rate of thyroglobulin iodination (167). The free 3,5-diiodotyrosine probably competes with a tyrosine residue in thyroglobulin for a binding site of ThP (167). Although iodide ion is necessary for the ThP catalyzed iodination reactions, it was shown that excess (i.e. millimolar) iodide can inhibit the iodination of thyroglobulin (168). Also, ThP will cause the tyrosine in a peptide to be preferentially iodinated if the sequence is Glu-Tyr, but no such preference was noted for LP or HRP (169).

Myeloperoxidase

Myeloperoxidase, MP, is a hemoprotein isolated from blood leukocytes (170-172), experimental rat chloroma tumor tissue (173,174), bone marrow cells of the guinea pig (175),

and the pus of infected dog uteri (176). The enzyme has a molecular weight of about 104,000 g/mole, depending upon its source (177,178). MP does not contain a carbohydrate moiety (179,180). MP from infected dog uteri has been crystallized (176).

The amino acid composition of MP varies with its source (178-180). Preparative disc electrophoretic separation of MP from normal human leukocytes demonstrated the presence of six isozymes (181). Each isozyme is dimeric and consists of any pair of three different subunit monomers. The existence of a dimeric structure of MP is supported by the fact that it can be split into two parts, each containing protein and heme, in the presence of 50% pyridine (176). This accounts for the heterogeneity of MP (182) for which up to ten components were observed (183).

MP was shown to contain two atoms of iron (176), and the paramagnetic susceptibility of MP shows the iron to be high spin (184). For an interpretation of the EPR spectrum of MP it was suggested that the two heme prosthetic groups have different environments (184) which is in accord with the idea that the two heme groups have different reactivities (176,178).

The structure of the heme groups and their modes of linkage to the protein are not yet known. Ferro-MP has spectral similarities with ferrosulfmyoglobin (185) indicating the possibility of a thiolate ligand. The pyridine hemochromogen of MP is similar to that of formyl or diacetyl

heme or heme *a* (179). It was suggested that at least one of the heme conjugated substituents is a carbonyl group and that the heme contains two electrophilic groups on opposite pyrroles as in cytochrome oxidase (186). MP, when modified with HCl, yields a new form of the enzyme, and this new form displays spectral characteristics similar to cytochrome oxidase (187). This supports the possibility that the prosthetic group of MP is analogous to heme *a*.

Acidic acetone will not cleave the heme from MP (188). Low yields of heme are obtained with reagents which cleave ester bonds (186,189). Recently, the rate of heme cleavage with sodium methoxide in methanol was used as an indication that the heme and protein may be linked by an amide bond (190).

Much of the present work with MP concerns the elucidation of its role in phagocytosis. The primary function of the leukocyte is the phagocytosis and destruction of microorganisms. The role of MP as an antimicrobial agent is the subject of extensive biochemical studies (191-195).

1.4 Oxidation-Reduction States of Peroxidase

There are five known oxidation-reduction states of peroxidase. These states are ferrous, ferric, Compound II, Compound I, and Compound III, in order of increasing oxidation state. These states are represented as shown in Fig. 1.3. The native enzyme, which is in the ferric state, can be reduced to the ferrous state by sodium dithionite,

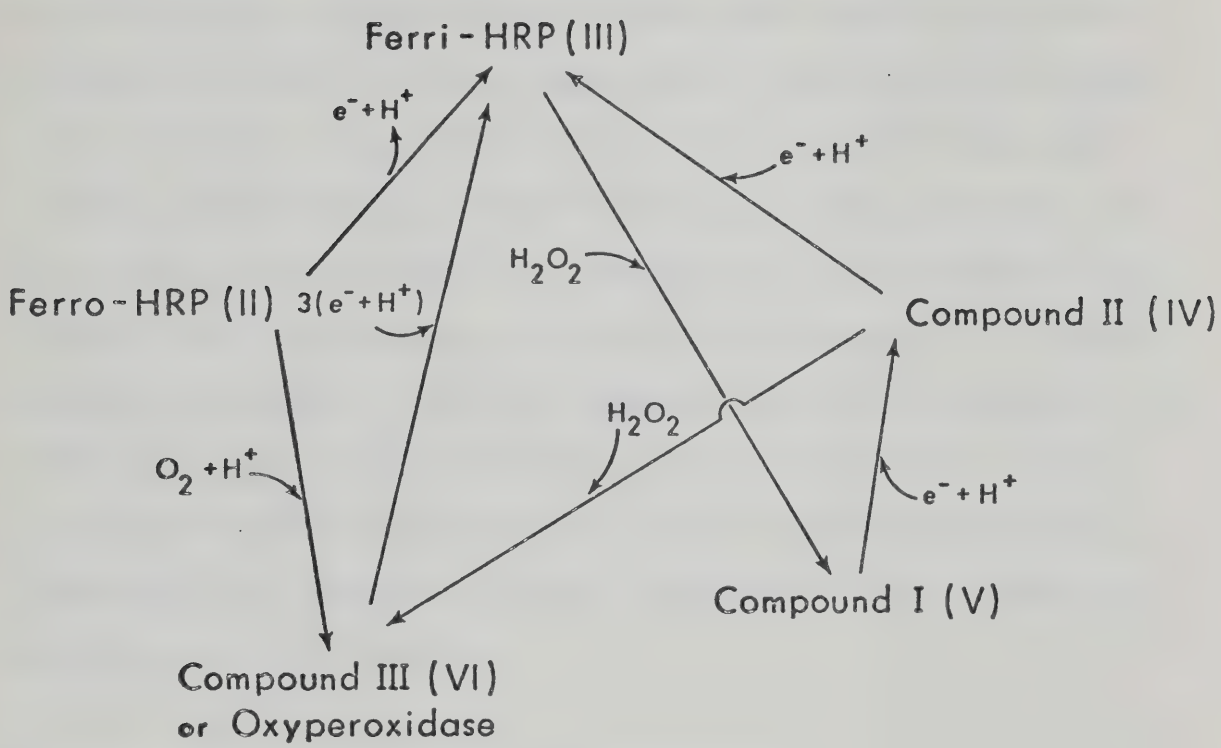

Fig. 1.3 The oxidation-reduction and proton balance relationships among the various forms of HRP. The formal oxidation state is indicated in the parentheses.

potassium borohydride, or by catalytic reduction over palladium or platinum on asbestos in the presence of a mediator such as methyl viologen (196). Compound I is the reaction product of hydrogen peroxide with the native enzyme and contains two oxidation equivalents more than the native state (21,23). Compound II is the one electron reduction product of Compound I. Compound III, or oxyperoxidase, can be formed by the reaction of Compound II with hydrogen peroxide or by the reaction of molecular oxygen with ferroperoxidase (196,197). Ferroperoxidase can reversibily form complexes with carbon monoxide, methyl isocyanide, cyanide, and nitric oxide; and ferriperoxidase can reversibily form complexes with cyanide, sulfide, fluoride, azide, hydroxylamine, and nitric oxide.

Ferroperoxidase and its Ligand Complexes

Ferroperoxidase must be formed in the absence of oxygen because oxygen is able to oxidize ferroperoxidase to ferriperoxidase (47). The oxidation-reduction potentials of the ferro- and ferri-HRP system have been determined potentiometrically from pH 4 to 11 (47). A variation of potential with pH was explained by an oxidation-linked proton equilibrium in both ferro- and ferri-HRP. This agrees with the results of a pH stat titration which showed that the formation of ferro-HRP from ferri-HRP is accompanied by the uptake of one proton (198). The oxidation-reduction potentials of HRP with different substituents on the 2 and 4 positions

of the heme group have been measured as a function of pH (199). The oxidation-linked proton equilibrium was attributed to a distal amino acid residue, and there appears to be strong hydrogen bonding between the base of the distal residue and the oxygen atom of water as a sixth ligand in the ferric state. Yamada *et al.* (198,199) consider it likely that ferroperoxidase has no water molecule coordinated at the sixth position as in the case of myoglobin. Oxidation-reduction potentials have been measured for turnip isoperoxidases P_1 and P_7 (50). From the presence of two oxidation-linked proton equilibria, it was concluded that the two isozymes have the same axial ligands, water and histidine; but they have different distal groups, a carboxyl group in P_1 and an imidazole group in P_7. The oxidation-reduction potentials of the ferro- and ferri-ClP couple have also been measured as a function of pH (200). Besides exhibiting an oxidation-linked proton equilibrium, this system also showed a sharp discontinuity in potential at pH 4.7 suggesting that either the ferric or ferrous form of ClP is drastically modified by changes in pH. Data on carbon monoxide binding indicate that ferro-ClP may be the species which is greatly modified near pH 4.7.

The absorption spectra of ferro-HRP and its carbon monoxide complex have been published (14,30), and they are very similar to the spectra of ferro-CcP and its carbon monoxide complex (81). However, the carbon monoxide complex of ferro-ClP is markedly different (120), which may be due to the

presence of a thiolate ligand instead of an imidazole ligand in the fifth coordination position. A carbon monoxide complex of ferro-MP has been observed (184), but only under restrictive conditions (201). A carbon monoxide complex of ferro-LP has also been observed (202). The cyanide complex of ferro-HRP has a dissociation constant 10^3-fold larger than the complex with ferri-HRP (203). The ferro-HRP cyanide complex has an absorption spectrum similar to the cyanide complexes of hemoglobin, myoglobin, and ferro-CcP (81). The cyanide and carbon monoxide complexes of ferro-HRP are both photodissociable (203). The kinetics of carbon monoxide (204) and cyanide (205) binding to ferro-HRP and their equilibrium constants of binding have been investigated. Carbon monoxide binds at pH 7 with a rate constant of 2.3×10^3 $M^{-1}s^{-1}$ (204). The kinetics of cyanide binding occurs in one step at pH 9.1 but is complicated and very different at pH 6.0, and the equilibrium constant of cyanide binding is highly pH dependent.

The Mössbauer spectrum of ferro-JRPa is characteristic of the ferrous high spin state, and the spectrum of the ferrous carbon monoxide complex is characteristic of the ferrous low spin state (106). This spin state elucidation by Mössbauer spectroscopy agrees with the magnetic susceptibility measurements of ferro-HRP and its carbon monoxide complex (25). As expected, the low spin cyanide complex of ferro-HRP (18) or ferro-CcP (81) has no EPR signal. Magnetic circular dichroism is sensitive to the spin and

oxidation state of the iron in hemoproteins. The MCD spectra of ferro-HRP and its carbon monoxide complex (206) are nearly identical with those of myoglobin and its carbon monoxide complex. The MCD spectrum of the cyanide complex of ferro-HRP is typical of a low spin ferrous derivative like oxymyoglobin. The CD spectrum of ferro-JRPa exhibits significantly different CD bands compared to native JRPa except for a close similarity in the ultraviolet region (107). This indicates a change in the heme group, but little or no change in the tertiary structure of the protein upon reduction.

The protonation of a heme-linked group causes changes in the visible spectrum of ferro-HRP (199), and the pK_a of this group changes upon the formation of the carbon monoxide complex (207). The pK_a value for the carbon monoxide complex of ferro-HRP varied by changing the substituents at the 2 and 4 positions of the heme group (208). The change in pK_a was interpreted in terms of hydrogen bonding between a distal amino acid residue and the ligand atom directly bound to the heme iron.

Compound III or Oxyperoxidase

The existence of a spectroscopically distinct Compound of HRP which was formed when a large excess of hydrogen peroxide was added to a solution of HRP was first noticed by Keilin and Mann (202). This Compound eventually became known as Compound III (14,209) because George (197) discovered

that it was formed by the reaction of hydrogen peroxide with Compound II. Chance (210) recorded the absorption spectrum of Compound III formed in this manner. Compound III was also formed in the aerobic dihydroxymaleic acid system in which HRP acts as an oxidase (211,212). HRP is reduced to ferro-HRP and in the presence of molecular oxygen forms Compound III. Yamazaki and Piette (213) concluded from a study of aerobic oxidase reactions catalyzed by HRP that Compound III and oxyperoxidase were one and the same derivative of HRP. Compound III can be formed in three ways: 1, ferro-HRP and molecular oxygen; 2, ferri-HRP and superoxide anion; and 3, Compound II and H_2O_2. HRP acts as an oxidase toward dihydroxyfumaric acid, and the free radical product of this substrate can reduce molecular oxygen to $O_2^{\cdot-}$, the superoxide anion radical. Compound III can be formed by reducing ferri- to ferro-HRP with NADH (214) and then introducing molecular oxygen (215). It can also be formed when indolacetic acid reduces HRP or TP (216) under aerobic conditions. Oxyperoxidase of TP isozyme P_7 is especially stable, and this may be a reflection of the oxygenase activity of this hemoprotein (50,216). During the xanthine oxidase reduction of *p*-benzoquinone, the $O_2^{\cdot-}$ formed is trapped by LP to form Compound III of LP (217). The amount of $O_2^{\cdot-}$ formed by photosensitization with fluorescein has been measured by using the extent of LP Compound III formation (218). Compound III of MP has been formed from the reaction between electrolytically produced $O_2^{\cdot-}$ and ferri-

MP (219).

The reaction of HRP Compound III with various oxidizable substrates showed it to be very much less reactive than Compound II (220,221).

Wittenberg *et al.* (197) have made an excellent study of Compound III. At pH 7 the reaction between ferro-HRP and molecular oxygen is first order in both reactants and has a rate constant of 5.8×10^4 $M^{-1}s^{-1}$. The reaction stoichiometry is 1:1, and oxyperoxidase is formed without detectable intermediates. Oxyperoxidase is able to oxidize a further three moles of ferroperoxidase indicating that it retains the four oxidation equivalents of molecular oxygen. Oxyperoxidase undergoes a slow first-order decomposition to ferri-HRP without detectable intermediates, and photodissociation does not occur even with intense light.

The optical spectrum of HRP oxyperoxidase shows little change with temperature indicating the absence of a thermal equilibrium between spin states, and the EPR spectrum shows no signal attributable to oxyperoxidase (30). Oxyperoxidase is probably diamagnetic as is oxyhemoglobin (222). CcP oxyperoxidase also has no EPR signal (81). Noble and Gibson (223) have demonstrated that hydrogen peroxide can oxidize ferro-HRP to oxyperoxidase in a sequence of two steps. Compound II is first formed from that reaction of ferro-HRP with hydrogen peroxide, and then Compound II reacts with more hydrogen peroxide to form oxyperoxidase. Both reactions are first order with respect to each reactant, and they

proceed without detectable intermediates. Phelps *et al.* (224) have found no detectable intermediates within the millisecond time range in the reaction of ferro-HRP with molecular oxygen to form oxyperoxidase and in the decomposition of oxyperoxidase to form ferri-HRP. The formation of $O_2^{\cdot-}$ during the decay of HRP oxyperoxidase has been detected (195).

The stability of HRP oxyperoxidase with the heme modified at the 2 and 4 positions increases in the order meso-, proto-, chlorocruoro-, and diacetylperoxidase (225). From these results it appeared that the stability of oxyperoxidase was affected by the electron density at the heme iron. For the stable diacetyldeutero-oxyperoxidase, a heme-linked proton equilibrium of pK_a=8.0 has been detected spectrophotometrically (208). Proton balance studies have shown no net amount of protons are gained or lost when forming oxyperoxidase from Compound II with H_2O_2 , but three protons are gained by the enzyme when ferri-HRP is formed from oxyperoxidase (198).

Ligand Complexes of Ferriperoxidase

A variety of inorganic ligands ligate to ferriperoxidase, presumably by displacing a water molecule from the sixth coordination position of the heme iron. Common ligands are fluoride, azide, cyanide, and possibly hydroxide ions. (The alkaline form of peroxidase may or may not be a hydroxide complex, and this point will be discussed further.)

Paramagnetic susceptibility measurements show that the binding of a ligand to native peroxidase causes a change in

the spin state of the heme iron. The paramagnetic susceptibility values of several hemoproteins including peroxidase have been summarized (25,226). When ligated with fluoride or water the ferric iron is usually predominantly high spin, whereas azide and cyanide produce complexes of intermediate and low spin states, respectively (14,25). The MP cyanide complex, however, has an unusually large paramagnetic susceptibility (184). A thermal equilibrium between the high and low spin states of the HRP azide complex has been demonstrated by magnetic susceptibility between -196° and room temperature (227). In contrast, the HRP complexes with fluoride and cyanide are purely high and low spin, respectively, over this temperature range, and their paramagnetic susceptibilities obey the Curie law (26). The EPR signal of the cyanide complex and the alkaline form of HRP is typical of low spin ferriheme (30). For native HRP the pH dependent magnetic susceptibility and optical spectra have been explained in terms of an acid and alkaline form, and each of these forms has high and low spin states populated in thermal equilibrium (26). Similar results have been obtained for CcP (77). The fluoride and cyanide complexes of CcP have optical spectra typical of high and low spin heme iron, respectively. These spectra are temperature independent. The Mössbauer spectrum of the CcP fluoride complex indicates high spin heme iron (228), and the CcP cyanide complex has an EPR spectrum typical of low spin heme iron (81). The temperature dependence of the optical spectrum of the CcP

azide complex indicates a spin state thermal equilibrium (77). The optical spectra of LP complexes with fluoride and cyanide are typical of the high and low spin states, respectively; but the alkaline form of LP could not be formed prior to denaturation (229). The EPR (104) and Mössbauer (106) spectra of the derivatives of JRPa show that its fluoride complex is high spin, and its alkaline form is low spin, as is its cyanide complex. The cyanide complex, however, is a temperature dependent mixture of spin states. Also, the Soret and visible CD spectra of the fluoride and cyanide complex and the alkaline form of JRPa have been recorded (107).

Chloride, bromide, and iodide all form spectroscopically distinct complexes with ClP at low pH, and this pH requirement for binding may be responsible for the low pH optimum of ClP catalyzed halogenation reactions (113). The fluoride and iodide complexes of ClP are high spin over a wide temperature range (118) as determined by their Mössbauer spectra. However, the Mössbauer spectrum of the ClP chloride complex is quite similar to that of native ClP suggesting that chloride may not bind as an axial ligand to the heme iron. Recent broad-line NMR results show a specific interaction between ClP and chloride at low pH which does not involve coordination to the heme iron (230). The oxidation-reduction potentials of ClP complexes with chloride, bromide, and iodide differ little from that of native ClP (201). This also suggested that these halide ions may not bind to the

heme iron.

ORD spectra of the fluoride and cyanide complexes of HRP (28) and LP (132), and the alkaline form of HRP, show that there is no gross change in protein conformation upon formation of these derivatives. No large orientational change of the heme with respect to the protein occurred in HRP, but a change apparently did occur in LP.

Recently, the magnetic circular dichroic spectra of the fluoride and cyanide complexes and the alkaline form of HRP were recorded (206). These spectra were compared to the corresponding derivatives of ferrimyoglobin. The MCD technique is sensitive to the spin and oxidation state of the heme iron. The MCD spectra for the cyanide complexes of ferri- and ferro-HRP and the carbon monoxide complex are nearly identical with the MCD spectra of the analogous ferrimyoglobin derivatives except for the alkaline forms. The alkaline form of HRP exhibited an entirely different MCD spectrum than that of ferrimyoglobin hydroxide. It could be that the alkaline form of HRP is not a hydroxide complex. There are other indications that fail to support the analogy between the alkaline form of HRP and ferrimyoglobin hydroxide. The magnetic moment of the alkaline form of HRP is much different from that of ferrimyoglobin hydroxide (90), and the pK_a value for the transition to their basic forms is a full two pK_a units higher for HRP than for ferrimyoglobin (231), pK_a=11 compared to 9, respectively. However, these differences might be caused by other factors than the possibility

that the alkaline form of HRP is not a hydroxide complex. It has been suggested on the basis of a kinetic study of the alkaline ionization of HRP that an amino acid side chain is ionized when HRP is brought to alkaline pH from neutral pH (232). A subsequent conformational change allows the side chain to ligate to the sixth position of the heme iron.

Kinetic studies of ligand binding to peroxidases has led to information about the nature of the heme active site. The pK_a values of catalytically important ionizable groups on both the enzyme and ligand can be determined by measuring the rate of complexation as a function of pH (233,234). The kinetics of cyanide binding to ferri-HRP between pH 4.2 and 11.3 was studied using the stopped-flow technique (235). The results were interpreted in terms of acid-base catalysis, and three ionizable groups on HRP and the ionization of hydrocyanic acid affect the binding rate. The rate of fluoride binding to HRP between pH 4.1 and 7.9 is affected by two ionizable groups on the enzyme of nearly the same pK_a value as those groups on the enzyme which affected the rate of cyanide binding (235,236). The kinetics of cyanide binding to LP between pH 4.6 and 10.6, studies by the temperature-jump method, showed that the rate of complex formation was affected by two ionizable groups on LP and by the ionization of hydrocyanic acid (237). A kinetic study of cyanide binding to TP isozymes P_1 and P_7 showed that binding occurred in one step (238). Fluoride binding to P_1 occurred in one step but fluoride binding to P_7 exhibited three distinct proces-

ses. Two ionizable groups on P_1 affect the rate of fluoride and cyanide binding, but three ionizable groups affect the binding rate of these ligands to P_7. Kinetic studies of fluoride (239) and cyanide (240) binding to CcP have been made as a function of pH. The rate of fluoride and cyanide binding is strongly influenced by the ionization of the acid form of the ligand and by a group on the enzyme pK_a=5.5. Above pH 7 the CcP cyanide complex undergoes two isomerization reactions.

Compound I and Compound II

Compounds I and II are oxidized intermediates in the peroxidatic enzymatic cycle previously shown in Equations [1] to [3]. Hydrogen peroxide reacts with peroxidase to form Compound I with no net gain or loss of protons (198). Compound I is reduced by an oxidizable substrate to Compound II with a net gain of one proton to the enzyme (198). When Compound II is reduced to HRP, the enzyme gains another proton (198).

Compound II was discovered (202) prior to Compound I because the much more reactive Compound I was quickly reduced to Compound II by oxidizable substrates which were present as impurities in the enzyme preparation. Theorell (19) with a purer preparation first noted the transient appearance of Compound I. The rapid-flow method was then used to measure the optical spectrum of Compound I (209,210). Titration with ferrocyanide established that Compound II requires one oxi-

dation equivalent of electrons (22,23) and Compound I requires two equivalents (21,241) to be reduced to native peroxidase. Since Compound I contains the two oxidation equivalents of the hydrogen peroxide, it was initially supposed that the oxidized intermediates were enzyme-substrate complexes (209,210,242-246). It was later demonstrated that spectroscopically identical preparations of HRP Compounds I and II could be formed from a variety of oxidizing agents (247-249). Much of the work on peroxidases has been directed toward the elucidation of the chemical structure, physical properties, amd mechanism of action of Compounds I and II.

Magnetic susceptibility measurements of HRP Compounds I and II showed that they contain three and two unpaired electrons, respectively (24,250). For Compound II this is consistent with a low spin ferryl peroxidase. In ferryl peroxidase the ferric heme is oxidized and can be formally represented as Fe(IV). The formulation of Compound II as a ferryl type structure is widely accepted, and the possibility of the existence of Fe(IV) porphyrins has been demonstrated by cyclic voltammetry (251). The location of the oxidized sites in Compound I is more elusive. The existence of three unpaired electrons in Compound I can be explained in three ways. Compound I could be in the Fe(V) oxidation state or it could be a low spin ferryl structure with a free radical in the porphyrin or protein moiety (252).

The free radical nature of HRP Compound I seems to be uncertain. Morita and Mason (104) found an EPR free radical

signal at g=2.003 for HRP Compound I at -175°, but its spin concentration was very low relative to the concentration of Compound I. Also, the decay of the signal did not correspond to the decay of the optical absorbance of Compound I. Blumberg *et al.* (30) found no EPR signal attributable to Compound I, but Douzou and Leterrier (31) found a free radical signal at g=2.003 during the conversion of Compound I to II. An EPR study of HRP Compound I by Aasa *et al.* (253) describes an asymmetric signal for Compound I below -253° at g=1.995. The spin concentration of this signal was approximately 1% of the concentration of Compound I. A titration of HRP with H_2O_2 demonstrated that the signal intensity was proportional to the amount of Compound I, and the signal intensity and optical absorbance decayed simultaneously. The low signal intensity may be due to a nearby fast-relaxing ferryl iron.

It has frequently been suggested that if a free radical is present in Compound I it may be contained in the prophyrin (222,251,254,255). One of these studies (255) is based on the two electron oxidation product of cobaltous octaethylporphyrin which is a stable π-cation radical with an optical spectrum very similar to HRP Compound I. The idea that the second oxidation equivalent in Compound I is not found in a Fe(V) configuration was supported by the Mössbauer spectra of both JRPa (256) and HRP (257) Compounds I and II. The same Mössbauer spectra are obtained for Compounds I and II indicating the same electronic configuration of the heme iron in both Compounds. The second oxidation equivalent

must be located at a site other than the heme iron.

Laser Raman spectra of HRP Compounds I and II (258) show that in contrast to native HRP (59) the heme iron in Compound II is in the plane of the porphyrin. The Raman spectrum of Compound I was typical of model porphyrin π-cation radicals (259).

The photolysis product of HRP Compound I at -196° (260-262) has been shown recently to produce a product of unusual paramagnetic character (263,264). The EPR signal intensity of the photolysis product is very much greater than the signal of Compound I or HRP. When the product is kept in the dark the signal diminishes but reappears when the sample is reirradiated.

CcP reacts with one mole of H_2O_2 to form a Compound known as ES (64,75,264,265). Compound ES can also be formed from CcP and chlorite (81), N-bromosuccinimide (266), and *o*-benzoylhydroxylamine (266). Compound ES retains both oxidizing equivalents of the hydrogen peroxide (265), but has an optical spectrum nearly identical to HRP Compound II (265). This observation was taken to suggest that one of the two oxidation equivalents may be retained in the protein moiety since the optical spectra are believed to reflect the electronic structure of heme groups (39). Unlike HRP Compound I, Compound ES showed an intense sharp free radical signal in the EPR spectrum at g=2.004 (79,81,267,268). The intensity of this signal corresponds to one unpaired electron per molecule of Compound ES. Large changes in the ultra-

violet absorption spectrum are observed upon the formation of Compound ES (79,268), and it appears likely that one of the two oxidation equivalents of Compound ES is retained as a free radical in an aromatic amino acid residue of the protein and not in the porphyrin π-orbitals as is suggested for HRP Compound I. In Compound ES the EPR signals for paramagnetic iron in native CcP have disappeared indicating that the iron has an even number of electrons as is expected for the ferryl or Fe(IV) oxidation state (75). This interpretation agrees with the magnetic susceptibility measurements on Compound ES (269).

An oxidized intermediate of CcP which is only one oxidation equivalent above the native enzyme was first noticed in the biphasic reduction of Compound ES by ferrocyanide (75). The second phase of this reaction corresponds to the reduction of the second oxidized intermediate known as CcP Compound II (270). It is not known which of the sites in Compound ES is reduced in the formation of CcP Compound II. Compound II could be Fe(IV) or Fe(III) and a free radical. An equilibrium between these two postulated forms of CcP Compound II might exist (270).

A possible chemical composition for ClP Compound I has been elucidated using ^{18}O labeled substrates (271). ClP was reacted simultaneously with unlabeled and doubly labeled ^{18}O *m*-chloroperbenzoic acid, and molecular oxygen which was released as a product was analyzed for isotopic distribution. Scrambling had occurred since molecular ^{16}O-^{18}O was obtained

as a product. A reasonable scheme which accounts for scrambling involves incorporation of one oxygen atom from the peracid into the enzyme probably as a ligand at the heme iron. There is a concomitant release of the parent carboxylic acid as Compound I is formed (272). This is followed by the reaction of Compound I with a second peracid molecule to form molecular oxygen (273). In contrast, the ClP catalyzed evolution of molecular oxygen from a mixture of unlabeled and doubly labeled ^{18}O H_2O_2 proceeds by a retention mechanism where no ^{16}O-^{18}O is produced (274)

The following overall formulations for Compounds I and II emerge from the presently available data. Compound I of HRP may contain an oxygen atom derived from H_2O_2 (271,273), and the oxygen atom is probably bound to Fe(IV) heme. The second oxidation equivalent may be located either on the porphyrin as a π-cation radical (255) or on an amino acid residue as a free radical. For CcP Compound ES this second oxidation equivalent is almost certainly located of the protein in an aromatic amino acid side chain (268). Since both HRP Compounds I and II have ferryl or Fe(IV) type structures (257), presumably it is the reduction of the free radical site which occurs when Compound I is reduced to Compound II. If Compoud II retains the oxygen atom (273) present in Compound I, then Compounds I and II can be represented by R·Fe(IV)O and RFe(IV)O, respectively. The free radical, ferryl heme, and the iron-bound oxygen atom are represented by R·, Fe(IV), and O.

The reactions of Compounds I and II with several oxidizable substrates have been studied by transient state kinetics. The stopped-flow apparatus using spectrophotometric detection is particulary suitable for this application because the reduction of Compound I or II is usually accompanied by sufficiently large absorbance changes in the Soret region even when the enzyme is in less than micromolar concentration. Compound I can be prepared by the addition of an equimolar amount of H_2O_2 to a solution of the native enzyme providing that the solution is free of oxidizable impurities. To prepare Compound II an equimolar amount of a one electron reductant is added to a solution of Compound I. The particular intermediate can then be reacted with an oxidizable substrate thereby measuring the reaction rate of a single relevant step from the overall enzymatic cycle.

Kinetic and equilibrium measurements of the properties of systems containing peroxidase have been the main research operations used in this laboratory. Reaction rate measurements, considerations of the rate-influencing factors, and the proposal of reaction mechanisms from these measurements is known as the discipline of chemical kinetics. Equilibrium and kinetic measurements are complementary by their nature. Measurements of a system at equilibrium serve to define the state of that system, whereas kinetic measurements define the manner in which one particular defined equilibrium state is converted into another defined equilibrium state. For example, equilibrium measurements can determine the state of

the reactants and products of an enzyme catalyzed reaction, but kinetics is required to determine the mode of enzyme action during the reaction. By means of chemical kinetics one attempts to define each individual concerted step of a reaction. However, the study of chemical kinetics seldom provides an exclusive reaction pathway, but it is very useful because of its ability to exclude one or more pathways so that the total number of possibilities is reduced. Since many life processes are catalyzed by enzymes, an understanding of the mode of enzymatic catalysis is fundamental to molecular biology. The measurement of the rate of an enzymatic reaction over a wide range of pH can reveal the existence and the pK_a values of catalytically important ionizable groups on the enzyme and on the substrate (233,234).

Since Chance (246) measured the effect of pH on the rate of oxidation of a few substrates by HRP Compound II, there have been several studies on the effect of pH on the rate of Compound I formation and on the reactions of Compounds I and II with a variety of substrates (275). The pH dependence of the rate of Compound I formation of LP (276,277), CcP (278), and HRP (279) with H_2O_2 has been studied. The rate of LP Compound I formation is independent of pH from 3.0 to 10.8 (277). For CcP the rate of Compound I formation is inhibited by the protonation of an ionizable group with a pK_a of 5.5 and by the deprotonation of a group with a pK_a of 9.8 (278). At pH values between these two pK_a values CcP reacts rapidly with H_2O_2. The rate of HRP Compound I

formation is pH independent from pH 5 to 9, but the protonation of two groups with pK_a values of 3.9 and 3.2 cause the rate to decrease (279). At low pH the rate of Compound I formation for CcP and HRP is base catalyzed. The pH dependence of the rate of HRP Compound I formation with several substituted perbenzoic acids indicated that the un-ionized form of the peracid is the reactive form, and the pattern of substituent effects did not agree with the expectations for electrophilic oxidation of the enzyme (280). The reactions of LP Compound II with iodide (281) and *p*-cresol (282) are acid catalyzed. The rates of iodide oxidation by HRP Compounds I and II (283,284) are acid catalyzed, and it was shown that iodide reduced Compound I directly to HRP without the transient appearence of Compound II (283). The rates of oxidation of ferrocyanide by CcP Compounds I and II (270) and by HRP Compounds I and II, formed with H_2O_2 (285) or with ethyl hydroperoxide (286) or *m*-chloroperbenzoic acid (286), have been studied as a function of pH. In the case of HRP the rate of ferrocyanide oxidation is independent of the oxidizing agent used in the preparation of Compounds I and II (286). The steady state rate of ferrocyanide oxidation by HRP was inhibited by cyanide (287). The cyanide bound only to HRP. The rate of oxidation of sulfite and nitrite by HRP Compounds I and II is acid catalyzed, and, like iodide (283), sulfite is able to reduce Compound I to HRP without the transient appearence of Compound II (288, 289). The reaction rate between HRP Compound II and *p*-

cresol, ferrocyanide, iodide (290,291), and *p*-aminobenzoic acid (292) have been studied in water and deuterium oxide over a wide range of pH or pD.

Fig. 1.4 is a compilation of the results of rate measurements as a function of pH for the reaction of HRP Compound II, HRP-II, with several substrates (262). The log of the second-order rate constant k is plotted as a function of pH. Except for the acid region of curve A for *p*-cresol as the substrate, all the reactions are acid catalyzed. A catalytically important ionization on HRP-II, pK_a=8.6, is indicated by ↓ for the substrates A *p*-cresol (290); B ferrocyanide (285); and D *p*-aminobenzoic acid (293). Important ionizations on *p*-cresol, pK_a=10.4 (290), and C bisulfite ion, pK_a=6.9 (288), are indicated by ↑. The plots for E and F, nitrite and iodide ions, show a single important ionization with a pK_a value beyond the pH range of the study (284,288).

Fig. 1.5 shows the rate of HRP Compound I reactions as a function of pH for several substrates. All the reactions shown are acid catalyzed. An ionizable group on Compound I with a pK_a value of about 5.1 is evident, ↓, with the substrates A ferrocyanide (285); B *p*-aminobenzoic acid (293); D iodide ion ; and E bisulfite ion (288). The pK_a of 6.9 for the dissociation of the bisulfite ion is indicated by ↑. The fast rate of the reaction of *p*-cresol with both Compound II and Compound I (see Chapter II) may suggest that phenolic compounds are the natural substrates for peroxidase.

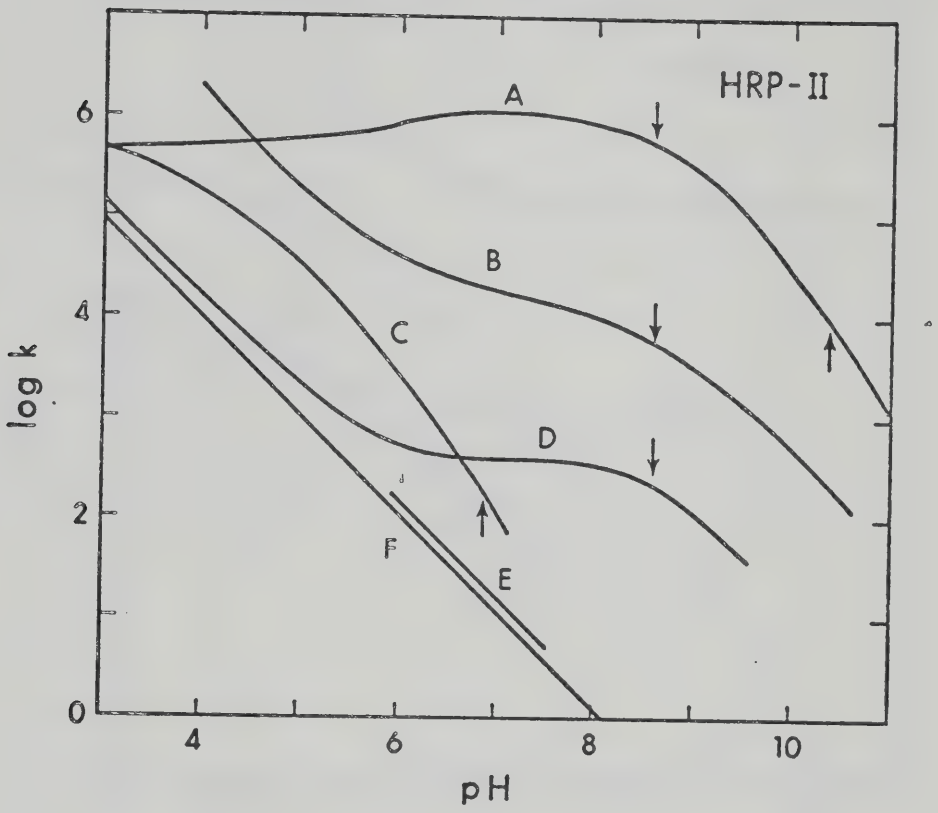

Fig. 1.4 Plots of the log of the second-order rate constant k *vs.* pH for the reaction of HRP Compound II with several substrates. A *p*-cresol, B ferrocyanide, C bisulfite, D *p*-aminobenzoic acid, E nitrite ion, and F iodide ion. The arrows indicate pK_a values on Compound II ↓ and on the substrate ↑ . These plots are taken from Dunford, H.B., and Stillman, J.S. (1976) *Coord. Chem. Rev.* 19, 187-251.

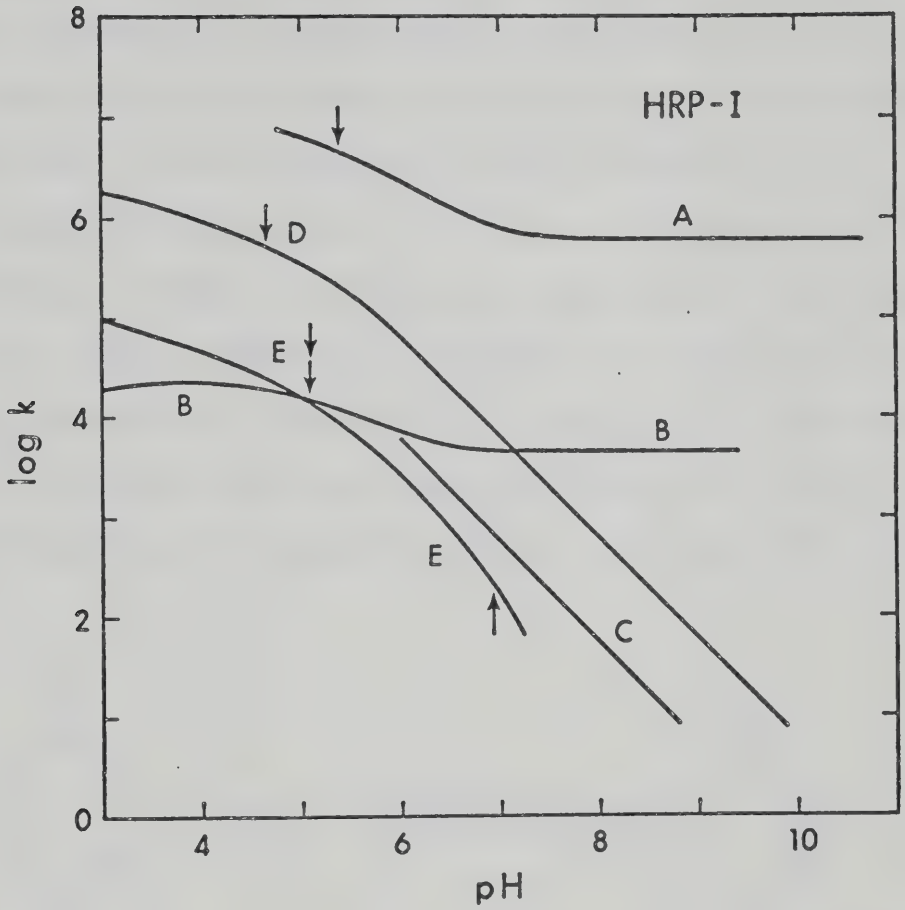

Fig. 1.5 Plots of the log of the second-order rate constant k *vs.* pH for the reaction of HRP Compound I with several substrates. A ferrocyanide, B *p*-aminobenzoic acid, C nitrite ion, D iodide ion, and E bisulfite ion. The arrows indicate pK_a values on Compound I ↓ and on the substrate ↑ . These plots are taken from Dunford, H.B., and Stillman, J.S. (1976) *Coord. Chem. Rev.* 19, 187-251.

1.5 Laccase

The presence of a substance responsible for the darkening and hardening of latex from the Japanese lacquer tree, *Rhus vernicifera*, was noted in 1883 (294). This substance is now known to be a copper-containing enzyme called laccase or *p*-diphenol oxidase (E.C. 1.10.3.2 *p*-diphenol: O_2 oxidoreductase). Laccase is found in a great many fungi (295) and plants (296). The early history of laccase has been reviewed (297-299). Laccase has a fairly low substrate specificity (300), but the catalyzed oxidation of *p*-diphenol to *p*-benzoquinone by molecular oxygen is especially facile.

[4] 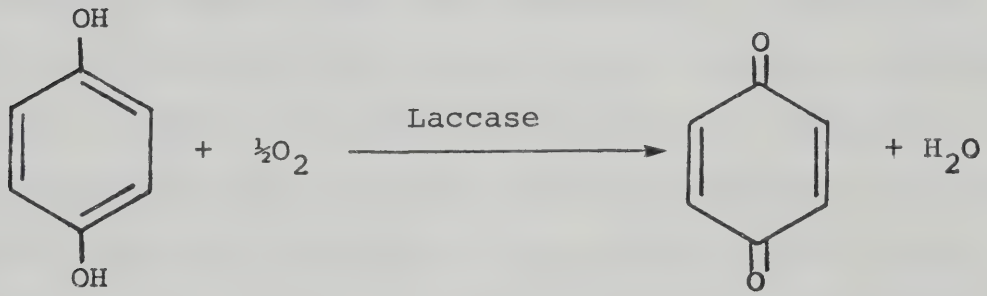

Thus, molecular oxygen is fully reduced to water.

Early reports were contradictory concerning the laccase catalyzed oxidations of monophenols such as *p*-cresol. Laccase was reported to be both inactive (301,302) and active (300, 303) with *p*-cresol. An attempt to resolve these discrepancies (300) indicated that *p*-cresol was only very incompletely oxidized by laccase because the enzyme had quickly become inactivated. However, this inactivation could be prevented

by the simultaneous presence of *p*-cresol and catechol, gelatin, or polysorbate 80 (a mixture of polyoxyethylene ethers of mixed oleic acid esters of sorbitol anhydride). In the presence of one of these additives which prevent inactivation, *p*-cresol and many other monophenols (304,305) can rapidly be oxidized by laccase. The oxidation products of *p*-cresol formed by laccase (300) and HRP (306) are the same. In an unusual application, laccase was used to catalyze the oxidation of steroidal hormones with a phenolic group in the A ring (307).

The most extensively studied laccases are from the Japanese lacquer tree, *Rhus vernicifera*, (308-312) and the Indo-Chinese lacquer tree, *Rhus succedanea*, (301,302,309) and from the wood-rotting white fungus, *Polyporus versicolor* (313,314). Laccase from *Rhus vernicifera* and especially from *Polyporus versicolor* are relatively available and hence the most completely studied of the laccases. The fungal laccase has two isozymes called A and B (314), and both isozymes contain four moles of copper per mole of enzyme (314,315). Laccase A and B have similar molecular weights, about 62,000 g/mole (313,315), but laccase A is 14% carbohydrate (313-315) whereas laccase B is less than 1% carbohydrate (314). Laccase from *Rhus vernicifera* has a molecular weight of 110,000 g/mole (308,309,316) and it is 45% carbohydrate (316). *Rhus succedanea* and *Rhus vernicifera* laccase have similar molecular weights (309). *Rhus vernicifera* laccase was once thought to have 5 to 6 moles of copper per

mole of enzyme (309,317,318), but this has been revised to 4 moles of copper (308,316). The blue color of laccase (sometimes these enzymes are referred to as the blue oxidases) is due to the presence of copper coordinated to the protein. The optical spectrum of laccase in its oxidized and reduced form is shown in Fig. 1.6. The copper is tightly bound to the protein as a prosthetic group since it is not removed by dialysis. The copper in *Rhus vernicifera* laccase does not exchange with $^{64}Cu(II)$ in solution, but the copper in the reduced form of the enzyme will exchange with $^{64}Cu(I)$ (310).

An oligomeric subunit structure was proposed for fungal laccase A (313), and this proposal was supported by hydrodynamic measurements of the enzyme made in the presence of guanidine hydrochloride (319). Laccase A may consist of four subunits of similar size which are linked by disulfide bridges and noncovalent interactions to form a tetramer (319). Electron microscopy of a different fungal laccase from the Ascomycete *Pdodspora anserina* indicates that this enzyme exists as a tetramer with the subunits arranged at the corners of a rectangle (320). The molecular weight of laccase from this source is 390,000 g/mole (320-322).

Oxidases generally require metals for their catalytic activity, and the copper in laccase may be involved in a mechanism in which high valence Cu(II) is reduced to Cu(I) by the substrate which is oxidized. The Cu(I) could then be reoxidized to Cu(II) by molecular oxygen which is eventually

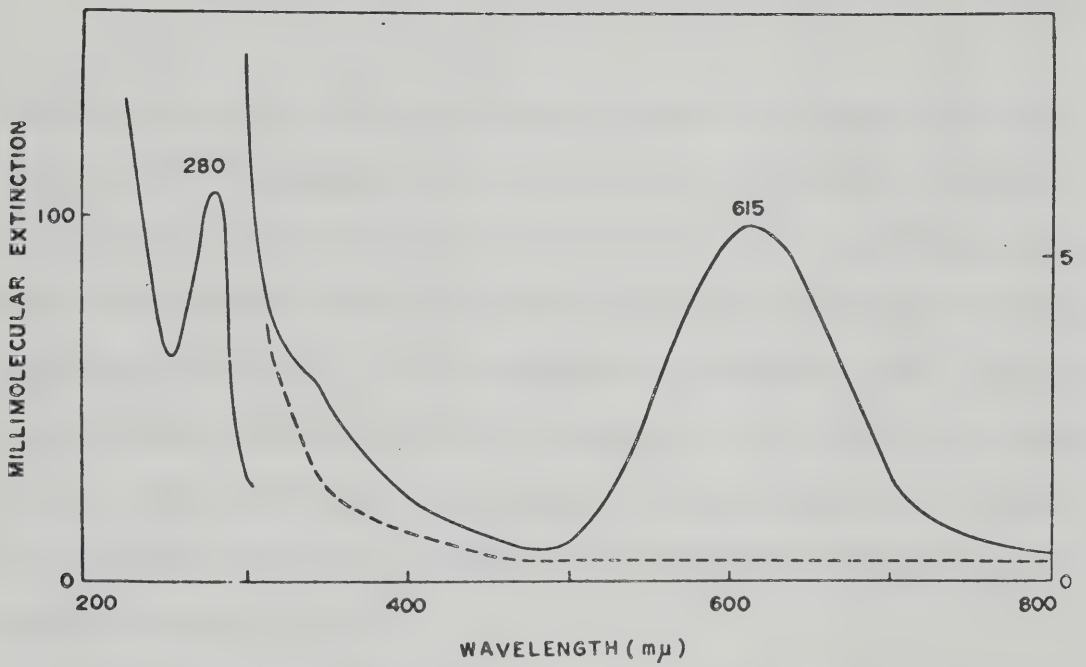

Fig. 1.6 Absorption spectra of laccase, ———, and reduced laccase, -----, in phosphate buffer at pH 7. These spectra are taken from Nakamura, T. (1958) *Biochim. Biophys. Acta* 30, 44-52.

reduced to water.

[5] Cu(II) + substrate $\longrightarrow$ Cu(I) + product

[6] Cu(I) + $\frac{1}{4}O_2$ + H^+ $\longrightarrow$ Cu(II) + $\frac{1}{2}H_2O$

A mechanism involving a valence change in copper has been established by Malmström *et al.* (323) using EPR. Since Cu(II), d^9, is paramagnetic and Cu(I), d^{10}, is diamagnetic, EPR spectroscopy has been widely applied to copper-containing proteins (324). This mechanism of action for laccase was further substantiated by Nakamura (308,325) who showed that 4 Cu(I) ions were oxidized by one molecule of oxygen. The valence change of copper was also detected by magnetic susceptibility (326).

The heterogeneity of the 4 moles of copper within a single molecule of laccase is well established (324). The copper ions have distinct environments in the enzyme which cause their nonequivalence. The nonequivalence of the copper ions was first detected by EPR for fungal laccase (327) and later for *Rhus vernicifera* laccase (328). The EPR signal intensity accounted for only 50% of the total copper content, and it was first concluded that half of the copper was present as Cu(I) (327,329). Magnetic susceptibility measurements also indicated that only half of the copper is paramagnetic in fungal (330) and *Rhus vernicifera* laccase (331). However, the presence of all divalent copper, but with two Cu(II) ions spin-paired, was included as a possibility (330).

Not only is half of the copper in laccase heterogeneous because half is paramagnetic and half is diamagnetic, but the copper is further heterogeneous because the EPR-detectable copper is of two unique types in both fungal laccase A and B (332) and *Rhus vernicifera* laccase (328). There are three types of copper in laccase which are referred to in the present literature as Type 1, 2, or 3. Type 1 has an unusual EPR spectrum characterized by an unusually small hyperfine splitting (328,333). Type 2 has a more normal EPR spectrum, and Type 3 refers to the diamagnetic copper. NMR proton relaxation measurements show that neither Type 1 nor Type 2 copper binds easily with exchangable water (332).

It has been pointed out that Type 1 copper is in a rather unique environment (328,329,333), and this unique bonding to copper is responsible for the strong blue color of laccase (327). The reduction or denaturation of fungal laccase causes a loss of blue color and a change in the EPR signal due to Type 1 Cu(II) (332). EPR experiments have shown that *p*-diphenol reduces Type 1 Cu(II) more readily than Type 2 Cu(II) (332). Type 1 Cu(II) of fungal laccase (334), but not of *Rhus vernicifera* laccase (328), has an exceptionally high redox potential, $E°=0.767$ V at pH 6.2 (334). As judged by the EPR spectrum, the Type 1, but not Type 2, Cu(II) of fungal laccase can be reduced to Cu(I) with simultaneous loss of blue color by raising the pH from 6 to 9 (335). Only one oxidation equivalent is required to restore the blue color and the EPR spectrum of Type 1 Cu(II)

(336).

Type 2 Cu(II) does not contribute significantly to the optical spectrum of laccase. Under certain conditions Type 2 Cu(II) can be selectively removed from fungal laccase (337). The removal of Type 2 Cu(II) does not change the optical characteristics of Type 1 Cu(II), but the enzyme is almost completely devoid of activity (337). This indicates a necessary role for Type 2 Cu(II) in the catalytic function. Activity can be restored by incubating the partially copper-depleted enzyme with Cu(II) and ascorbate (337). Treatment of fungal laccase with azide does not affect the optical absorption band at 615 nm, but it does alter the EPR signal of the Type 2 Cu(II) (332). Several anions are known to bind to Type 2 Cu(II) of both fungal (332,338) and *Rhus vernicifera* (339) laccase, and these anions also inhibit the oxidase activity (332,338,339). This provides more support for the catalytic role of the Type 2 Cu(II). The EPR spectrum of the cyanide complex of Type 2 Cu(II) in fungal laccase has a hyperfine structure which indicates that the Type 2 Cu(II) may be coordinated to three or four nitrogen atoms (332,338).

Type 3 or diamagnetic copper in laccase could exist as Cu(I) or as two spin-paired Cu(II) ions. The first experimental evidence for two spin-paired Cu(II) ions came from the anaerobic titrations of fungal laccase (340). Type 1 Cu(II) could be fully reduced, but Type 2 Cu(II) could be only partially reduced. Since 3.7 equivalents of

electrons were required to reduce the enzyme, there must be two additional electron accepting sites. Electron accepting sites on the protein appeared unlikely, so the cupric-cupric pair was an attractive choice. The presence of a closely linked Cu(II) pair in laccase is supported by the finding that the closely related copper-containing protein ceruloplasmin has an EPR spectrum typical of a cupric-cupric pair when reduced and treated with nitric oxide (341). A degree of positive cooperativity among all four electron accepting sites was also noted (340). Type 1 Cu(II) could not be fully reduced until 3.7 equivalents of electrons were added, and the enzyme showed an increased affinity for the second and third electron. This two-electron accepting site in fungal laccase (342) and *Rhus vernicifera* laccase (343) has been associated with an intense absorption band at about 330 nm. The difference absorption spectrum of reduced relative to oxidized laccase has bands at 330 and 615 nm which are due to Type 3 and Type 1 copper, respectively. These two bands are reduced simultaneously with 3.5 equivalents of ascorbate (342). This indicates cooperativity between Type 1 and Type 3 copper. The redox potential of the two-electron accepting site in *Rhus vernicifera* laccase is 0.782 V at pH 5.5 (344). At high pH where Type 1 Cu(II) of fungal laccase is reduced, the two-electron accepting site can be reduced by two electrons from octacyanotungstate(IV) (336).

Cooperativity between Type 2 and Type 3 copper has been noted during the anaerobic reduction of fungal laccase B

(345). The rate of oxidation by molecular oxygen of Type 2 and Type 3 copper is similar, and their rate of oxidation change in a similar manner as a function of pH (345). Super-hyperfine lines in the high-field part of the EPR spectrum of partially reduced Type 2 copper indicated that Type 2 copper is ligated with nitrogen (345). Neither anaerobic reduction of fungal laccase A by ferrocyanide and *p*-diphenol nor its reoxidation by molecular oxygen follows second-order kinetics (346). The Type 1 copper is only reoxidized by molecular oxygen after the other sites are reduced. The kinetic results are consistent with a mechanism involving the cooperation of several electron accepting sites (346). The kinetics of the anaerobic reduction of fungal laccase B by *p*-diphenol, ascorbate, or ferrocyanide show a second-order reduction of the Type 1 Cu(II) (347). The rate of reduction of Type 3 copper, which is associated with the absorption band at 330 nm, is independent of the substrate concentration (347). This rate may be limited by a transition within the laccase molecule. The rate of Type 3 copper reduction is inhibited by fluoride (347), an anion which selectively binds to Type 2 copper (338). It appears that Type 2 Cu(II) is a redox mediator between Type 1 and Type 3 copper. For example, nearly four equivalents of electrons are required to fully reduce Type 1 Cu(II) to Cu(I) (340). The reducing substrate may initially transfer an electron to Type 1 Cu(II), and this electron may proceed to Type 3 copper via Type 2 copper. The binding of anions to Type 2 Cu(II) (332,338) inhibits

laccase perhaps by inhibiting the rate limiting mediator function of Type 2 copper.

The mechanism of reoxidation of laccase by molecular oxygen is an interesting aspect of this enzyme. The reduction of molecular oxygen to water occurs in cell respiration and is a very important biochemical process. A comparison of the experimental evidence for the reoxidation of laccase and the modes of reduction of molecular oxygen may suggest a reasonable pathway for this reaction.

Oxygen is a good oxidizing agent from the thermodynamic point of view, but, depending upon its environment, it is

[7] $\frac{1}{4}O_2 + e^- + H^+ = \frac{1}{2}H_2O$ $E°=0.82$ V at pH 7

often rather inert kinetically. Equations [8] to [11] summa-

				E°, pH 7
[8]	$O_2 + e^-$	=	O_2^-	-0.45 V
[9]	$O_2^- + e^- + 2H^+$	=	H_2O_2	0.98 V
[10]	$H_2O_2 + e^- + H^+$	=	$H_2O + HO\cdot$	0.38 V
[11]	$HO\cdot + e^- + H^+$	=	H_2O	2.33 V

rise four possible stages for the reduction of molecular oxygen. (The values of E° are from reference 348.) Mechanistic conclusions cannot be deduced from half-cell potentials. However, the last free radical intermediate, HO·, is extremely reactive and may lead to side reactions which appear not to be observed. The presence of HO· will not occur if

the reduction of oxygen to water occurs via two double-electron transfers, Equations [12] and [13].

			E°, pH 7
[12]	$\frac{1}{2}O_2 + e^- + H^+$	$= \frac{1}{2}H_2O_2$	0.27 V
[13]	$\frac{1}{2}H_2O_2 + e^- + H^+$	$= H_2O$	1.35 V

The two double-electron transfers from the reduced form of laccase may be possible via the cooperative nature of the oxidation-reduction sites in the enzyme. This is in accord with the kinetic studies which showed the Type 1 Cu(I) is only reoxidized by molecular oxygen when the other sites in the enzyme are reduced (346). The first intermediate produced by the first double-electron transfer is hydrogen peroxide. From EPR studies it was deduced that hydrogen peroxide binds to the Type 2 Cu(II) in native fungal laccase and causes the appearance of a new optical absorption band at 400 nm (350). An intermediate has been found in the reoxidation of fungal laccase by molecular oxygen (351). The optical and EPR properties of this new intermediate are similar to those of the complex between Type 2 Cu(II) and hydrogen peroxide. The detection of bound hydrogen peroxide as an intermediate does not help to decide the question of a four or two step reduction of molecular oxygen since hydrogen peroxide would be present from either mechanism.

Tripositive copper, Cu(III), may be a possible oxidation state in some copper-containing oxidases. Cu(III) bound to the protein of the enzyme may be relatively stable since it

is quite stable when bound to deprotonated peptides in aqueous solution (352). D-galactose oxidase may involve Cu(III) in its catalytic cycle (353,354).

1.6 References

1. Lascelles, J. (1964) in Tetrapyrrole Biosynthesis and its Regulation pp. 17-37, Benjamin, New York
2. Yamazaki, I. (1974) in Molecular Mechanisms of Oxygen Activation (Hayaishi, O., ed) pp. 551-553, Academic Press, New York
3. de Due, C. (1974) in Alcohol and Aldehyde Metabolizing Systems (Thurman, R.G., Yonetani, T., Williamson, J.R., and Chance, B., eds) pp. 161-168, Academic Press, New York
4. Thomson, R.H. (1964) in Biochemistry of Phenolic Compounds (Harborne, J.B., ed) pp. 1-32, Academic Press, New York
5. Brown, B.R. (1967) in Oxidative Coupling of Phenols Taylor, W.I., and Battersby, A.R., eds) Vol. 1, pp. 167-201, Marcel Dekker, New York
6. Neish, A.C. (1968) in Constitution and Biosynthesis of Lignin (Kleinzeller, A., Springer, G.F., and Wittman, H.G., eds) pp. 30-31, Springer-Verlag, New York
7. Williams, A.H. (1963) in Enzyme Chemistry of Phenolic Compounds, Proceedings of the Plant Phenolics Group Symposium (Pridham, J.B., ed) pp. 87-95, Pergamon, New York

8. Schonbein, C.F. (1855) *Verh. Naturf. Ges. Basel* 1, 339-373

9. Linossier, M.G.C.R. (1898) *Soc. Biol. Paris* 50, 373-375

10. Bach, A.N., and Chodat, R. (1903) *Ber. Dtsch. Chem. Ges.* 36, 606-608

11. Willstäter, R., and Polinger, A. (1923) *Liebigs. Annln.* 430, 269-319

12. Saunders, B.C., Holmes-Siedle, A.-G., and Stark, B.P. (1964) in Peroxidase, Butterworths, London

13. Paul, K.-G., and Stigbrand, T. (1970) *Acta Chem. Scand.* 24, 3607-3617

14. Keilin, D., and Hartree, E.F. (1951) *Biochem. J.* 49, 88-104

15. Cecil, R., and Ogston, A.G. (1951) *Biochem. J.* 49, 105-106

16. Shannon, L.M., Kay, E., and Lew, J.Y. (1966) *J. Biol. Chem.* 241, 2166-2172

17. Klapper, M.H., and Hackett, D.P. (1965) *Biochim. Biophys. Acta* 96, 272-282

18. Theorell, H. (1942) *Arkiv. Kemi* 16A, No. 2

19. Theorell, H. (1941) *Enzymologia* 10, 250-252

20. Delincee, H., and Radola, B.J. (1970) *Biochim. Biophys. Acta* 200, 404-407

21. Chance, B. (1952) *Arch. Biochem. Biophys.* 37, 235-239

22. George, P. (1952) *Nature* 169, 612-613

23. George, P. (1953) *Biochem. J.* 54, 267-276

24. Theorell, H., and Ehrenberg, A. (1952) *Arch. Biochem. Biophys.* 41, 442-461

25. Hartree, E.F. (1946) *Ann. Rept. Progr. Chem. (Chem. Soc. London)* 43, 287-296

26. Tamura, M. (1971) *Biochim. Biophys. Acta* 243, 249-258

27. Osbar, A.J., and Eichhorn, G.L. (1962) *J. Biol. Chem.* 237, 1820-1824

28. Ellis, W.D., and Dunford, H.B. (1968) *Can. J. Biochem.* 46, 1231-1235.

29. Strickland, E.H., Kay, E., Shannon, L.M., and Horwitz, J. (1968) *J. Biol. Chem.* 243, 3560-3565

30. Blumberg, W.E., Peisach, J., Wittenberg, B.A., and Wittenberg, J.B. (1968) *J. Biol. Chem.* 243, 1854-1862

31. Douzou, P., and Leterrier, F. (1970) *Biochim. Biophys. Acta* 220, 338-340

32. Welinder, K.G., Smillie, L.B., and Schonbaum, G.R. (1972) *Can. J. Biochem.* 50, 44-62

33. Welinder, K.G., and Smillie, L.B. (1972) *Can. J. Biochem.* 50, 63-90

34. Welinder, K.G. (1973) *F.E.B.S. Lett.* 30, 243-245

35. Welinder, K.G., and Mazza, G. (1975) *Eur. J. Biochem.* 57, 415-424

36. Moss, T.H., Bearden, A.J., Bartsch, R.G., and Cusanovich, M.A. (1968) *Biochemistry* 7, 1583-1590

37. Lang, G., and Marshall, W. (1966) *Proc. Phys. Soc. (London)* 87, 3-34

38. Theorell, H. (1943) *Ark. Kem. Min. Geol.* 16, No. 14

39. Brill, A.S., and Williams, R.J.P. (1961) *Biochem. J.* 78, 246-253

40. Brill, A.S., and Sandberg, H.E. (1968) *Biophys. J.* 8, 669-690

41. Brill, A.S., and Sandberg, H.E. (1968) *Biochemistry* 7, 4254-4260

42. Mauk, M.R., and Girotti, A.W. (1974) *Biochemistry* 13, 1757-1763

43. Yonetani, T., Yamamoto, H., Erman, J.E., Leigh, Jr. J.S., and Reed, G.H. (1972) *J. Biol. Chem.* 247, 2447-2455

44. Williams, R.J.P., Wright, P.E., Mazza, G. and Ricard, J. (1975) *Biochim. Biophys. Acta* 412, 127-147

45. McDonald, C.C., and Philips, W.D. (1973) *Biochemistry* 12, 3170-3186

46. Chance, B. (1952) *Arch. Biochem. Biophys.* 40, 153-164

47. Harbury, H.A. (1957) *J. Biol. Chem.* 225, 1009-1024

48. George, P., and Lyster, R.L.J. (1958) *Proc. Nat. Acad. Sci.* 44, 1013-1039

49. Ellis, W.D., and Dunford, H.B. (1969) *Arch. Biochem. Biophys.* 133, 313-317

50. Ricard, J., Mazza, G., and Williams, R.J.P. (1972) *Eur. J. Biochem.* 28, 566-578

51. Lanir, A., and Schejter, A. (1975) *Biochem. Biophys. Res. Commun.* 62, 199-203

52. Vuk-Pavlovic, S., and Benko, B. (1975) *Biochem. Biophys. Res. Commun.* 66, 1154-1159

53. Burns, P.S., Dwek, R.A., Williams, R.J.P., and Wright, P.E. (1975) *Biochim. Biophys. Acta* 'submitted for publication'

54. Teale, F.W.J. (1959) *Biochim. Biophys. Acta* 35, 543

55. Tamura, M., Asakura, T., and Yonetani, T. (1972) *Biochim. Biophys. Acta* 268, 292-304

56. Spiro, T.G. (1975) *Biochim. Biophys. Acta* 416, 169-189

57. Strekas, T.C., and Spiro, T.G. (1972) *Biochim. Biophys. Acta* 263, 830-833

58. Strekas, T.C., and Spiro, T.G. (1972) *Biochim. Biophys. Acta* 278, 188-192

59. Rakshit, G., and Spiro, T.G. (1974) *Biochemistry* 13, 5317-5323

60. Altschul, A.M., Abrams, R., and Hogness, T.R. (1940) *J. Biol. Chem.* 136, 777-794

61. Ellfolk, N. (1967) *Acta Chem. Scand.* 21, 175-181

62. Ellfolk, N. (1967) *Acta Chem. Scand.* 21, 1921-1924

63. Yonetani, T., and Ray, G.S. (1965) *J. Biol. Chem.* 240, 4503-4508

64. Yonetani, T., Chance, B., and Kajiwara, S. (1966) *J. Biol. Chem.* 241, 2981-2982

65. Yonetani, T. (1967) *J. Biol. Chem.* 242, 5008-5013

66. Ellfolk, N. (1967) *Acta Chem. Scand.* 21, 2736-2742

67. Yonetani, T. (1970) in Advances in Enzymology (Nord, F.F., ed) Vol. 33, pp. 309-335, Interscience, New York

68. Chance, B. (1951) in Enzymes and Enzyme Systems (Edsall, J.T., ed) pp. 93-104, Harvard University Press, Cambridge

69. Nicholls, P., and Mochan, E. (1971) *Biochem. J.* 121, 55-67

70. Mochan, E., and Nicholls, P. (1971) *Biochem. J.* 121, 69-82

71. Yamanaka, T. (1972) *Ann. Rep. Biol. Works, Fac. Sci. Osaka Univ.* 19, 75-87

72. Gupta, R.K., and Yonetani, T. (1973) *Biochim. Biophys. Acta* 292, 502-508

73. Vanderkooi, J., and Erecinska, M. (1974) *Arch. Biochem. Biophys.* 162, 385-391

74. George, P. (1953) *Biochem. J.* 55, 220-230

75. Coulson, A.F.W., Erman, J.E., and Yonetani, T. (1971) *J. Biol. Chem.* 246, 917-924

76. Yonetani, T., and Ehrenberg, A. (1967) in Magnetic Resonance in Biological Systems (Ehrenberg, A., Malmström, B.G., and Vänngård, T., eds) pp. 155-158, Pergamon Press, New York

77. Yonetani, T., Wilson, D.F., and Seamonds, B. (1966) *J. Biol. Chem.* 241, 5347-5352

78. Iizuka, T., Masao, K., and Yonetani, T. (1968) *Biochim. Biophys. Acta* 167, 257-267

79. Yonetani, T., Schleyer, H., and Ehrenberg, A. (1966) *J. Biol. Chem.* 241, 3240-3243

80. Rein, H., and Ristau, O. (1965) *Biochim. Biophys. Acta* 94, 516-524

81. Wittenberg, B.A., Kampa, L., Wittenberg, J.B., Blumberg, W.E., and Peisach, J. (1968) *J. Biol. Chem.* 243, 1863-1870

82. Yonetani, T., and Asakura, T. (1968) *J. Biol. Chem.* 243, 4715-4721

83. Asakura, T., and Yonetani, T. (1969) *J. Biol. Chem.* 244, 4573-4579

84. Asakura, T., and Yonetani, T. (1969) *J. Biol. Chem.* 244, 537-544

85. Yonetani, T., and Asakura, T. (1969) *J. Biol. Chem.* 244, 4580-4588

86. Yamazaki, I., Fujinaga, K., Takehara, I., and Takahashi, H. (1956) *J. Biochem.* 43, 377-386

87. Hosoya, T. (1960) *J. Biochem.* 47, 369-381

88. Mazza, G., Charles, C., Bouchet, M., Ricard, J., and Raynaud, J. (1968) *Biochim. Biophys. Acta* 167, 89-98

89. Mazza, G., Job, C., and Bouchet, M. (1973) *Biochim. Biophys. Acta* 322, 218-223

90. Smith, D.W., and Williams, R.J.P. (1970) *Struct. Bonding* 7, 1-45

91. Henry, Y., and Mazza, G. (1974) *Biochim. Biophys. Acta* 371, 14-19

92. Morita, Y., and Kameda, K. (1957) *Mem. Res. Inst. Food Sci., Kyoto Univ.* 12, 1-13

93. Morita, Y. (1957) *Koso Kagaku Shinpojiumu* 12, 98-103

94. Morita, Y., Yoshida, C., and Kitamura, I. (1970) *Agr. Biol. Chem.* 34, 1191-1197

95. Morita, Y., and Kameda, K. (1957) *Mem. Res. Inst. Food Sci., Kyoto Univ.* 12, 14-23

96. Morita, Y., Kameda, K., and Mizuno, M. (1961) *Agr. Biol. Chem.* 25, 136-140

97. Morita, Y., and Kameda, K. (1962) *Mem. Res. Inst. Food Sci., Kyoto Univ.* 24, 1-12

98. Morita, Y., and Kameda, K. (1959) *Bull. Agr. Chem. Soc. Japan* 23, 28-33

99. Morita, Y., and Kameda, K. (1958) *Mem. Res. Inst. Food Sci., Kyoto Univ.* 14, 61-76

100. Morita, Y., and Kameda, K. (1958) *Mem. Res. Inst. Food Sci., Kyoto Univ.* 14, 49-60

101. Morita, Y., Shimizu, K., and Kada, N. (1968) *Agr. Biol. Chem.* 32, 671-677

102. Morita, Y., and Yoshida, C. (1970) *Agr. Biol. Chem.* 34, 590-598

103. Yoshida, C., and Morita, Y. (1970) *Mem. Res. Inst. Food Sci., Kyoto Univ.* 31, 1-9

104. Morita, Y., and Mason, H.S. (1965) *J. Biol. Chem.* 240, 2654-2659

105. Maeda, Y., Higashimura, T., and Morita, Y. (1967) *Biochem. Biophys. Res. Commun.* 29, 362-367

106. Maeda, Y. (1968) *J. Phys. Soc. Japan* 24, 151-159

107. Hamaguchi, K., Ikeda, K., Yoshida, C., and Morita, Y. (1969) *J. Biochem.* 66, 191-201

108. Hager, L.P. (1970) in Methods in Enzymology (Colowick, S.P., and Kaplan, N.O., eds) Vol. 17 Part A, pp. 648-652, Academic Press, New York

109. Morris, D.R., and Hager, L.P. (1966) *J. Biol. Chem.* 241, 1763-1768

110. Shaw, P.D., and Hager, L.P. (1961) *J. Biol. Chem.* 236, 1626-1630

111. Hager, L.P., Morris, D.R., Brown, F.S., and Eberwein, H. (1966) *J. Biol. Chem.* 241, 1769-1777

112. Thomas, J.A., Morris, D.R., and Hager, L.P. (1970) *J. Biol. Chem.* 245, 3129-3134

113. Thomas, J.A., Morris, D.R., and Hager, L.P. (1970) *J. Biol. Chem.* 245, 3135-3142

114. Thomas, J.A., and Hager, L.P. (1968) *Biochem. Biophys. Res. Commun.* 32, 770-775

115. Brown, F.S., and Hager, L.P. (1967) *J. Am. Chem. Soc.* 89, 719-720

116. Thomas, J.A., and Hager, L.P. (1969) *Biochem. Biophys. Res. Commun.* 35, 444-450

117. Jone, C., and Hager, L.P. (1976) *Biochem. Biophys. Res. Commun.* 68, 16-20

118. Champion, P.M., Münck, E., Debrunner, P.G., Hollenberg, P.F., and Hager, L.P. (1973) *Biochemistry* 12, 426-435

119. Stern, J.O., and Peisach, J. (1974) *J. Biol. Chem.* 249, 7495-7498

120. Hollenberg, P.F., and Hager, L.P. (1973) *J. Biol. Chem.* 248, 2630-2633

121. Collman, J.R., Sorrell, T.N., and Hoffman, B.M. (1975) *J. Am. Chem. Soc.* 97, 913-914

122. Koch, S., Tang, S.C., Holm, R.H., and Frankel, R.B. (1975) *J. Am. Chem. Soc.* 97, 914-916

123. Koch, S., Tang, S.C., Holm, R.H., Frankel, R.B., and Ibers, J.A. (1975) *J. Am. Chem. Soc.* 97, 916-918

124. Chiang, R., Makino, R., Spomer, W.E., and Hager, L.P. (1975) *Biochemistry* 14, 4166-4171

125. Champion, P.M., Liscomb, J.D., Münck, E., Debrunner, P., and Gunsalas, I.C. (1975) *Biochemistry* 14, 4151-4158

126. Champion, P.M., Chiang, R., Münck, E., Debrunner, P., and Hager,L.P. (1975) *Biochemistry* 14, 4159-4166

127. Dawson, J.H., Trudell, J.R., Barth, G., Linder, R.E., Bunnenberg, R.E., Djerassi, C., Chiang, R., and Hager, L.P. (1976) *J.Am. Chem. Soc.* 98, 3709-3710

128. Theorell, H., and Åkeson, Å. (1943) *Arkiv Kemi, Minerol. Geol.* 17B, No. 7

129. Morrison, M., Allen, P.Z., Bright, J., and Jayasinghe, W. (1965) *Arch. Biochem. Biophys.* 111, 126-133

130. Morrison, M., and Allen, P.Z. (1966) *Science* 152, 1626-1628

131. Rombauts, W.A., Schroeder, W.A., and Morrison, M. (1967) *Biochemistry* 6, 2965-2977

132. Maguire, R.J., and Dunford, H.B. (1971) *Can. J. Chem.* 49, 666-670

133. Morell, D.B. (1953) *Austral. J. Exp. Biol.* 31, 567-572

134. Hultquist, D.E., and Morrison, M. (1963) *J. Biol. Chem.* 238, 2843-2846

135. Morell, D.B., and Clezy, P.S. (1963) *Biochim. Biophys. Acta* 71, 157-164

136. Carlström, A. (1969) *Acta Chem. Scand.* 23, 203-313

137. Chang, J.Y., and Schroeder, W.A. (1973) *Arch. Biochem. Biophys.* 156, 475-479

138. Bayse, G.S., and Morrison, M (1971) *Arch. Biochem. Biophys.* 145, 143-148

139. Hosoya, T., and Morrison, M (1967) *Biochemistry* 6, 1021-1026

140. Morrison, M., Rombauts, W.A., and Schroeder, W.A. (1966) in Hemes and Hemoproteins (Chance, B., Estabrook, R.W., and Yonetani, T., eds) pp. 345-348, Academic Press, New York

141. Bayse, G.S., Michaels, A.W., and Morrison, M (1972) *Biochim. Biophys. Acta* 284, 30-33

142. David, G.S., and Reisfeld, R.A. (1974) *Biochemistry* 13, 1014-1021

143. Marchalonis, J.J., Cone, R.E., and Santer, V. (1971) *Biochem. J.* 124, 921-927

144. Arntzen, C.J., Armond, P.A., Zettinger, C.S., Vernotte, C., and Briantais, J.M. (1974) *Biochim. Biophys. Acta* 347, 329-339

145. Barber, A.J., and Jamieson G.A. (1971) *Biochemistry* 10, 4711-4717

146. Nachman, R.L., Hubbard, A., and Ferris, B. (1973) *J. Biol. Chem.* 248, 2928-2936

147. Phillips, D.R., and Morrison, M. (1971) *Biochemistry* 10, 1766-1771

148. Shin, B.C., and Carraway, K.L. (1974) *Biochim. Biophys. Acta* 345, 141-153

149. Bayse, G.S., Michaels, A.W., and Morrison, M. (1972) *Biochim. Biophys. Acta* 284, 34-42

150. Levitt, A.E. (1969) *Chem. Eng. News* Sept. 22, 38-39

151. Hogg, D.McC., and Jago, G.R. (1970) *Biochem. J.* 117, 779-790

152. Jone, C., and Hager, L.P. (1976) *Biochem. Biophys. Res. Commun.* 68, 16-20

153. DeGroot, L.J., and Dunn, A.D. (1964) *Biochim. Biophys. Acta* 92, 205-222

154. Yip, C.C. (1966) *Biochim. Biophys. Acta* 128, 262-271

155. DeGroot, L.J., and Davis, A.M. (1962) *Endocrinology* 70, 505-510

156. Hosoya, T., and Morrison, M. (1967) *J. Biol. Chem.* 242, 2828-2836

157. Taurog, A., Lothrop, M.L., and Estabrook, R.W. (1970) *Arch. Biochem. Biophys.* 139, 221-229

158. Danner, D.J., and Morrison, M. (1971) *Biochim. Biophys. Acta* 235, 44-51

159. Krinsky, M.M., and Alexander, N.M. (1971) *J. Biol. Chem.* 246, 4755-4758

160. Coval, M.L., and Taurog, A. (1967) *J. Biol. Chem.* 242, 5510-5523

161. Taurog, A. (1970) in Recent Progress in Hormone Research (Astwood, E.B., ed) Vol. 26, pp. 189-247, Academic Press, New York

162. Hosoya, T., Matsukawa, S., and Nagai, Y. (1971) *Biochemistry* 10, 3086-3093

163. Fawcett, D.M., and McLeod, L.E. (1963) *Endocrinology* 73, 279-284

164. Neary, J.T., Armstrong, A., Davidson, B., Maloof, F., and Soodak, M. (1975) *Biochim. Biophys. Acta* 379, 262-270

165. Neary, J.T., Davidson, B., Armstrong, A., Strout, H.V., Maloof, F., and Soodak, M. (1976) *J. Biol. Chem.* 251, 2525-2529

166. Hosoya, T. (1968) *Gumma Symp. Endocrinol., Proc.* 5, 219-230

167. Deme, D., Fimiani, E., Pommier, J., and Nunez, J. (1975) *Eur. J. Biochem.* 51, 329-336

168. Taurog, A. (1970) *Arch. Biochem. Biophys.* 139, 212-220

169. Krinsky, M.M., and Fruton, J.S. (1971) *Biochem. Biophys. Res. Commun.* 43, 935-940

170. Agner, K. (1941) *Acta Physiol. Scand.* 2, Suppl. 8, 1-62

171. Schultz, J., and Kaminker, K. (1962) *Arch. Biochem. Biophys.* 96, 465-467

172. Schultz, J., Corlin, R., Oddi, F., Kaminker, K., and Jones, W. (1965) *Arch. Biochem. Biophys.* 111, 73-79

173. Schultz, J., Gordon, A., and Shay, H. (1957) *J. Am. Chem. Soc.* 79, 1632-1635

174. Newton, N., Morell, D.B., and Clarke, L. (1965) *Biochim. Biophys. Acta* 96, 463-475

175. Himmelhoch, S.R., Evans, W.H., Mage, M.G., and Peterson, E.A. (1969) *Biochemistry* 8, 914-921

176. Agner, K. (1958) *Acta Chem. Scand.* 12, 89-94

177. Ehrenberg, A., and Agner, K. (1958) *Acta Chem. Scand.* 12, 95-100

178. Odajima, T., and Yamazaki, I. (1972) *Biochim. Biophys. Acta* 284, 360-367

179. Schultz, J., and Shmukler, H.W. (1964) *Biochemistry* 3, 1234-1238

180. Felberg, N.T., Putterman, G.J., and Schultz, J. (1969) *Biochem. Biophys. Res. Commun.* 37, 213-218

181. Felberg, N.T., and Schultz, J (1972) *Arch. Biochem. Biophys.* 148, 407-413

182. Felberg, N.T., and Schultz, J. (1968) *Anal. Biochem.* 23, 241-246

183. Schultz, J., Felberg, N., and John, S. (1967) *Biochem. Biophys. Res. Commun.* 28, 543-549

184. Ehrenberg, A. (1962) *Arkiv Kemi* 19, 119-128

185. Nicholls, P. (1961) *Biochem. J.* 81, 374-383

186. Newton, N., Morell, D.B., and Clarke, L. (1965) *Biochim. Biophys. Acta* 96, 476-486

187. Odajima, T., and Yamazaki, I. (1972) *Biochim. Biophys. Acta* 284, 368-374

188. Agner, K (1943) in Advances in Enzymology (Nord, F.F., and Werkman, C.H., eds) Vol. 3, pp. 137-148, Interscience, New York

189. Nichol, A.W., Morell, D.B., and Thomson, J. (1969) *Biochem. Biophys. Res. Commun.* 36, 576-581

190. Wu, N.C., and Schultz, J. (1975) *F.E.B.S. Lett.* 60, 141-144

191. Schultz, J. (1970) in Biochemistry of the Phagocytic Process pp. 89-129, North-Holland, London

192. Klebanoff, S.J. (1968) *J. Bacteriol.* 95, 2131-2138

193. Klebanoff, S.J. (1970) *Science* 169, 1095-1097

194. Klebanoff, S.J. (1974) *J. Biol. Chem.* 249, 3724-3728

195. Rotilio, G., Falcioni, G., Fioretti, E., and Brunori, M. (1975) *Biochem. J.* 145, 405-407

196. Wittenberg, J.B., Noble, R.W., Wittenberg, B.A., Antonini, E., Brunori, M., and Wyman, J. (1967) *J. Biol. Chem.* 242, 626-634

197. George, P. (1953) *J. Biol. Chem.* 201, 427-434

198. Yamada, H., and Yamazaki, I. (1974) *Arch. Biochem. Biophys.* 165, 728-738

199. Yamada, H., Makino, R., and Yamazaki, I. (1975) *Arch. Biochem. Biophys.* 169, 344-353

200. Makino, R., Chiang, R., and Hager, L.P. (1976) 'submitted for publication'

201. Odajima, T., and Yamazaki, I. (1970) *Biochim. Biophys. Acta* 206, 71-77

202. Keilin, D., and Mann, T (1937) *Proc. Roy. Soc. B (London)* 122, 119-133

203. Keilin, D., and Hartree, E.F. (1955) *Biochem. J.* 61, 153-171

204. Kertesz, D., Antonini, E., Brunori, M., Wyman, J., and Zito, R. (1965) *Biochemistry* 4, 2672-2676

205. Phelps, C., Antonini, E., and Brunori, M. (1971) *Biochem. J.* 122, 79-87

206. Nozawa, T., Kobayashi, N., and Hatano, M. (1976) *Biochim. Biophys. Acta* 427, 652-662

207. Hayashi, Y., Yamada, H., and Yamazaki, I. (1976) *Biochim. Biophys. Acta* 427, 608-616

208. Yamada, H., and Yamazaki, I. (1975) *Arch. Biochem. Biophys.* 171, 737-744

209. Chance, B. (1949) *Arch. Biochem. Biophys.* 21, 416-430

210. Chance, B. (1952) *Arch. Biochem. Biophys.* 41, 404-415

211. Swendin, B., and Theorell, H. (1940) *Nature* 145, 71-72

212. Chance, B. (1952) *J. Biol. Chem.* 197, 577-589

213. Yamazaki, I., and Piette, L.H. (1963) *Biochim. Biophys. Acta* 77, 47-64

214. Yamazaki, I., and Yokota, K. (1965) *Biochem. Biophys. Res. Commun.* 19, 249-254

215. Ricard, J., and Nari, J. (1967) *Biochim. Biophys. Acta* 132, 321-329

216. Ricard, J., and Job, D. (1974) *Eur. J. Biochem.* 44, 359-374

217. Nakamura. S., and Yamazaki, I. (1969) *Biochim. Biophys. Res. Commun.* 189, 29-37

218. Balny, C., and Douzou, P. (1974) *Biochem. Biophys. Res. Commun.* 56, 386-391

219. Odajima, T., and Yamazaki, I. (1972) *Biochim. Biophys. Acta* 284, 355-359

220. Yokota, K., and Yamazaki, I. (1965) *Biochem. Biophys. Res. Commun.* 18, 48-53

221. Tamura, M., and Yamazaki, I. (1972) *J. Biochem.* 71, 311-319

222. Peisach, J., Blumberg, W.E., Wittenberg, B.A., and Wittenberg, J.B. (1968) *J. Biol. Chem.* 243, 1871-1880

223. Noble, R.W., and Gibson, Q.H. (1970) *J. Biol. Chem.* 245, 2409-2413

224. Phelps, C.F., Antonini,E., Giacometti, G., and Brunori, M. (1974) *Biochem. J.* 141, 265-272

225. Makino, R., Yamada, H., and Yamazaki, I. (1976) *Arch. Biochem. Biophys.* 173, 66-70

226. Brill, A.S. (1966) in Comprehensive Biochemistry (Florkin, M., and Stotz, E.H., eds) Vol. 14, pp. 447-479, Elsevier, Amsterdam

227. Tamura, M. (1971) *Biochim. Biophys. Acta* 243, 239-248

228. Lang, G., Asakura, T., and Yonetani, T. (1969) *J. Phys. C* 2, 2246-2261

229. Morell, D.B. (1954) *Biochem. J.* 56, 683-690

230. Krejcarek, G.E., Bryant, R.G., Smith, R.J., and Hager, L.P. (1976) *Biochemistry* 15, 2508-2511

231. George, P., and Hanania, G. (1952) *Biochem. J.* 52, 517-523

232. Epstein, N., and Shejter, A. (1972) *F.E.B.S. Lett.* 25, 46-48

233. Critchlow, J.E., and Dunford, H.B. (1972) *J. Theor. Biol.* 37, 307-320

234. Dunford, H.B., Critchlow, J.E., Maguire, R.J., and Roman, R. (1974) *J. Theor. Biol.* 48, 283-298

235. Ellis, W.D., and Dunford, H.B. (1968) *Biochemistry* 7, 2054-2062

236. Dunford, H.B., and Alberty, R.A. (1967) *Biochemistry* 6, 447-451

237. Dolman, D., Dunford, H.B., Chowdhury, D.M. and Morrison, M. (1968) *Biochemistry* 7, 3991-3996

238. Job, D., and Ricard, J. (1975) *Arch. Biochem. Biophys.* 170, 427-437

239. Erman, J.E. (1974) *Biochemistry* 13, 34-39

240. Erman, J.E. (1974) *Biochemistry* 13, 39-44

241. Chance, B. (1952) *Arch. Biochem. Biophys.* 41, 416-424

242. Chance, B. (1943) *J. Biol. Chem.* 151, 553-577

243. Chance, B. (1948) *Nature* 161, 914-917

244. Chance, B. (1949) *Science* 109, 204-208

245. Chance, B. (1949) *Arch. Biochem. Biophys.* 24, 389-409

246. Chance, B. (1949) *Arch. Biochem. Biophys.* 24, 410-421

247. George, P. (1953) *J. Biol. Chem.* 201, 413-426

248. George, P. (1953) *Science* 117, 220-221

249. Chance, B. (1952) *Arch. Biochem. Biophys.* 41, 425-431

250. Theorell, H., Ehrenberg, A., and Chance, B. (1952) *Arch. Biochem. Biophys.* 37, 237-239

251. Felton, R.H., Owen, G.S., Dolphin, D., and Fajer, J. (1971) *J. Am. Chem. Soc.* 93, 6332-6334

252. Brill, A.S., and Williams, R.J.P. (1961) *Biochem. J.* 78, 253-262

253. Aasa, R., Vänngård, T., and Dunford, H.B. (1975) *Biochim. Biophys. Acta* 391, 259-264

254. Weinryb, I. (1968) *Biochem. Biophys. Res. Commun.* 31, 110-112

255. Dolphin, D., Forman, A., Borg, D.C., Fajer, J., and Felton R.H. (1971) *Proc. Nat. Acad. Sci. U.S.* 68, 614-618

256. Maeda, Y., and Morita, Y. (1967) *Biochem. Biophys. Res. Commun.* 29, 680-685

257. Moss, T.H., Ehrenberg, A., and Bearden A.J. (1969) *Biochemistry* 8, 4159-4162

258. Felton, R.H., Romans, A.Y., Nai-Teng, Y., and Schonbaum, G.R. (1976) *Biochim. Biophys. Acta* 434, 82-89

259. Dolphin, D., and Felton, R.H. (1974) *Acc. Chem. Res.* 7, 26-32

260. Stillman, J.S., Stillman, M.J., and Dunford, H.B. *Biochem. Biophys. Res. Commun.* 63, 32-35

261. Stillman, J.S., Stillman,M.J., and Dunford, H.B. *Biochemistry* 14, 3183-3188

262. Dunford, H.B., and Stillman, J.S. (1976) *Coord. Chem. Rev.* 19, 187-251

263. Chu, M., Dunford, H.D., and Job, D. (1976) 'submitted for publication'

264. Yonetani, T. (1965) *J. Biol. Chem.* 240, 4059-4514

265. Yonetani, T. (1966) *J. Biol. Chem.* 241, 2562-2571

266. Coulson, A.F.W., and Yonetani, T. (1975) *Biochemistry* 14, 2389-2396

267. Yonetani, T., Schleyer, H., and Chance, B. (1966) *Science* 152, 678

268. Yonetani, T., Schleyer, H., and Ehrenberg, A. (1966) in Magnetic Resonance in Biological Systems (Ehrenberg, A., Malmström, B., and Vänngård, T., eds) pp. 151-158, Pergamon, Oxford

269. Iizuka, T., Kotani, M., and Yonetani, T. (1968) *Biochim. Biophys. Acta* 167, 257-267

270. Jordi, H.C., and Erman, J.E. (1974) *Biochemistry* 13, 3734-3745

271. Hager, L.P., Doubek, D.L., Silverstein, R.M., Hargis, J.H., and Martin, J.C. (1972) *J. Am. Chem. Soc.* 94, 4364-4366

272. Schonbaum, G.R., and Lo, S. (1972) *J. Biol. Chem.* 247, 3353-3360

273. Hager, L.P., Doubek, D.L., Silverstein, R.M., Lee, T.T., Thomas, J.A., Hargis, J.H., and Martin, J.C. (1973) in Oxidases and Related Redox Systems (King, T.E., Mason, H.S., and Morrison, M., eds) pp. 311-332, University Park Press, Baltimore

274. Hager, L.P., Hollenberg, P.F., Rand-Meir, T., Chiang, R., and Doubek, D.L. (1975) *Ann. N.Y. Acad. Sci.* 244, 80-93

275. Critchlow, J.E., and Dunford, H.B. (1973) in Oxidases and Related Redox Systems (King, T.E., Mason, H.S., and Morrison, M. eds) pp. 355-366, University Park Press, Baltimore

276. Chance, B. (1950) *J. Am. Chem. Soc.* 72, 1577-1583

277. Maguire, J.R., Dunford, H.B., and Morrison, M. (1973) *Can. J. Biochem.* 49, 1165-1171

278. Loo, S., and Erman, J.E. (1975) *Biochemistry* 14, 3467-3470

279. Dolman, D., Newell, G.A., Thurlow, M.D., and Dunford, H.B. (1975) *Can. J. Biochem.* 53, 495-501

280. Davies, D.M., Jones, P., and Mantle, D. (1976) *Biochem. J.* 157, 247-253

281. Maguire, J.R., and Dunford, H.B. (1972) *Biochemistry* 11, 937-941

282. Maguire, J.R., and Dunford, H.B. (1973) *Can. J. Chem.* 51, 1721-1723

283. Roman, R., and Dunford, H.B. (1972) *Biochemistry* 11, 2076-2082

284. Roman, R., Dunford, H.B., and Evett, M. (1971) *Can. J. Chem.* 49, 3059-3063

285. Hasinoff, B.B., and Dunford, H.B. (1970) *Biochemistry* 9, 4930-4939

286. Cotton, M.L., and Dunford, H.B. (1973) *Can. J. Chem.* 51, 582-587

287. Cotton, M.L., Dunford, H.B., and Raycheba, J.M.T. (1973) *Can. J. Biochem.* 51, 627-631

288. Roman, R., and Dunford, H.B. (1973) *Can. J. Chem.* 51, 588-596

289. Araiao, T., Miyoshi, K., and Yamazaki, I. (1976) *Biochemistry* 15, 3059-3063

290. Critchlow, J.E., and Dunford, H.B. (1972) *J. Biol. Chem.* 247, 3703-3713

291. Critchlow, J.E., and Dunford, H.B. (1972) *J. Biol. Chem.* 247, 3714-3725

292. Hubbard, C.D., Dunford, H.B., and Hewson, W.D. (1975) *Can. J. Chem.* 53, 1563-1569

293. Dunford, H.B., and Cotton, M.L. (1975) *J. Biol. Chem.* 250, 2920-2932

294. Yoshida, H. (1883) *J. Chem. Soc. (London)* 43, 472-486

295. Boidin, J. (1951) *Rev. Mycol.* 16, 173-197

296. Franke, W. (1960) in Handbuch der Pflanzenphysiologie (Ruhland, W., ed) Vol. 12, pp. 424-430, Springer-Verlag, Berlin

297. Dawson, C.R., and Tarpley, W.B. (1951) in The Enzymes (Sumner, J.B., and Myrbäck, K., eds) Vol. 2, pp.454-498, Academic Press, New York

298. Levine, W.G. (1966) in The Biochemistry of Copper (Peisach, J., Aisen, P., and Blumberg, W.E., eds) pp. 371-387, Academic, Press, New York

299. Malkin, R., and Malmström, B.G. (1970) in Advances in Enzymology (Nord, F.F., ed) Vol. 33, pp. 177-244, Interscience, New York

300. Fåhraeus, G., and Ljunggren, H. (1961) *Biochim. Biophys. Acta* 46, 22-32

301. Keilin, D., and Mann, T. (1939) *Nature* 143, 23-24

302. Keilin, D., and Mann, T. (1940) *Nature* 145, 304

303. Higuchi, J. (1958) *J. Biochem.* 45, 515-528

304. Fåhraeus, G. (1961) *Biochim. Biophys. Acta* 54, 192-194

305. Benfield, G., Bocks, S.M., Bromley, K., and Brown, B.R. (1964) *Phytochemistry* 3, 79-88

306. Westerfeld, W.W., and Lowe, C. (1942) *J. Biol. Chem.* 145, 463-470

307. Lugaro, G., Carrea, G., Cremonesi, P., Casellato, M. M., and Antonini, E. (1973) *Arch. Biochem. Biophys.* 159, 1-6

308. Nakamura, T. (1958) *Biochim. Biophys. Acta* 30, 44-52

309. Omura, T. (1961) *J. Biochem.* 50, 264-272

310. Omura, T. (1961) *J. Biochem.* 50, 305-311

311. Omura, T. (1961) *J. Biochem.* 50, 389-393

312. Osaki, S. and Walaas, O. (1968) *Arch. Biochem. Biophys.* 123, 638-639

313. Fåhraeus, G., and Reinhammar, B. (1967) *Acta Chem. Scand.* 21, 2367-2378

314. Malmström, G., Fåhraeus, G., and Mosbach, R. (1958) *Biochim. Biophys. Acta* 28, 652-653

315. Mosbach, R. (1963) *Biochim. Biophys. Acta* 73, 204-212

316. Reinhammar, B. (1970) *Biochim. Biophys. Acta* 205, 35-47

317. Blumberg, W.E., Levine, W.G., Margolis, S., and Peisach, J. (1964) *Biochem. Biophys. Res. Commun.* 15, 277-283

318. Peisach, J., and Levine, W.G. (1965) *J. Biol. Chem.* 240, 2284-2289

319. Butzow, J.J. (1968) *Biochim. Biophys. Acta* 168, 490-506

320. Molitoris, H.P., Van Breemen, J.F.L., Van Bruggen, E.F.J. and Esser, K. (1972) *Biochim. Biophys. Acta* 271, 286-291

321. Esser, K., and Minuth, W. (1971) *Eur. J. Biochem.* 23, 484-488

322. Molitoris, H.P., and Reinhammar, B. (1975) *Biochim. Biophys. Acta* 386, 493-502

323. Malmström, B.G., Mosbach, R., and Vänngård, T. (1959) *Nature* 183, 321-322

324. Vänngård, T. (1972) in Biological Applications of Electron Spin Resonance (Swartz, H.M., Bolton, J.R., and Borg, D.C., eds) pp. 411-447, Interscience, New York

325. Nakamura, T. (1958) *Biochim. Biophys. Acta* 30, 538-542

326. Nakamura, T. (1958) *Biochim. Biophys. Acta* 30, 640-641

327. Broman, L. Malmström, B.G., Aasa, R., and Vänngård, T. (1962) *J. Mol. Biol.* 5, 301-310

328. Malmström, B.G., Reinhammar, B., and Vänngård, T. (1970) *Biochim. Biophys. Acta* 205, 48-57

329. Malmström, B.G. (1965) in Oxidases and Related Redox Systems (King, T.E., Mason, H.S., and Morrison, M., eds) pp. 207-216, Wiley, New York

330. Ehrenberg, A., Malström, B.G., Broman, L., and Mosbach, R. (1962) *J. Mol. Biol.* 5, 450-452

331. Moss, T.H., and Vänngård, T. (1974) *Biochim. Biophys. Acta* 371, 39-43

332. Malmström, B.G., Reinhammar, B., and Vänngård, T. (1968) *Biochim. Biophys. Acta* 156, 67-76

333. Malmström, B.G., and Vänngård, T. (1960) *J. Mol. Biol.* 2, 118-124

334. Fee, J.A., and Malmström, B.G. (1968) *Biochim. Biophys. Acta* 153, 299-302

335. Malmström, B.G., Aasa, R., and Vänngård, T. (1965) *Biochim. Biophys. Acta* 110, 431-434

336. Fee, J.A., Malmström, B.G., and Vänngård, T. (1970) *Biochim. Biophys. Acta* 197, 136-142

337. Malkin, R., Malmström, B.G., and Vänngård, T. (1969) *Eur. J. Biochem.* 7, 253-259

338. Malkin, R., Malmström, B.G., and Vänngård, T. (1968) *F.E.B.S. Lett.* 1, 50-54

339. Morpurgo, L., Rotilio, G., Agrò, A.F., and Mondovì, B. (1974) *Biochim. Biophys. Acta* 336, 324-328

340. Fee, J.A., Malkin, R., Malmström, B.G., and Vänngård, T. (1969) *J. Biol. Chem.* 244, 4200-4207

341. Van Leevwen, F.X.R., Wever, R., and Van Gelder, B.F. (1973) *Biochim. Biophys. Acta* 315, 200-203

342. Malkin, R., Malmström, B.G., and Vänngård, T. (1969) *Eur. J. Biochem.* 10, 324-329

343. Reinhammar, B.R.M., and Vänngård, T.I. (1971) *Eur. J. Biochem.* 18, 463-468

344. Reinhammar, B.R.M. (1972) *Biochim. Biophys. Acta* 275, 245-259

345. Brändén, R., and Reinhammar, B. (1975) *Biochim. Biophys. Acta* 405, 236-242

346. Malmström, B.G., Agrò, A.F., and Antonini, E. (1969) *Eur. J. Biochem.* 9, 383-391

347. Andréasson, L.-E., Malmström, B.G., Strömberg, C., and Vänngård, T. (1973) *Eur. J. Biochem.* 34, 434-439

348. George, P. (1965) in Oxidases and Related Redox Systems (King, T.E., Mason, H.S., and Morrison, M., eds) pp. 3-33, Wiley, New York

349. Malmström, B.G. (1970) *Biochem. J.* 117, 15-16P

350. Brändén, R., Malmström, B.G., and Vänngård, T. (1971) *Eur. J. Biochem.* 18, 238-241

351. Andréasson, L.-E., Bränden, R., Malmström, B.G.,

352. (1975) *Chem. Eng. News* December 8, 26-27

353. Hamilton, G.A., Libby, R.D., and Hartzell, C.R. (1973) *Biochem. Biophys. Res. Commun.* 55, 333-340

354. Cleveland, L., Coffman, R.E., Coon, R., and Davis, L. (1975) *Biochemistry* 14, 1108-1115

CHAPTER II. THE OXIDATION OF *p*-CRESOL BY HORSERADISH PEROXIDASE COMPOUND I

2.1 Summary

Rate constants for the reaction between horseradish peroxidase Compound I and *p*-cresol have been determined at several values of pH between 2.98 and 10.81. These rate constants were used to construct a log (rate) *vs.* pH profile from which it is seen that the most reactive form of the enzyme is its most basic form within this pH range so that base catalysis is occurring. At the maximum rate a second-order rate constant of $(5.1\pm0.3)\times10^{7}$ $M^{-1}s^{-1}$ at 25° is obtained. The activation energy of the reaction at the maximum rate was determined from an Arrhenius plot to be 5.0±0.5 kcal/mole. Evidence for an exception to the generally accepted enzymatic cycle of horseradish peroxidase is presented. One half molar equivalent of *p*-cresol can convert Compound I quantitatively to Compound II at high pH, whereas, usually this step requires one molar equivalent of reductant. The stoichiometry of this reaction is pH dependent.

2.2 Introduction

The facility of oxidation and the formation of colored products are perhaps the reasons that the reaction of phenols with peroxidase has been known since 1900 (1). Phenols also represent a class of substrates supposed to behave as the usual reductant, AH, in the following general mechanism which

depicts the enzymatic cycle (2-4)

[1] $HRP + H_2O_2 \longrightarrow HRP\text{-}I$

[2] $HRP\text{-}I + AH \longrightarrow HRP\text{-}II + A\cdot$

[3] $HRP\text{-}II + AH \longrightarrow HRP + A\cdot$

Native horseradish peroxidase (E.C.1.11.1.7 donor-H_2O_2 oxidoreductase) and its two spectroscopically and kinetically distinct intermediates, Compounds I and II, are abbreviated as HRP, HRP-I, and HRP-II. In this general mechanism one mole of reducing substrate is required to convert one mole of HRP-I to HRP-II, and a further mole is necessry to complete the cycle by reducing HRP-II back to native HRP. Exceptions to this general mechanism occur with the substrates sulfite (5) and iodide (6), which have been shown to transfer two electrons in one step thereby converting HRP-I directly to HRP without intermediate formation of HRP-II.

p-Cresol and at least one other phenol, guaiacol (7), are another but different type of exception to this general mechanism. Under certain conditions either of the phenols need be present in only half molar equivalent quantities to convert HRP-I quantitatively to HRP-II, and an additional half molar equivalent of the phenol will convert HRP-II to HRP. Therefore a total of only one molar equivalent of phenol will complete the enzymatic cycle.

This cnapter gives an analysis of the kinetic parameters of the reaction between HRP-I and *p*-cresol obtained by

studying the reaction over as large as possible pH range using pseudo first-order kinetics with single turnovers of the enzyme. The temperature dependence of the reaction rate was also studied. The pH dependence of the conversion of HRP-I to HRP-II using *p*-cresol in half molar quantities is discussed.

2.3 Experimental

Materials

Horseradish peroxidase (Lot 7344226) was purchased from Boehringer-Mannheim Corp. as an ammonium sulfate precipitate and was prepared for use by extensive dialysis against multiply distilled water and subsequent Millipore filtration. The enzyme was stored in the cold. Isozyme C, using the notation of Shannon *et al.*, (8) and of Paul and Stigbrand (9), has been determined to be the major component of HRP obtained from this supplier (10), and there has never been any evidence from this lab of a second isozyme component of detectably different reactivity (11).

Enzyme purity was determined from the absorbance ratio of 403 to 280 nm which was greater than 3.45. This is close to the value of the crystalline enzyme. The concentration of HRP was determined spectrophotometrically at 403 nm using a molar absorptivity of 1.02×10^5 $M^{-1}cm^{-1}$ (12). Highest grade *p*-cresol with 99+% purity obtained from Aldrich Chemical Co., Inc. was used without further purification. Its gas

chromatogram showed a single sharp peak. Potassium nitrate and buffer components were reagent grade.

The stability of Compound I depends greatly upon the extent that the water in which it is dissolved is free of oxidizable impurities. Water from this department's central distillation system was further purified in the following manner. A second distillation (from alkaline permanganate) was performed using a Corning AG-3 distillation apparatus. The distillate was fed into a 3-liter round-bottomed flask containing more alkaline permanganate and equipped with a Glas-Col heating mantle. A third distillation was effected through an 18 inch column packed with 1/8 inch I.D. glass helices obtained from SGA Scientific. The condenser was only partially cooled by running tap water very slowly through the outer jacket from top to bottom so that it did not fill with water. The vapor was partially condensed with the uncondensed portion vented to the atmosphere through an 8 mm O.D. tube loosely packed with Pyrex glass wool. This procedure facilitated a steam distillation of trace contaminants. Two more identical distillations, except without alkaline permanganate, completed the water purification procedure. The resultant water had a resistance of 6.2×10^5 ohms (cell constant 0.8) which can be compared to a resistance of $(1\text{-}4) \times 10^6$ ohms for water purified elsewhere in this department using ion exchange. The higher conductivity (lower resistance) of our preparation is more than offset by the elimination of trace organic contaminants which are

always present in ion-exchange purified water.

Apparatus

The rate measurements were performed with a Gibson-Durrum stopped-flow spectrophotometer model D-110 using at least a tenfold excess of *p*-cresol to maintain pseudo first-order conditions. For each set of reaction conditions between six and nine, usually eight, individual determinations of the rate constants were performed which were then averaged for a single best value. The progress of the reaction resulted in a decrease in transmittance and was followed at the isosbestic wavelength between HRP-II and HRP. At the isosbestic wavelength, no change in transmittance could be attributed to the further reaction of HRP-II to HRP which occurs in the presence of excess *p*-cresol. The isosbestic wavelength was slightly pH dependent and varied between 410.0 and 410.8 nm according to the wavelength scale on the Durrum instrument. The isosbestic wavelength could be accurately determined at a certain pH value by comparing the transmittance at the end of the HRP-I reaction with the transmittance at time infinity. Also, if the wavelength was close to the isosbestic value, but not exactly equal to it, a small reproducible irregularity occurred in the oscilloscope trace at the point where HRP-II became present in sufficient quantity to react with *p*-cresol and cause a transmittance change.

The data collection and storage system for the stopped-

flow experiments have been previously described (13). The stopped-flow spectrophotometer was equipped with a two centimeter cuvette, and temperature was maintained constant (±0.1°) by circulating thermostated water. All rate constants except those used to construct the Arrhenius plot were measured at 25°.

All absorbance measurements were performed on a Cary 14 spectrophotometer, and pH was measured with an Orion 801 pH meter outfitted with a Fisher combination electrode calibrated with standard buffers.

Methods

For the stopped-flow experiments one drive syringe contained the *p*-cresol solution and buffer (ionic strength 0.02); and the second drive syringe contained HRP-I at a concentration of 1.2 μM, while both syringes contained potassium nitrate (0.1 M). Therefore the total ionic strength of the reaction mixture was 0.11. Having the buffer in only one drive syringe avoided the increased speed of decay of the moderately labile HRP-I at pH values other than 7. This pH-jump method is viable because the proton equilibria are complete well within the dead time of the instrument. Kinetic measurements were performed in subdued light and with the storage syringe containg the HRP-I masked with opaque tape to avoid the recently discovered photochemical reaction of HRP-I (14).

Drive and storage syringes were copiously rinsed with

multiply distilled water between kinetic runs, and before filling they were rinsed twice with the appropriate solution. Just prior to adding the enzyme solution to the storage syringe, a 95% molar equivalent of hydrogen peroxide contained in a few microliters of solution was added to convert the native enzyme to HRP-I. Excess hydrogen peroxide had to be avoided to ensure only a single turnover in the relevant single step of the overall enzymatic cycle.

The rapidity of the HRP-I reaction with *p*-cresol at pH 7 to 8 even with only a tenfold excess of *p*-cresol, led to pseudo first-order rate constants larger than 400 s^{-1}. This corresponds to a half-life of less than 2 ms, and this pushed the stopped-flow method to its limits. However, the beauty of first-order kinetics is that half-life is not a function of concentration thereby making possible accurate determinations of the rate constant even when the dead time obscured the first part of the reaction. The dead time of the instrument was determined to be about 3 ms.

The pseudo first-order rate constant of each determination was obtained as a parameter from a weighted nonlinear least squares analysis of the oscilloscope trace (each data point weighted equally). The first-order kinetics were described by Equation [4]

$$[4] \qquad \frac{-d[HRP\text{-}I]}{dt} = k_{obs}[HRP\text{-}I]$$

where k_{obs} is the observed pseudo first-order rate constant

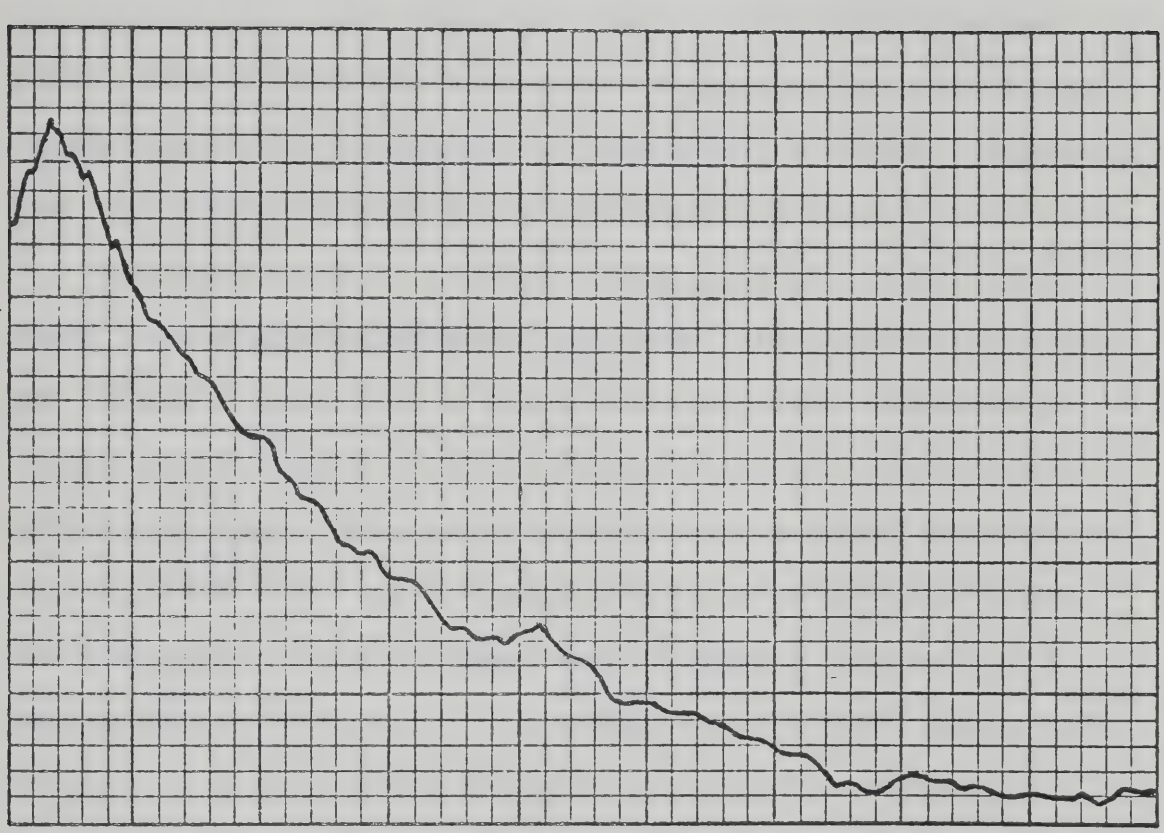

Fig. 2.1 A stopped-flow oscilloscope trace of the reaction of HRP-I (0.6 μM) with *p*-cresol (6.0 μM) at pH 8.74 in tris buffer. Ordinate: 100 mV per large division, absicissa: 2 ms per large division, RC time constant: 0.5 ms.

including the excess concentration of *p*-cresol. As shown in Fig. 2.1, simple exponential traces were obtained for data collection on a time scale as fast a 2 ms per division. The amount of noise on the trace is due to the low resistance-capacitance (RC) time constant necessary to avoid dampening and thus distorting of the exponential curve.

The solutions of *p*-cresol were made up immediately prior to a day's experiments and kept for the duration of use (about 5 hours) in a black-painted flask immersed in an ice-water bath at 0°. The concentration of *p*-cresol was determined spectrophotometrically using a molar absorptivity of 1.7×10^3 $M^{-1}cm^{-1}$ at 277 nm (15). Isolation from light and low temperature storage were necessary to avoid the photooxidation reaction of *p*-cresol (16). With these precautions a check of the absorbance at 277 nm showed no significant change in the *p*-cresol concentration over the 5 hour interval. The concentration of hydrogen peroxide was determined as described elsewhere using the HRP assay (17) and was checked weekly.

Spectra were run on a Cary 14 spectrophotometer. The 1 cm cuvette contained a 2 ml solution of potassium nitrate (0.1 M), buffer (ionic strength 0.01) and HRP (6.3 μM). HRP-I was formed by the addition of a molar equivalent of hydrogen peroxide in a few microliters of solution on the end of a Teflon plumper. The plumper technique was repeated for the addition of the *p*-cresol.

2.4 Results

A very good method for testing for adherence to true second-order kinetics performed under pseudo first-order conditions is to plot the observed pseudo first-order rate constant from Equation [4] against the concentration of the excess reactant for several concentrations. Two types of this plot were obtained for the HRP-I oxidation of *p*-cresol: linear above about pH 6 and nonlinear below this pH. Typical results are shown in Figs. 2.2 and 2.3.

The plot of the log of the second-order rate constant, $k_{1,app}$, for the reaction of HRP-I with *p*-cresol *vs.* pH is shown in Fig 2.4. The shape of this profile at lower pH indicates that a basic HRP-I species is reactive. From the shape of the profile at higher pH, it can be deduced that the reactive form of *p*-cresol is the acid (electrically neutral) species. (The pK_a of *p*-cresol, pK_s is 10.12.) *p*-Cresol is the first substrate to be shown to be reactive with basic HRP-I.

The large value of the rate constant from pH 6 to 10 shows that *p*-cresol is very readily oxidized. At pH 8.74 where the rate is maximal, the rate was investigated as a function of temperature. The activation energy, E_a, was computed to be 5.0±0.5 kcal/mole from the slope of the Arrhenius plot in Fig. 2.5 using a linear least squares analysis. The error in E_a was estimated from the average fractional deviations for all the rate constants. The rate constant at the highest temperature was increased and the

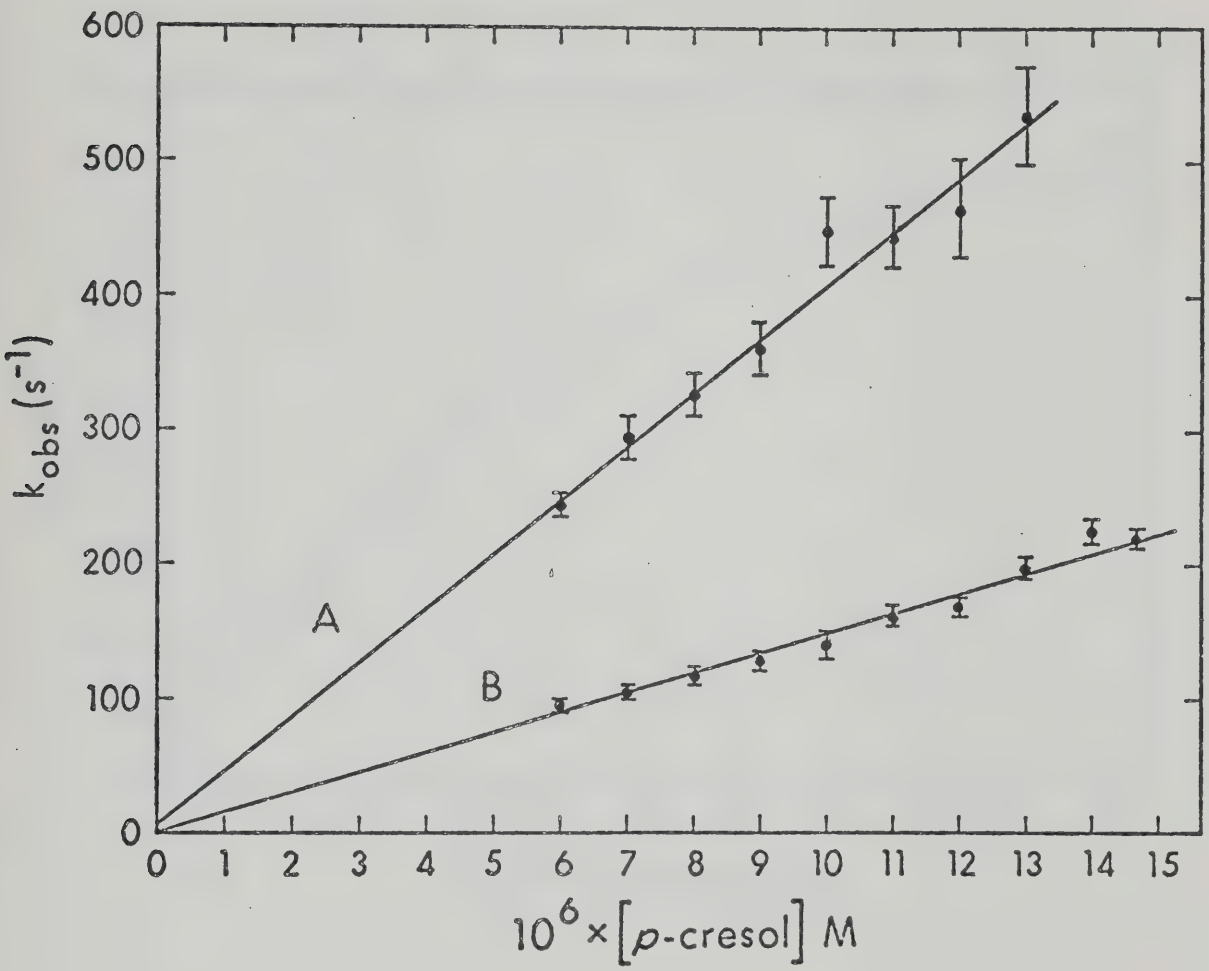

Fig. 2.2 Examples of linear plots of k_{obs} *vs.* the concentration of *p*-cresol with slopes calculated with a weighted linear least squares analysis using Equation [8]. Plot A: phosphate buffer, pH 6.03. Plot B: carbonate buffer, pH 10.54. The slope is the apparent second-order rate constant, $k_{1,app}$, and the intercepts are zero within standard deviation.

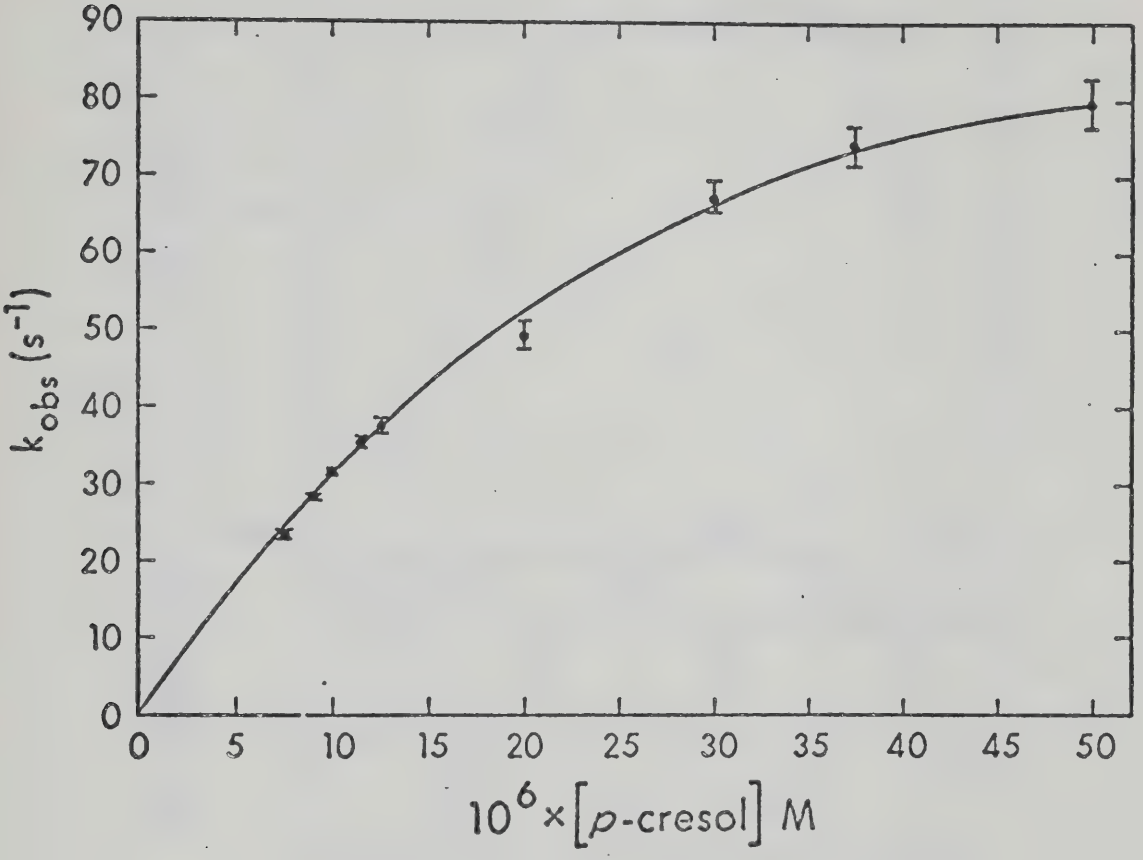

Fig. 2.3 Example of a nonlinear plot in citrate buffer at pH 3.70 analyzed using Equation [7].

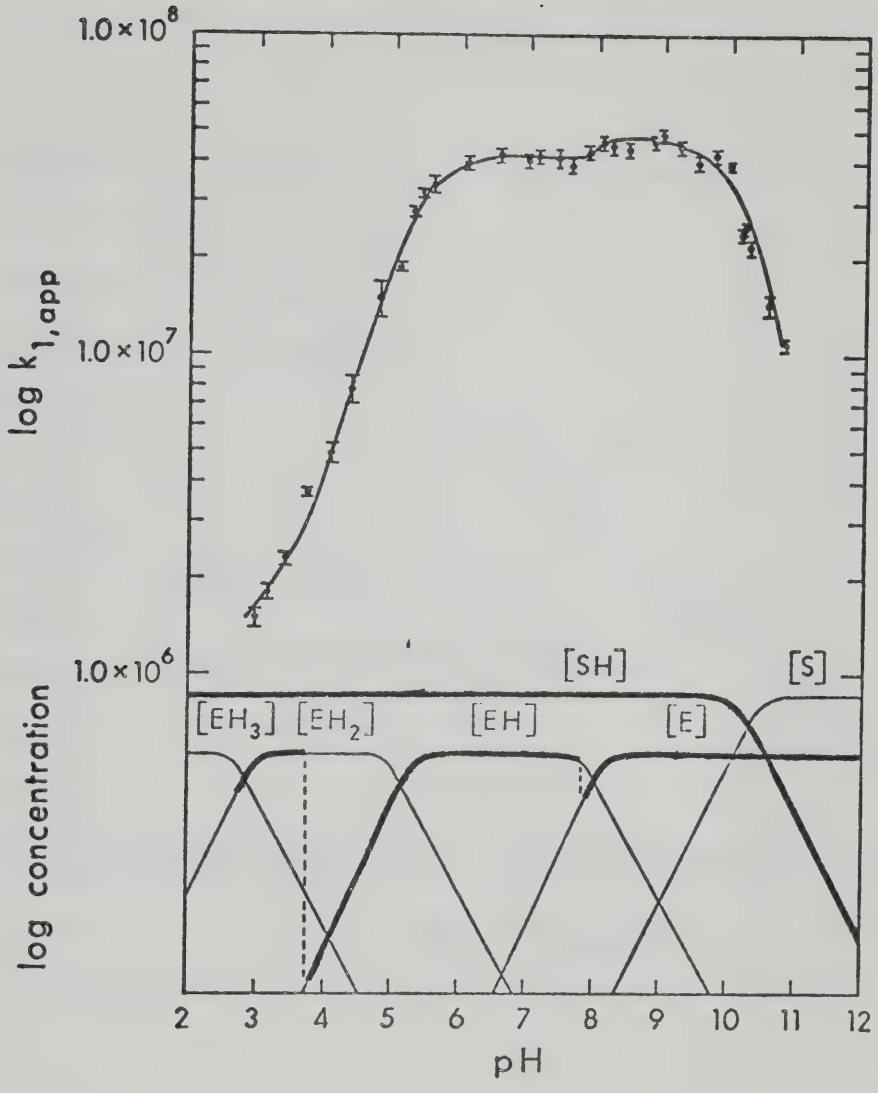

Fig. 2.4 Log ($k_{1,app}$) *vs.* pH profile for the reaction of HRP-I with *p*-cresol. Base catalysis is evident. The best line through the data was calculated using a weighted non-linear least squares analysis of Equation [9] or [10]. The schematic log (concentration) *vs.* pH plots explain the shape of the log ($k_{1,app}$) profile using three enzyme and one *p*-cresol dissociation constants. Bold lines indicate forms contributing most to the apparent rate. The vertical dashed lines indicate the calculated pH at which forms of the enzyme differing by one proton contribute equally to the rate.

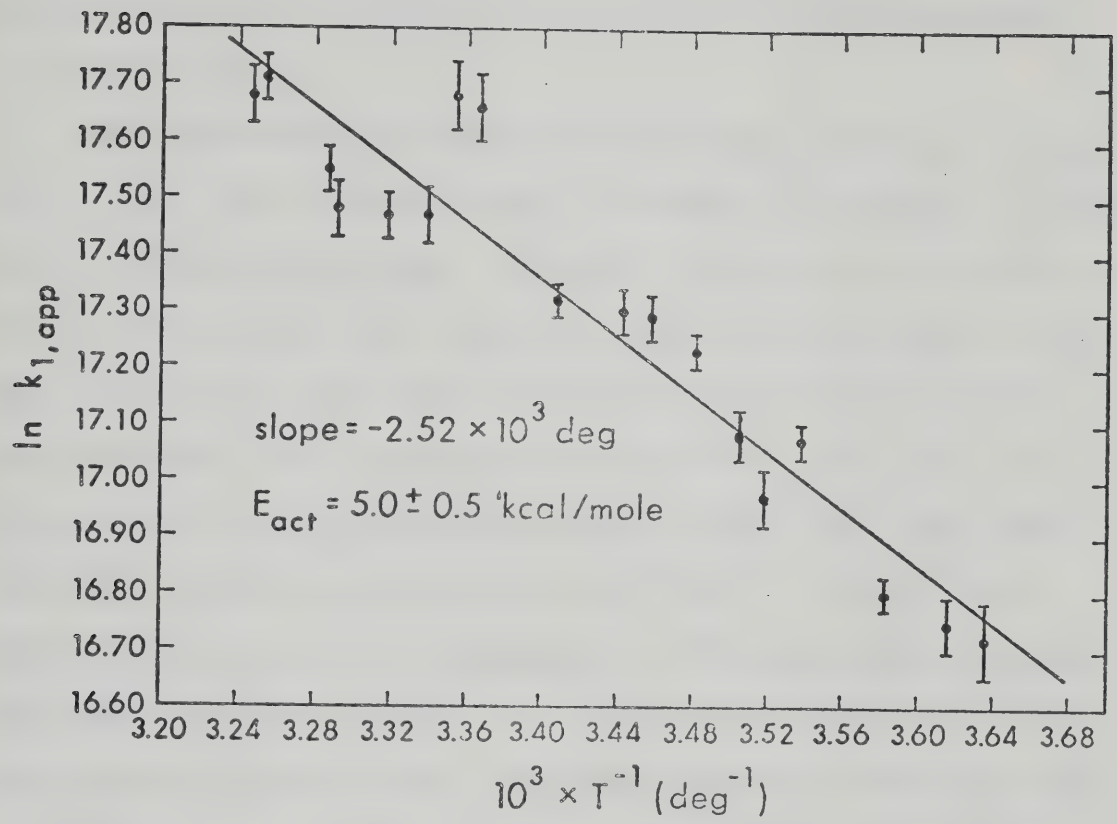

Fig. 2.5 Arrhenius plot for the reaction of HRP-I with *p*-cresol at pH 8.74. At this pH the most basic form of HRP-I is the predominant enzyme species contributing to the observed rate. The best straight line was calculated by a linear least squares analysis.

rate constant at the lowest temperature was decreased by this average fractional deviation. A new slope was calculated using these two new points which gave an E_a different by 0.5 kcal/mole.

When second-order kinetics are obeyed strictly, a plot of k_{obs} *vs.* the concentration of *p*-cresol will have a linear slope and zero intercept. However, such was not the case at low pH where nonlinear (concave towards the abscissa) plots were obtained. This type of nonlinearity has previously been detected for the following reactions, also only at certain values of pH: HRP-II with *p*-cresol (18), and HRP-I and HRP-II with *p*-aminobenzoic acid (11). All of these substrates are aromatic compounds. This nonlinear response has been described as due to a binding interaction between the enzyme and substrate. The most commonly cited case of such a phemomenon occurs in Michaelis-Menten kinetics in which an enzyme-substrate complex reacts unimolecularly as illustrated by Equation [5]

$$\text{[5]} \qquad \text{HRP-I} + \text{PC} \underset{}{\overset{K_M}{\rightleftharpoons}} \text{HRP-I-PC} \xrightarrow{k} \text{Products}$$

where K_M is the Michaelis constant and PC is *p*-cresol. However, conventional double-reciprocal plots of the data showed marked deviations from linearity.

In the previous examples of nonlinear plots involving HRP-I or HRP-II this Michaelis-Menten scheme was also proven to be inadequate and was supplanted by a scheme in which both

uncomplexed enzyme and a nonproductive enzyme-substrate complex can react bimolecularly with a substrate molecule (11,18).

$$[6] \qquad \begin{matrix} & & & k_{1,app} & \\ & \text{HRP-I} + \text{PC} & & \longrightarrow & \\ K_M & \uparrow\downarrow & & & \Big\} \text{ Products} \\ & \text{HRP-I-PC} + \text{PC} & & k_{2,app} & \\ & & & \longrightarrow & \end{matrix}$$

which leads to

$$[7] \qquad k_{obs} = \frac{k_{1,app}[PC] + k_{2,app}[PC]^2/K_M}{1 + [PC]/K_M}$$

An equivalent alternative scheme, as far as kinetic arguments are concerned, is one in which productive binding occurs, but in which a step corresponding to the lower half of Equation [6] as well as Equation [5] is included (18,19). From Equation [7], the nonlinear plots of k_{obs} *vs.* the concentration of *p*-cresol with a decrease in slope towards high concentration indicate that $k_{1,app}$ is larger than $k_{2,app}$ (Table 2.1). Whether productive or nonproductive binding occurs, reactions of this type indicate a type of negative cooperativity for a single subunit enzyme. The kinetic parameters were found by fitting Equation [7] to the data using a nonlinear least squares analysis. The kinetic parameters for the nonlinear plots of k_{obs} *vs.* the concentration of *p*-cresol are summarized in Table 2.1.

As a value of pH 6 was approached from the acid region

Table 2.1 The kinetic parameters[a] for nonlinear plots of k_{obs} *vs.* the concentration of *p*-cresol using a weighted nonlinear least squares analysis (Equation [7]).

pH[b]	Buffer[c]	$k_{1,app}(M^{-1}s^{-1})$	$k_{2,app}(M^{-1}s^{-1})$	$K_M(M)$
2.98	G	$(1.5\pm0.1)\times10^{6}$	$(2\pm1)\times10^{5}$	$(5\pm2)\times10^{-5}$
3.12	G	$(1.8\pm0.2)\times10^{6}$	$(9.7\pm0.9)\times10^{5}$	$(2\pm2)\times10^{-5}$
3.40	CI	$(2.3\pm0.1)\times10^{6}$	$(3\pm3)\times10^{5}$	$(9\pm4)\times10^{-5}$
3.70	CI	$(3.7\pm0.1)\times10^{6}$	$(2\pm2)\times10^{6}$	$(8\pm5)\times10^{-5}$
4.36	CI	$(7.9\pm0.9)\times10^{6}$	$(4\pm7)\times10^{6}$	$(5\pm19)\times10^{-5}$
4.76	A	$(1.5\pm0.2)\times10^{7}$	$(3\pm8)\times10^{6}$	$(5\pm6)\times10^{-5}$

[a] Errors represent standard deviations computed in the analysis.

[b] Error in pH values estimated at ±0.02.

[c] Buffer key: see footnote *a* of Table 2.2.

Table 2.2 Values of $k_{1,app}$ as a function of pH.

pH	Buffer[a]	$k_{1,app}$[b] ($M^{-1}s^{-1}$)	Calculation Method	10^6 x concentration range of *p*-cresol (M)
10.81	C	$(1.09\pm0.05)\times10^7$	3	6.0 - 12.5
10.54	C	$(1.45\pm0.08)\times10^7$	2	6.0 - 15.0
10.31	C	$(2.2\pm0.1)\times10^7$	3	6.0 - 10.0
10.19	C	$(2.5\pm0.1)\times10^7$	3	6.0 - 10.0
10.18	C	$(2.4\pm0.1)\times10^7$	3	6.0 - 10.0
9.99	C	$(3.9\pm0.1)\times10^7$	2	6.0 - 10.0
9.76	C	$(4.2\pm0.2)\times10^7$	3	6.0 - 10.0
9.50	C	$(4.0\pm0.2)\times10^7$	3	6.0 - 10.0
9.21	T	$(4.5\pm0.2)\times10^7$	3	6.0 - 10.0
8.94	T	$(4.9\pm0.2)\times10^7$	3	6.0 - 10.0
8.85	T	$(4.7\pm0.2)\times10^7$	2	6.0 - 10.0
8.46	AN	$(4.4\pm0.2)\times10^7$	2	6.0 - 15.0
8.23	T	$(4.5\pm0.2)\times10^7$	3	6.0 - 9.0
8.07	T	$(4.6\pm0.2)\times10^7$	3	6.0 - 10.0

Table continued on next page

pH	Buffer[a]	$k_{1,app}^{b}$ ($M^{-1}s^{-1}$)	Calculation Method	10^6 x concentration range of *p*-cresol (M)
7.85	T	$(4.3\pm0.2)\times10^7$	3	6.0 - 10.0
7.59	P	$(3.9\pm0.2)\times10^7$	3	6.0 - 10.0
7.40	P	$(4.1\pm0.2)\times10^7$	3	6.0 - 10.0
7.09	P	$(4.2\pm0.2)\times10^7$	3	6.0 - 10.0
6.98	P	$(4.1\pm0.2)\times10^7$	2	6.0 - 10.0
6.55	P	$(4.2\pm0.2)\times10^7$	3	6.4 - 10.0
6.03	P	$(4.0\pm0.2)\times10^7$	2	6.0 - 13.0
5.54	A	$(3.4\pm0.2)\times10^7$	3	6.0 - 10.0
5.44	A	$(3.2\pm0.1)\times10^7$	3	6.0 - 10.0
5.26	A	$(2.8\pm0.1)\times10^7$	3	6.0 - 10.0
5.10	A	$(1.89\pm0.05)\times10^7$	2	6.0 - 11.0
4.76	A	$(1.5\pm0.2)\times10^7$	1	6.0 - 58.4
4.36	CI	$(7.9\pm0.9)\times10^6$	1	6.0 - 50.0
4.01	A	$(4.9\pm0.3)\times10^6$	2	6.0 - 50.0
3.70	CI	$(3.7\pm0.1)\times10^6$	1	7.5 - 50.0

Table continued on next page

pH	Buffer[a]	$k_{1,app}^{b}$ ($M^{-1}s^{-1}$)	Calculation Method	10^6 x concentration range of *p*-cresol (M)
3.40	CI	$(2.3\pm0.1)\times10^6$	1	6.0 - 40.0
3.12	G	$(1.8\pm0.2)\times10^6$	1	6.0 - 50.0
2.98	G	$(1.5\pm0.1)\times10^6$	1	14.0 - 117.0

[a] Buffer key: C, carbonate; T, tris/HNO_3; AN, ammonium/ammonium nitrate; P, phosphate, A, acetate; CI, citrate; G, glycine/HNO_3.

[b] Errors are standard deviations calculated by the least square analysis. For calculation method 3, errors are average deviations from the mean.

plots of the type shown in Fig. 2.3 become more nearly linear, and reliable values of $k_{2,app}$ and K_M could not be obtained. At this pH and higher values the linear plots were fitted using Equation [8]

[8] $$k_{obs} = k_{1,app}[PC]$$

It should be noted that obedience of Equation [8] does not disprove the existence of a enzyme-substrate complex, but it does impose limits on the pertinent rate constants. For instance, if productive binding were occurring linear plots would still be obtained if the unimolecular reaction of the complex going to products was very much faster than the rate of formation of the complex. Futhermore, if the Michaelis constant (a dissociation constant) is large, the terms in Equation [7], $k_{2,app}[PC]^2/K_M$ and $[PC]/K_M$, become vanishingly small whereupon Equation [7] becomes equal to Equation [8].

Fig. 2.4 shows the log ($k_{1,app}$) *vs.* pH profile for the oxidation of *p*-cresol by HRP-I. The rate constants which define the profile, $k_{1,app}$, were obtained in three ways: 1, from $k_{1,app}$ in the nonlinear plots of k_{obs} *vs.* the concentration of *p*-cresol (Equation [7]); 2, from the linear plots (Equation [8]); and 3, when two to four determinations of k_{obs}, the pseudo first-order rate constants at different concentrations of *p*-cresol, were divided by the appropriate concentration of *p*-cresol for that determination to obtain a few values of $k_{1,app}$ which were then averaged for a best

value. Values of $k_{1,app}$ obtained in these ways are listed in Table 2.2. Plots of k_{obs} *vs.* the concentration of *p*-cresol were made at several pH values in all parts of the profile to ensure the validity of calculating $k_{1,app}$ by the third and least tedious method.

2.5 Discussion

p-Cresol appears to be unique among the substrates whose reactions with HRP-I have been studied intensively as a function of pH, because it is the only substrate for which HRP-I exhibits base catalysis and because of its fast reaction rate. The HRP-I substrates for which extensive pH dependent rate studies have been performed are the iodide ion (6), ferrocyanide ion (17), bisulfite ion (5), and *p*-aminobenzoic acid (11). For these substrates HRP-I exhibits acid catalysis.

Referring to Fig. 2.4, there are three observed negative inflections which are most readily assigned to pK_a estimates of 5.0, 8.0, and 10.0 for acid groups on the reactant molecules. Under the conditions of the kinetic experiments, the dissociation constant of *p*-cresol has been spectrophotometrically measured to have the value pK_a = 10.12±0.01 (18). Therefore the pK_a value of about 10.0 can be assigned to the substrate, and since *p*-cresol has no other ionizations within the experimental pH range the remaining pK_a values must be assigned to the enzyme. By use of the diffusion-controlled limit for bimolecular reactions

in solution it can be shown that only the acid form of *p*-cresol is reactive (20). Upon more rigorous inspection of the log ($k_{1,app}$) profile, the slope of the linear part in the acid region should have a value of +1 if a single kinetically important ionization occurs (20). The slope of this section is about +0.6 however, and therefore the value of log ($k_{1,app}$) does not decrease as rapidily as it should with decreasing pH. *p*-Cresol reacts only in the un-ionized, and therefore uncharged form, and this eliminates the possibility of enzyme-substrate electrostatic interactions affecting the magnitude of $k_{1,app}$ (21). A plausible explanation is that other kinetically important forms of the enzyme become important; and that these are further protonated species also capable of reacting with *p*-cresol but at a reduced rate.

To explain the entire log ($k_{1,app}$) profile in terms of acid-base catalysis it was necessary to use four different catalytically important forms of the enzyme and the acid form of *p*-cresol. This scheme is represented in different ways in Figs. 2.4 and 2.6. Two equations that represent the log ($k_{1,app}$) profile can be deduced from Figs. 2.4 and 2.6. These equations, [9] and [10], are fundamentally equivalent yet contain different terms in their numerators. Equation [9] is derived from the collision theory of acid-base catalysis and uses molecular (macroscopic) ionization constants (22). The symbols k_a through k_d represent second-order pH independent rate constants corresponding to Fig. 2.6.

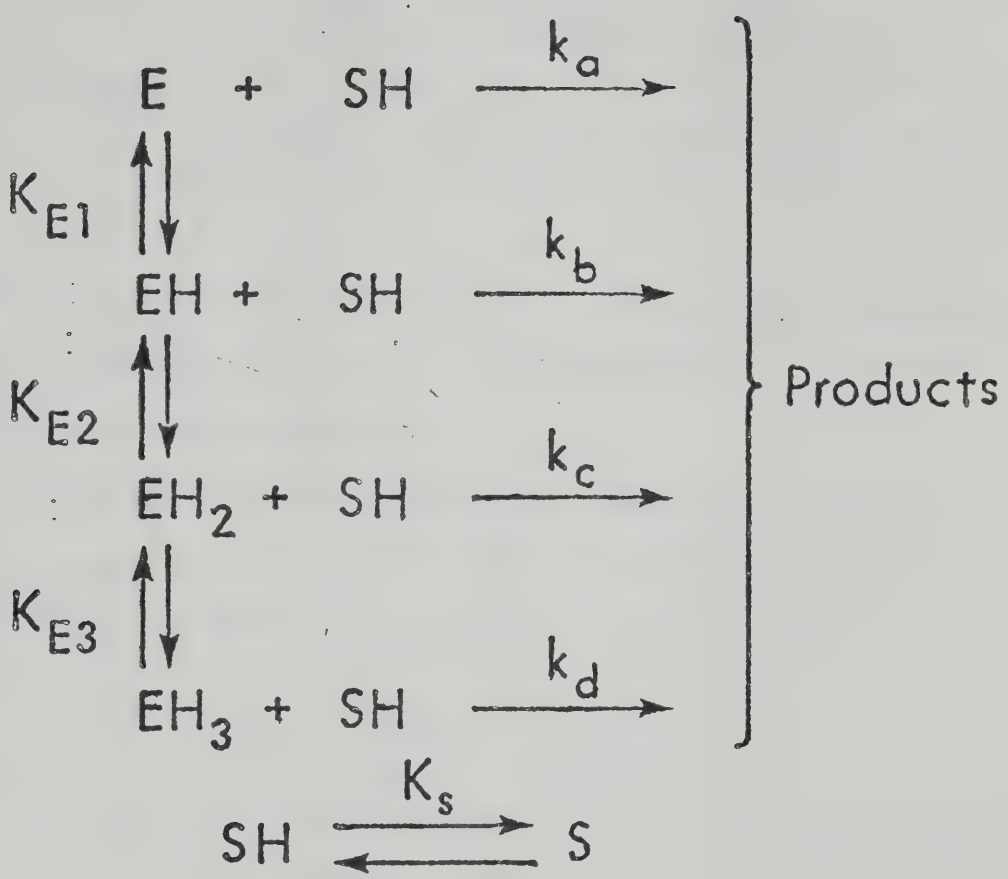

Fig. 2.6 Reaction scheme proposed to explain the log ($k_{1,app}$) *vs.* pH profile involving four forms of the enzyme (three acid dissociation constants, K_{En}) and two forms of *p*-cresol (one acid dissociation constant, K_S). All four enzymes forms react with the acid form of *p*-cresol, SH, and no enzyme form is able to react with the *p*-cresolate anion, S. k_a through k_d represent pH independent second-order rate constants.

$$[9] \qquad k_{1,app} = \frac{k_a + \frac{k_b[H^+]}{K_{E1}} + \frac{k_c[H^+]^2}{K_{E1}K_{E2}} + \frac{k_d[H^+]^3}{K_{E1}K_{E2}K_{E3}}}{\left(1 + \frac{[H^+]}{K_{E1}} + \frac{[H^+]^2}{K_{E1}K_{E2}} + \frac{[H^+]^3}{K_{E1}K_{E2}K_{E3}}\right)\left(1 + \frac{K_S}{[H^+]}\right)}$$

The acid dissociation constants on the enzyme and substrate are represented by K_{En} and K_S. The derivation of Equation [9] is given in the Appendix.

Equation [10] can be written by inspection of the log ($k_{1,app}$) profile (23,24). and has its origins in the transition state theory of acid-base catalysis (25).

$$[10] \qquad k_{1,app} = \frac{k_a\left(1 + \frac{[H^+]}{K_{E1}^{\ddagger}} + \frac{[H^+]^2}{K_{E1}^{\ddagger}K_{E2}^{\ddagger}}\right)}{\left(1 + \frac{[H^+]}{K_{E1}} + \frac{[H^+]^2}{K_{E1}K_{E2}} + \frac{[H^+]^3}{K_{E1}K_{E2}K_{E3}}\right)\left(1 + \frac{K_S}{[H^+]}\right)}$$

In Equation [10], k_a is the pH independent rate constant at high pH, $K_{En}^{\ddagger}$ is a transition state acid dissociation constant and corresponds to a positive inflection (increase in slope) in the log ($k_{1,app}$) profile, whereas K_{En} represents initial state ionization constants corresponding to a negative inflection.

Comparing equations, note that only from Equation [9] can all the pH independent rate constants be obtained; and in only Equation [10] are the $K_{En}^{\ddagger}$ values obtainable, while both equations yield all the initial state dissociation

Table 2.3 The parameters for the log ($k_{1,app}$) *vs.* pH profile calculated by nonlinear least squares analysis.

kinetic parameter	Collision Theory Equation [9]	Transition Theory Equation [10]
k_a ($M^{-1}s^{-1}$)	$(5.1\pm0.3)\times10^{7}$	$(5.3\pm0.4)\times10^{7}$
k_b ($M^{-1}s^{-1}$)	$(4.0\pm0.2)\times10^{7}$	$(4.2\pm0.2)\times10^{7}$ [a]
k_c ($M^{-1}s^{-1}$)	$(2\pm10)\times10^{6}$	----------
k_d ($M^{-1}s^{-1}$)	$(1\pm2)\times10^{6}$	----------
$pK_{E1}^{\ddagger}$	----------	8.0 ± 0.4
$pK_{E2}^{\ddagger}$	----------	3.8 ± 0.1 [b]
$K_{E1}^{\ddagger}K_{E2}^{\ddagger}$ (M^2)	----------	$(2\pm5)\times10^{-12}$
pK_{E1}	8.0 ± 0.3	8.1 ± 0.4
pK_{E2}	5.08 ± 0.01 [b]	5.10 ± 0.04 [b]
pK_s	10.19 ± 0.05	10.22 ± 0.06
$K_{E1}K_{E2}$ (M^2)	$(8\pm15)\times10^{-14}$	$(7\pm17)\times10^{-14}$
$K_{E2}K_{E3}$ (M^2)	$(7\pm170)\times10^{-9}$ [a]	$(8\pm24)\times10^{-8}$ [b]
pK_{E3}	3.1 ± 1.6 [a]	2.0 ± 0.7 [b]
$K_{E1}K_{E2}K_{E3}$ (M^3)	$(7\pm364)\times10^{-17}$	$(7\pm56)\times10^{-16}$

[a] value obtained from equation [11]

[b] value obtained from equation [12]

constants. Note that Equation [10] does not require a cubed hydrogen ion concentration term in the numerator as $K_{E3}^{\ddagger}$ lies outside the range of the experimental data (in other words there are only two positive inflections in the experimentally determined log ($k_{1,app}$) *vs.* pH plot). The best fit values for the kinetic parameters in Equations [9] and [10] were obtained by a nonlinear least squares analysis and are compiled in Table 2.3. The best fit line drawn through the data of the log ($k_{1,app}$) profile can be generated using Equation [9] or [10], and the curves virtually overlap over the entire range of pH.

It was found advantageous to fit the log ($k_{1,app}$) profile only from pH = 7.85 to 2.98 as this allowed a much more precise determination of K_{E2}, the most catalytically significant enzyme dissociation constant. If K_{E2} and $K_{E2}^{\ddagger}$ were calculated from Equations [9] or [10], the single minimizing value from the nonlinear least squares analysis for the product of $K_{E1}K_{E2}$ or $K_{E1}^{\ddagger}K_{E2}^{\ddagger}$ must be divided by K_{E1} or $K_{E1}^{\ddagger}$. These last two terms contain a large error because they represent a small inflection in the log ($k_{1,app}$) profile, and consequently the product of $K_{E1}K_{E2}$ or $K_{E1}^{\ddagger}K_{E2}^{\ddagger}$ also incorporate this large error. Further, the large error in K_{E3} is mainly due to the value of pK_{E3} not being sufficiently within the experimental pH range. The two equations for each theory, collision and transition state, which correspond to the data between pH = 7.85 and 2.98 are

$$[11] \qquad k_{1,app} = \frac{k_b + \frac{k_c[H^+]}{K_{E2}} + \frac{k_d[H^+]^2}{K_{E2}K_{E3}}}{1 + \frac{[H^+]^2}{K_{E2}} + \frac{[H^+]^2}{K_{E2}K_{E3}}}$$

and

$$[12] \qquad k_{1,app} = \frac{k_b\left(1 + \frac{[H^+]}{K_{E2}^{\ddagger}}\right)}{1 + \frac{[H^+]}{K_{E2}} + \frac{[H^+]^2}{K_{E2}K_{E3}}}$$

The kinetic parameters are compiled in Table 2.3.

The difference, $pK_{E1}^{\ddagger} - pK_{E1} = -0.1 \pm 0.08$, is negative indicating base catalysis, and the small difference reflects the small magnitude of base catalysis in the vicinity of pH 8. A much larger base catalysis effect occurs in more acid solution. The difference, $pK_{E2}^{\ddagger} - pK_{E2} = -1.4 \pm 0.1$, for the second enzyme ionization has a very pronounced effect on the value of $k_{1,app}$. The value of $pK_{E3}^{\ddagger}$ could not be determined, and thus no comparison with pK_{E3} is possible. The acid dissociation constant with the largest effect on catalysis is $pK_{E2} = 5.08 \pm 0.01$, and a compilation of the important pK_E values for HRP-I reactions with the substrates *p*-aminobenzoic acid, ferrocyanide, bisulfite

ion, and iodide ion shows kinetically important values of $pK_E \simeq 5$ (26). The values of pK_S obtained from both Equations [9] and [10] are the same within their standard deviations and agree very favorably with the spectrophotometrically measured value of $pK_S = 10.12 \pm 0.01$.

The schematic log (concentration) *vs.* pH plot in the bottom of Fig. 2.4 explains the shape of the log ($k_{1,app}$) profile in terms of the concentrations of the initial reactants. The reactive forms giving the largest contribution to the apparent rate over a certain pH range are emphasized with bold lines. The dashed vertical lines connect these forms and mark the calculated pH value where the rate contributions are equal for two forms of HRP-I differing by one proton. The percentage of the acid form of *p*-cresol, SH, remains essentially constant for pH values significantly less than the value of pK_S. The shape of the log ($k_{1,app}$) profile at pH values greater than pK_S can be explained by the slope of -1 for log [SH] *vs.* pH and a slope of zero for log [E] *vs.* pH. At pH values less than pK_S any parts of the log ($k_{1,app}$) profile with a nonzero slope are attributed to catalytically important ionizations on the enzyme. The slight dip, moving toward lower pH, occurs at pH = pK_{E1} = 8.0 where an acid form of the enzyme, EH, starts to provide the largest contribution to the apparent rate. The contribution to the rate by E has been curtailed due to its low concentration. Moving to yet lower pH the more acid form of HRP-I, EH_2, becomes catalytically important. When

the pH is less than the pK_{E2} value of 5.08 the concentration of EH_2 is larger than the concentration of EH, but the former does not contribute equally to the apparent rate until a pH of 3.8. This occurs because EH_2 is only 1/20 as reactive as EH with *p*-cresol. (Compare k_b and k_c.) At even higher acidity where $pH = pK_{E3} \simeq 2 - 3$, a further protonated form of HRP-I, EH_3, contributes to the apparent rate although the form EH_3 is probably never predominant within the experimental range of pH. Since the value of pK_{E3} corresponds to a pH value of the edge of the accessible data it is not well defined. The abatement in rate upon entering the acid region is due to the diminished concentration of the two very reactive forms of HRP-I represented by E and EH, which are replaced with the much less reactive forms EH_2 and EH_3. Since less acid forms of HRP-I are more reactive, the reaction is properly described as base catalyzed.

The uniqueness of *p*-cresol as a substrate for HRP-I can be attributed to a different proton transfer mechanism during oxidation when compared to the previously studied substrates. Since the iodide ion (6), ferrocyanide ion (17), bisulfate ion (5), and *p*-aminobenzoic acid (11) as substrates for HRP-I all have similar $\log(k_{app})$ *vs.* pH curves, approximately the same proton transfer mechanism applies to each substrate. The apparent second-order rate constants for these substrates increase when a kinetically important ionizable group with a pK_a of about 5.1 is protonated.

The most kinetically important ionizable group determined with *p*-cresol as the substrate is pK_{E2} with a value of 5.08. It is plausible that this refers to the same ionizable group on HRP-I found for the other substrates, but for *p*-cresol the protonation of this ionizable group inhibits the reaction, indicating a substantially different mechanism. Many phenolic compounds including *p*-cresol have been studied by electron spin resonance by Shiga and Imaizumi (27) and are known to be oxidized with HRP in the steady state by dehydrogenation to yield the corresponding phenoxy radical. This indicates that for *p*-cresol both a proton and an electron are removed by oxidation. Therefore there may be a mandatory proton transfer from *p*-cresol to the group with a pK_a of 5.1 to facilitate the electron transfer, hence base catalysis. Perhaps *p*-aminobenzoic acid and the inorganic ions require the positive charge of a proton on the ionizable group to facilitate electron transfer, which is not accompanied by proton transfer and therefore their rates of oxidation are acid catalyzed.

The magnitudes of k_a and k_b may be large enough to represent a bimolecular reaction rate that approaches the diffusion-controlled limit (28). The rate of a bimolecular reaction in solution is usually thought to be diffusion controlled when a limit of about 10^{10} $M^{-1}s^{-1}$ is approached. However, enzyme reactions are likely to have very important steric requirements, and it has been suggested that a bimolecular reaction rate between an enzyme and a substrate

Table 2.4 The second-order rate constants for the reaction of *p*-cresol with HRP-I at several temperatures at pH 8.74 where the most basic enzyme species is predominant.

T(°C)	$10^{-7} \times k_{1,app} (M^{-1}s^{-1})$
1.9	1.8±0.1
3.4	1.9±0.1
6.0	2.0±0.1
9.5	2.6±0.1
11.1	2.4±0.1
12.1	2.6±0.2
14.0	3.0±0.1
16.0	3.2±0.1
17.3	3.3±0.1
20.3	3.3±0.1
23.8	4.7±0.3
25.0	4.8±0.2
26.3	3.8±0.2
28.4	3.9±0.2
30.6	3.9±0.2
31.1	4.2±0.2
34.1	4.9±0.2
34.8	4.8±0.3

in the range of 10^7 to 10^8 $M^{-1}s^{-1}$ may be diffusion controlled (29,30). The activation energy can provide an aid in deciding if a reaction rate is diffusion controlled. Fig. 2.5 shows the Arrhenius plot for the oxidation of *p*-cresol by HRP-I at pH 8.74. At this pH the most basic form of HRP-I is the predominant reactive species (Fig. 2.4). Values of $k_{1,app}$ as a function of temperature are given in Table 2.4. The value of E_a is 5.0±0.5 kcal/mole and is not much above the activation energy for diffusion in aqueous solutions (28). The value of the entropy of activation, $\Delta S^{\ddagger}$, is (-6±1) cal/mole-deg as calculated from the Arrhenius pre-exponential factor, A, obtained from the intercept in Fig. 2.5. The negative value of $\Delta S^{\ddagger}$ correlates with an important steric factor, according to the collision theory. A recent study of the reaction of many phenolic compounds with HRP-I in the pH independent region has shown that a rate constant of 2×10^8 $M^{-1}s^{-1}$ could be attained at 27° (31).

As mentioned earlier, the reduction of HRP-I by *p*-cresol has revealed an unusual 2:1 stoichiometry. For this to occur *p*-cresol must contain two reducing equivalents, and yet these two electrons cannot be transferred simultaneously because if they were, HRP-I would be reduced directly to HRP without intermediate formation of HRP-II. The conversion of HRP-I to HRP-II is known to be a one electron reduction (32). Conversions of HRP-I to HRP-II at three different values of pH using only a half mole of *p*-cresol have shown that the HRP-II yield decreases with decreasing pH. Qualitative

features of the unusual stoichiometry for the reaction of HRP-I with *p*-cresol were observed earlier (33), but the pH dependence was not studied. Advantage was taken of the upper limit of the 2:1 stoichiometry to form HRP-II from HRP-I and *p*-cresol in such a manner that HRP-I caused no interference with a study of the reactions of HRP-II. A variable yield of HRP-II, mixed with native HRP, obtained as a function of pH, was not important to the kinetic studies since the studies were conducted under pseudo first-order conditions where neither absolute concentrations nor absolute molar absorptivities are required to obtain accurate results (33). The stoichiometry of the reaction of HRP-I with *p*-cresol has been investigated in detail and the results are presented in the following chapter.

2.6 References

1. Saunders, B.C., Holmes-Siedle, A.G., and Stark, B.P. (1964) in Peroxidase pp. 25-27, Butterworths, London
2. Chance, B. (1952) *Arch. Biochem. Biophys.* 41, 416-424
3. George, P. (1952) *Nature* 169, 612-613
4. George, P. (1953) *Biochem. J.* 54, 267-276
5. Roman, R., and Dunford, H.B. (1973) *Can. J. Chem.* 51, 588-596
6. Roman, R., and Dunford, H.B. (1972) *Biochemistry* 11, 2076-2082
7. Santimone, M. (1975) *Can. J. Biochem.* 53, 649-657
8. Shannon, L.M., Kay, E., and Lew, J.Y. (1966) *J. Biol. Chem.* 241, 2166-2172
9. Paul, K.-G., and Stigbrand, T. (1970) *Acta Chem. Scand.* 24, 3607-3617
10. Phelp, C., and Antonini, E. (1969) *Biochem. J.* 114, 719-724
11. Dunford, H.B., and Cotton, M.L. (1975) *J. Biol. Chem.* 250, 2920-2932
12. Schonbaum, G.R., and Lo, S. (1972) *J. Biol. Chem.* 247, 3353-3360
13. Roman, R., Dunford, H.B., and Evett, M. (1971) *Can. J. Chem.* 49, 3059-3063
14. Stillman, J.S, Stillman, M.J., and Dunford, H.B. (1975) *Biochemistry* 14, 3183-3188
15. Herington, E.F.G., and Kynatson, W. (1957) *Trans. Faraday Soc.* 53, 138-142

16. Joschek, H.-I., and Miller, S.I. (1966) *J. Am. Chem. Soc.* 88, 3273-3281

17. Cotton, M.L., and Dunford, H.B. (1973) *Can. J. Chem.* 51, 582-587

18. Critchlow, J.E., and Dunford, H.B. (1972) *J. Biol. Chem.* 247, 3703-3713

19. Dunford, H.B., and Stillman, J.S. (1976) *Coord. Chem. Revs.* 19, 187-251

20. Dunford, H.B. (1974) *J. Theor. Biol.* 46, 467-479

21. Hammes, G.G., and Alberty, R.A. (1959) *J. Phys. Chem.* 63, 274-279

22. Dixon, M., and Webb E.C. (1964) in Enzymes 2nd Ed., p. 119, Longmans Green, London

23. Dunford, H.B., Critchlow, J.E., Maguire, R.J., and Roman, R. (1974) *J. Theor. Biol.* 48, 283-298

24. Critchlow, J.E., and Dunford, H.B. (1972) *J. Theor. Biol.* 37, 307-320

25. Dunford, H.B. (1975) *J. Chem. Ed.* 52, 578-580

26. Dunford, H.B. (1974) *Physiol. Veg.* 12, 13-23

27. Shiga, T., and Imaizumi, K. (1975) *Arch. Biochem. Biophys.* 167, 469-479

28. Hewson, W.D., and Dunford, H.B. (1975) *Can. J. Chem.* 53, 1928-1932

29. Gutfreund, H. (1972) in Enzymes: Physical Principals p. 159, Wiley-Interscience, Toronto

30. Schmitz, K.S., and Schurr, J.M. (1972) *J. Phys. Chem.* 76, 534-545

31. Job, D., and Dunford, H.B. (1976) *Eur. J. Biochem.* 66, 607-614

32. Chance, B. (1952) *Arch. Biochem. Biophys.* 37, 235-237

33. Hassinoff, B.B., and Dunford, H.B. (1970) *Biochemistry* 9, 4930-4939

2.7 Appendix

Refer to Fig 2.6.

$$v = k_{1,app}[E]_{total}[S]_{total} = k_a[E][SH] + k_b[EH][SH] + k_c[EH_2][SH] + k_d[EH_3][SH]$$

$$[E]_{total} = [E] + [EH] + [EH_2] + [EH_3]$$

$$[S]_{total} = [S] + [SH]$$

$$k_{1,app} = \frac{[SH](k_a[E] + k_b[EH] + k_c[EH_2] + k_d[EH_3])}{([E] + [EH] + [EH_2] + [EH_3])([SH] + [S])}$$

K_{En} and K_S represent acid dissociation constants.

$$k_{1,app} = \frac{k_a + \frac{k_b[H^+]}{K_{E1}} + \frac{k_c[H^+]^2}{K_{E1}K_{E2}} + \frac{k_d[H^+]^3}{K_{E1}K_{E2}K_{E3}}}{\left(1 + \frac{[H^+]}{K_{E1}} + \frac{[H^+]^2}{K_{E1}K_{E2}} + \frac{[H^+]^3}{K_{E1}K_{E2}K_{E3}}\right)\left(1 + \frac{K_S}{[H^+]}\right)}$$

CHAPTER III. STOICHIOMETRY OF THE REACTION BETWEEN HORSERADISH PEROXIDASE AND *p*-CRESOL

3.1 Summary

Over a wide range of pH horseradish peroxidase Compound I can be reduced quantitatively via Compound II to the native enzyme by only one molar equivalent of *p*-cresol. Since two molar equivalents of electrons are required for the single turnover of the enzymatic cycle, *p*-cresol behaves as a two electron reductant. With *p*-cresol and Compound I in a 1:1 ratio, Compound II and *p*-methylphenoxy radicals are obtained in the transient state. Compound II is then reduced to the native enzyme. A possible explanation for the facile reduction of Compound II involves reaction with the dimerization product of these radicals, a half molar equivalent of 2,2'-dihydroxy-5,5'-dimethylbiphenyl. If only one-half molar equivalent of *p*-cresol is present, then at high pH the reduction stops at Compound II. The major steady state peroxidase oxidation product of *p*-cresol (with *p*-cresol in large excess compared to the enzyme concentration) is Pummerer's ketone. Pummerer's ketone is only reactive at pH values greater than about 9 where significant amounts of the enol can be formed via the enolate anion. Therefore, in alkaline solution it is reactive with Compound I, but not with Compound II which is converted into an unreactive basic form. These results indicate that Pummerer's ketone cannot be the intermediate free radical product responsible for

reducing Compound II in the single turnover experiments. It is postulated that Pummerer's ketone is formed only in the steady state by the reaction of the *p*-methylphenoxy radical with excess *p*-cresol.

3.2 Introduction

Horseradish peroxidase (E.C. 1.11.1.7 donor-H_2O_2 oxidoreductase) and its two intermediates, Compound I and Compound II, are all spectroscopically distinct. The characteristic nature of the spectra between 350 and 450 nm is frequently used for monitoring their interconversion.

For some time we have been aware of a unusual 2:1 stoichiometry for the reaction of Compound I with *p*-cresol (1,2). The yield of Compound II was maximized when only a half mole of *p*-cresol was used as a reductant per mole of Compound I (2). Two moles of reductant are usually necessary to complete a single turnover of the enzyme. The 2:1 stoichiometry provides an interesting exception to the widely accepted general mechanism which depicts the enzymatic cycle (3-5)

[1] $\text{HRP} + H_2O_2 \longrightarrow \text{HRP-I}$

[2] $\text{HRP-I} + \text{AH} \longrightarrow \text{HRP-II} + \text{A}\cdot$

[3] $\text{HRP-II} + \text{AH} \longrightarrow \text{HRP} + \text{A}\cdot$

Horseradish peroxidase, Compound I, and Compound II are represented by HRP, HRP-I, and HRP-II; and AH represents an

oxidizable substrate. Many phenolic compounds are oxidized by peroxidase. The visual changes of color and precipitation which accompanied the formation of the oxidation products of *p*-cresol were recorded (6) and the identification of several of the main oxidation products was undertaken (7,8). Shiga and Imaizumi (9) have used electron spin resonance spectroscopy in combination with a continous flow system to determine the initial formation of the *p*-methylphenoxy radical from the oxidation of *p*-cresol by peroxidase.

It is the purpose of this chapter to present experimental evidence for a mechanism of the reduction of HRP-I by *p*-cresol which explains the 2:1 stoichiometry of the reaction. The major steady state peroxidase oxidation product of *p*-cresol is 4a,9b-dihydro-8,9b-dimethyl-3(4H)-dibenzofuranone (I) which is better known as Pummerer's ketone (10).

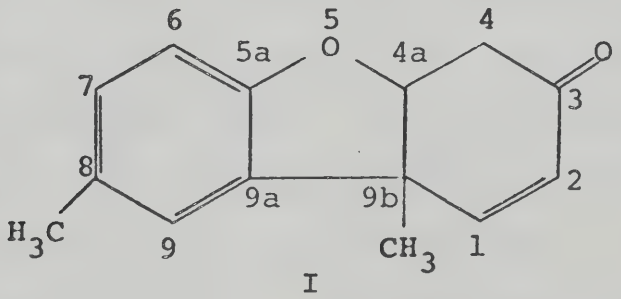

I

An extensive kinetic and equilibrium study of Pummerer's ketone indicates that it cannot be the same oxidation product formed in the transient state single turnover experiments.

3.3 Experimental

Horseradish peroxidase was purchased from Boehringer

Mannheim GmbH as a purified ammonium sulfate precipitate (Lot 7394427). The enzyme was prepared as described elsewhere (11). The purity number of the enzyme, determined by the ratio of absorbances at 403 and 280 nm, was 3.34. The concentration of HRP was determined spectrophotometrically at 403 nm using a molar absorptivity of 1.02×10^5 $M^{-1}cm^{-1}$ (12). *p*-Cresol with a stated purity of 99+% was obtained from Aldrich Chemical Co., Inc. and was used without further purification. Potassium nitrate and buffer components were reagent grade. Very pure water free from oxidizable contaminants was used for all experiments that involved solutions of the enzyme. The method used to purify the water has been described in the previous chapter.

Spectra were obtained with a Cary 14 spectrophotometer by the following procedure. HRP (0.244 ml of 57.4 μM) was pipetted into a 1 cm cell along with potassium nitrate (0.200 ml of 1 M), buffer (0.100 ml of ionic strength 0.2), and 1.456 ml of purified water. This gave a total volume of 2 ml which was 7.0 μM (14 nmole) in HRP, 0.1 M in potassium nitrate, and buffer with an ionic strength of 0.01 for a total ionic strength of 0.11. The spectrum of native HRP was recorded. To obtain the spectrum of HRP-I, 5.13 μl of 2.73 mM hydrogen peroxide (14 nmole) were deposited with a Hamilton microliter syringe on the end of a Teflon plumper which was then used to mix the hydrogen peroxide solution with the solution in the cell. The spectrum of HRP-I was immediately recorded. The same plumper technique was used

to add a substrate to the solution of Compound I. The sum of the volumes of the hydrogen peroxide solution and substrate solution never exceeded 10 µl so that the dilution of the original solution in the cell was insignificant. The spectra were scanned from 450 to 350 nm at a rate of 2.5 nm/s. The Cary 14 was also used to measure the absorbance at 295 nm of Pummerer's ketone as a function of pH. From pH 7.10 to 10.18 phosphate, tris, and carbonate buffers were used to control the pH; and from pH 10.09 to 14.30 the pH was calculated from the known amount of sodium hydroxide added to an unbuffered aqueous solution of Pummerer's ketone with a microliter syringe. Corrections were made for the change in absorbance caused by dilution with the sodium hydroxide titer volume. For the buffer and titration technique the reference cell contained all the solutes in the sample cell except Pummerer's ketone.

The concentration of hydrogen peroxide was determined by the HRP assay method of Cotton and Dunford (13), and the concentration of *p*-cresol was determined spectrophotometrically at 277 nm using a molar absorptivity of 1.7×10^3 $M^{-1}cm^{-1}$ (14). The pH was measured with an Orion model 801 pH meter equipped with a Fisher combination glass electrode. The meter was calibrated to ±0.02 using commercial standard buffers.

Pummerer's ketone was isolated from a mixture of the enzyme oxidation products of *p*-cresol formed in the steady state. *p*-Cresol (10.49 g, 97 mmole) was dissolved in 900 ml

of pH 7.2 phosphate buffer (ionic strength 0.01). Hydrogen peroxide (97 mmole) in 25 ml of purified water was slowly added to the continuously stirred solution of *p*-cresol with 7 intermittant additions of 0.5 ml of 57.4 μM HRP over a period of two hours. This allowed HRP to cycle in the steady state. A cream-white oily precipitate formed immediately which was removed by centrifugation. It showed at least five spots on a silica gel thin layer chromatogram developed with 20% v/v ethyl ether in chloroform. Pummerer's ketone was separated from the other compounds using dry column chromatography (15) with fluorescent silica gel (grade II-III) as the adsorbent and chloroform as the solvent. Fluorescent silica gel was used so that the adsorbed compound could be located by the absence of fluorescence under ultraviolet light. A column of Nylon tubing permitted the section containing the compound to be sliced from the column rather than eluted.

Pummerer's ketone was also prepared nonenzymatically using a variation of the original preparation by Pummerer *et al.* (10) *p*-Cresol (64.24 g, 0.594 mole) was dissolved with sodium carbonate (84.65 g, 0.799 mole) in 1.2 l of water. Potassium ferricyanide (236 g, 0.717 mole) was added intermittantly over a period of 30 minutes to the continuously stirred solution. After 24 hours of stirring at 30° the pH was lowered from 8 to 5 with concentrated HCl, and the reaction mixture was extracted with 800 ml (total volume of several extractions) of methylene chloride. The

dark brown residue after evaporation of the methylene chloride was vacuum distilled at 2-3 mm. The first fraction, 66°, was unreacted *p*-cresol (identified by NMR); and the second fraction, 155-160°, proved to be Pummerer's ketone (identified by NMR and mass spectroscopy) in 14% yield. It was recrystallized twice from boiling methanol and had a melting point of 125°.

A Hewlett-Packard 5750 gas chromatograph was used to determine the number of components in some reaction mixtures. The column (8 feet by 1/8 inch O.D.) was 15% SE-30 supported on 80-100 mesh Chromosorb W. The oven temperature was 200°, and the He flow rate was 23 ml/min. The same column and conditions were used for the coupled gas chromatograph and mass spectrometer. The analysis system consisted of a Varian 1200 gas chromatograph coupled with an A.E.I. MS2 mass spectrometer with the computations performed by a Nova 2-10 computer with an A.E.I. DS50 program.

The kinetic experiments were performed with a Durrum model D-110 stopped-flow apparatus. One drive syringe contained HRP-I and 0.1 M potassium nitrate while the second drive syringe contained substrate, 0.1 M potassium nitrate, and 0.02 ionic strength buffer. The mixing volumes were equal, and the concentrations quoted later refer to initial reactant concentrations in the cuvette.

The three α-carbonyl protons of Pummerer's ketone were exchanged with deuterium by dissolving the ketone in a warm solution of sodium deuteroxide, 1.35 M, in deuterium oxide

(prepared by the addition of freshly cut sodium metal to deuterium oxide). Partially deuterated Pummerer's ketone precipitated upon cooling the solution. No resonances in the NMR spectrum due to the α-carbonyl protons could be detected. The sodium salt of Pummerer's ketone was prepared by the dropwise addition of sodiun ethoxide in ethanol to a solution of the ketone in ethyl ether. The yellow salt precipitated immediately.

3.4 Results and Discussion

Transient State Results for HRP-I and *p*-Cresol in a 1:1 Ratio

From pH 3.5 to 10.2 the addition of one mole of *p*-cresol to one mole of HRP-I (both at 7.0 μM concentration) produced a complete single turnover in the enzymatic cycle regenerating native HRP. When another mole of hydrogen peroxide was added to the solution of regenerated HRP a stable preparation of HRP-I was formed indicating the absence of any further oxidizable substrate. The stopped-flow apparatus was used to demonstrate that this reduction of one mole of HRP-I to HRP by one mole of *p*-cresol proceeded via HRP-II. By monitoring the reaction course at 420 nm (HRP-I and *p*-cresol, each 1.0 μM) it was possible to observe a fast initial absorbance increase followed by a slower absorbance decrease. The initial increase is due to the reduction of HRP-I to HRP-II, and the subsequent decrease corresponds to the reduction of HRP-II to HRP. For all experiments conducted at pH values from 3.5 to 10.2 HRP-II was present in the

transient state.

The quantitative reduction of one mole of HRP-I to HRP-II to native HRP by one mole of *p*-cresol requires that *p*-cresol must relinquish two moles of electrons because the conversion of HRP-I to HRP-II is a known one electron reduction (16) as is the reduction of HRP-II to HRP (5). It is also obligatory that *p*-cresol does not lose its two available electrons simultaneously because this would permit the direct reduction of HRP-I to HRP (which is known to occur with bisulfite (17) and iodide (18) ions as substrates). The transient state observations require that a single molecule of *p*-cresol must lose one electron to one molecule of HRP-I thereby reducing it to HRP-II, and the reaction product containing one less electron than *p*-cresol must in turn reduce a molecule of HRP-II to native HRP and itself be further oxidized.

A scheme that meets the above requirements for the single turnover experiments in illustrated in Equations [4] and [5] and their sum in Equation [6]

[4] $$\text{HRP-I} + \text{PC} \longrightarrow \text{HRP-II} + \text{PC}\cdot$$

[5] $$\text{HRP-II} + \text{PC}\cdot \longrightarrow \text{HRP} + \text{Products}$$

[6] $$\text{HRP-I} + \text{PC} \longrightarrow \text{HRP} + \text{Products}$$

p-Cresol is represented by PC, and the *p*-methylphenoxy free radical is represented by PC·. The initially formed *p*-methylphenoxy free radical has been detected by EPR so that the

reaction of Equation [4] does occur (9). However, the validity of Equation [5] can be questioned because of evidence presented by Ohnishi *et al.* (19). It was found that the free radical derived from *p*-cresol by the action of HRP and hydrogen peroxide can remove an electron from hydrogen donors which are slowly reacting substrates for HRP. Since the free radical is itself an oxidizing agent, it seems unlikely that it could be further oxidized by HRP-II.

In the normal enzymatic cycle, Equations [1] to [3], the fate of the enzyme is emphasized. It is usually thought that the substrate, if it is an organic molecule, is dehydrogenated to form a free radical. The typical conjecture, deduced from product identification, concerning the further events of the free radicals involves oligomerization reactions with predominant dimerization. For the peroxidase oxidation of *p*-cresol three products were isolated by Westerfeld and Lowe (7): Pummerer's ketone, 2,2'-dihydroxy-5,5'-dimethyl-biphenyl, and an analogous terphenyl (isolated in a weight ratio of 1 : 0.2 : 0.5, respectively). The original assignment of the structural formula of Pummerer's ketone by Pummerer *et al.* was incorrect (20). The structure was later revised by Barton *et al.* (21), and the revision was confirmed by Arkley *et al.* (22) to the presently accepted structure (I). At least two of the enzymatic oxidation products of *p*-cresol appear capable of being further oxidized because they are phenols, and this might help to explain the 2:1 stoichiometry. A wide variety of phenols and naphthols can react with

peroxidase except those with extremely high oxidation potentials like *p*-nitrophenol (9,23). It is therefore postulated that the *p*-methylphenoxy radicals combine to form products which are responsible for the subsequent reduction of HRP-II to native HRP in the single turnover experiments where HRP-I and *p*-cresol are in a 1:1 ratio. Danner *et al.* (24) have shown that both phenol and its dimeric oxidation product, 2,2'-biphenol, are oxidizable by HRP.

In a titration study, Santimone (25) has shown that guaiacol can also donate two molar equivalents of electrons to reduce HRP-I to HRP. To explain this 2:1 stoichiometry, Santimone postulated a mechanism in which the *o*-methoxyphenoxy free radical, G·, formed from the dehydrogenation of guaiacol, G, loses an electron to dissolved molecular oxygen thereby forming the superoxide radical anion, $O_2^{\dot{-}}$. These events are depicted by Equations [7] to [10]

[7] $\text{HRP-I} + \text{G} \longrightarrow \text{HRP-II} + \text{G}\cdot$

[8] $\text{G}\cdot + O_2 \longrightarrow O_2^{\dot{-}} + \text{Products}$

[9] $\text{HRP-II} + O_2^{\dot{-}} \longrightarrow \text{HRP} + O_2$

---

[10] $\text{HRP-I} + \text{G} \longrightarrow \text{HRP} + \text{Products}$

The superoxide radical anion has been shown to react rapidly with HRP-I but to be unreactive with HRP-II (26,27), so that the validity of Equation [9] is doubtful. This scheme might also be criticized in terms of relative redox potentials. If G· can be oxidized by oxygen to form $O_2^{\dot{-}}$, and even if $O_2^{\dot{-}}$

could then be oxidized by HRP-II; then the relative potentials must also permit G· to be oxidized by HRP-II (because the free energy change makes a reaction feasible, it does not prove it must occur).

A mechanism consistent with all the observations concerning the reduction of one mole of HRP-I via HRP-II to native HRP by one mole of *p*-cresol in a single turnover is introduced in Equations [4] and [11] to [13]

[4] $$\text{HRP-I} + \text{PC} \longrightarrow \text{HRP-II} + \text{PC}\cdot$$

[11] $$\text{PC}\cdot \longrightarrow \tfrac{1}{2}(\text{PC})_2$$

[12] $$\text{HRP-II} + \tfrac{1}{2}(\text{PC})_2 \longrightarrow \text{HRP} + \text{Products}$$

[13] $$\text{HRP-I} + \text{PC} \longrightarrow \text{HRP} + \text{Products}$$

The fate of the *p*-methylphenoxy radicals generated in the first step is described in Equation [11] as a dimerization. One half mole of this dimer $(PC)_2$ is then able to react with one mole of HRP-II as shown by Equation [12] so that it must behave as a bifunctional molecule. The dimerization of the free radical is indicated by the identification of products from *p*-cresol oxidation (7,8), of which the most complete study was performed by Chen *et al.* (28). Ferric chloride or HRP was used as an oxidant. The dimer 2,2'-dihydroxy-5,5'-biphenyl (and the analogous trimer) and Pummerer's ketone (a dimer) were isolated along with two previously unidentified compounds from the HRP oxidation mixture. It might be noted that $\frac{1}{2}(PC)_2$ in Equations [11] and [12] might be

partially replaced by $1/3(PC)_3$ or $\frac{1}{4}(PC)_4$, etc.

Transient State Results for HRP-I and *p*-Cresol in a 2:1 Ratio

Fig. 3.1 illustrates the pH dependence of the reaction of HRP-I with a half molar equivalent of *p*-cresol. Spectrum A is that of native HRP at pH 10.51, and at this pH half a molar equivalent reduces HRP-I quantitatively to HRP-II as shown by spectrum B. At pH values of 7.06 and 4.01, spectra C and D, the 2:1 stoichiomtery is no longer obvious, and these spectra both indicate that the solution contains a large amount of HRP. A possible explanation for this pH dependence of the HRP-II yield might be found in the relative rates of the reactions of HRP-I and HRP-II with *p*-cresol which have been measured over a wide pH range (1,29) as shown in Fig. 3.2. It can be seen that HRP-I reacts approximately 10^4 times faster than HRP-II at pH 10.5 and only 40 and 10 times faster at pH values of 7.1 and 4.0. The rate of reaction of HRP-II with *p*-cresol is so slow compared with the rate of HRP-I at pH 10.5 that virtually none of the HRP-II formed in the initial stages of the reaction of HRP-I with *p*-cresol can compete effectively for the remaining *p*-cresol. At lower pH values similar arguments apply, but since a factor of 10 between the rate constants for two consecutive competitive bimolecular reactions is known to separate the two rates sufficiently so that each rate can be measured independently (30,31). Consequently there should be an insignificant amount of competitive interference by

HRP-II at any pH for the *p*-cresol substrate. However, the fate of the *p*-methylphenoxy radicals must also be considered. If the radicals combine quickly to form a new product which is also reactive, the HRP-II can compete with the remaining HRP-I to oxidize the new product. If HRP-II is reduced to native HRP at a rate comparable to that for HRP-I reduction to HRP-II (32) by the radical combination product then both the reduction of HRP-I and the yield of HRP-II will be non-quantitative as is indicated by the lack of an isosbestic point in Fig. 3.1. Stopped-flow traces indicated that the reduction of HRP-I by a half molar equivalent of *p*-cresol does not follow second-order kinetics, in accord with the above explanation of the complexities of the reaction. The quantitative yield of HRP-II observed at only high pH (Fig. 3.1, spectrum B) can be explained by the conversion of HRP-II into a nonreactive basic form. At high pH the reduction would proceed as illustrated in Equations [4], [11], [14], and [15]

[4] $\text{HRP-I} + \text{PC} \longrightarrow \text{HRP-II} + \text{PC}\cdot$

[11] $\text{PC}\cdot \longrightarrow \tfrac{1}{2}(\text{PC})_2$

[14] $\text{HRP-I} + \tfrac{1}{2}(\text{PC})_2 \longrightarrow \text{HRP-II} + \text{Products}$

---

[15] $2\text{HRP-I} + \text{PC} \longrightarrow 2\text{HRP-II} + \text{Products}$

The possible role of $O_2^{\dot{-}}$ in the reaction of HRP-I with a half mole of *p*-cresol was tested by repeating the experiments discussed in Fig. 3.1 with solutions deoxygenated by bubbling with 99.997% nitrogen. There was no observable

change in the results.

Steady State Results

We also undertook the isolation and identification of the products of *p*-cresol oxidized in the steady state by HRP, primarily performed as a means of their synthesis, so that their possible reactions with the enzyme could be studied independently of the *p*-cresol reaction. Pummerer's ketone was by far the most abundant volatile product and was identified by infrared and NMR spectroscopy and by gas chromatography combined with mass spectroscopy. The mass and NMR spectra were identical to those already published (28,33). The chromatogram of the volatile products obtained from the precipitate of the enzyme oxidation of *p*-cresol is shown in Fig. 3.3, and the large peak at about 17 minutes corresponds to Pummerer's ketone as identified by mass spectometry. Since the area under the peak of the chromatogram is directly proportional to the amount of the compound, it was possible to show that about 90% of the volatile products is Pummerer's ketone, M.W. = 214 g/mole. The small peak at about 12 minutes corresponds to 2,2'-dihydroxy-5,5'-dimethylbiphenyl, also 214 g/mole. In the steady state both HRP-I and HRP-II oxidize *p*-cresol, and it was assumed that they give the same products. The validity of this assumption is supported by the fact that a diversity of oxidizing agents form these products from *p*-cresol (34-37). A very high yield of Pummerer's ketone was obtained by

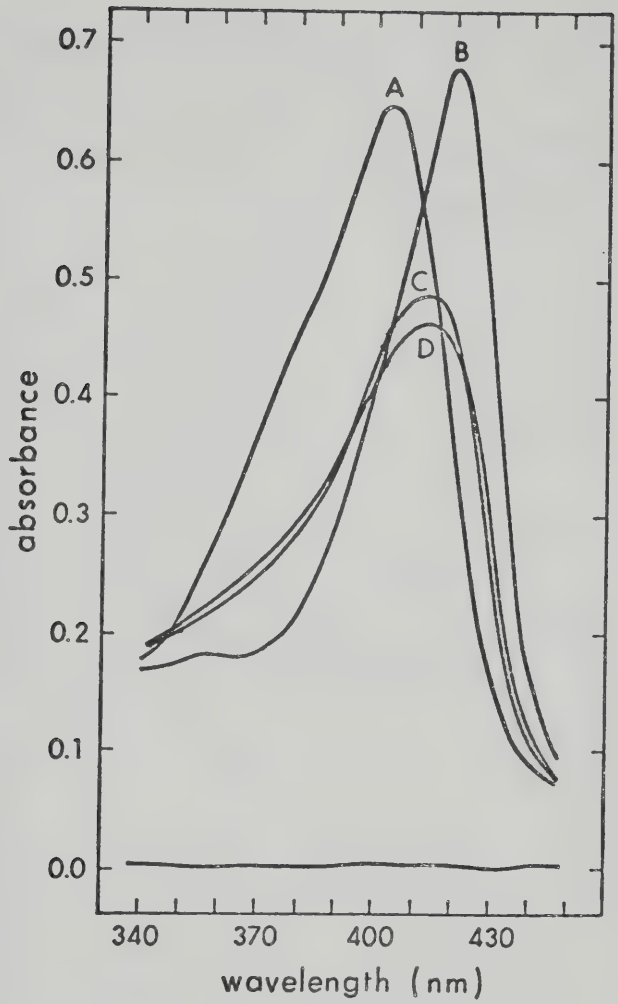

Fig. 3.1 The spectra obtained at different pH values by adding one half molar equivalent of *p*-cresol to HRP-I. The spectra were recorded immediately after mixing. A: the spectrum of native HRP at pH 10.51, B: at pH 10.51 showing a quantitative conversion to HRP-II, C: nonquantitative conversion at pH 7.06, D: nonquantitative conversion at pH 4.01. The solutions were 0.1 M with respect to potassium nitrate, and buffers contributed an ionic strength of 0.01. (A: carbonate, B: phosphate, C: acetate.) The H_2O baseline is included.

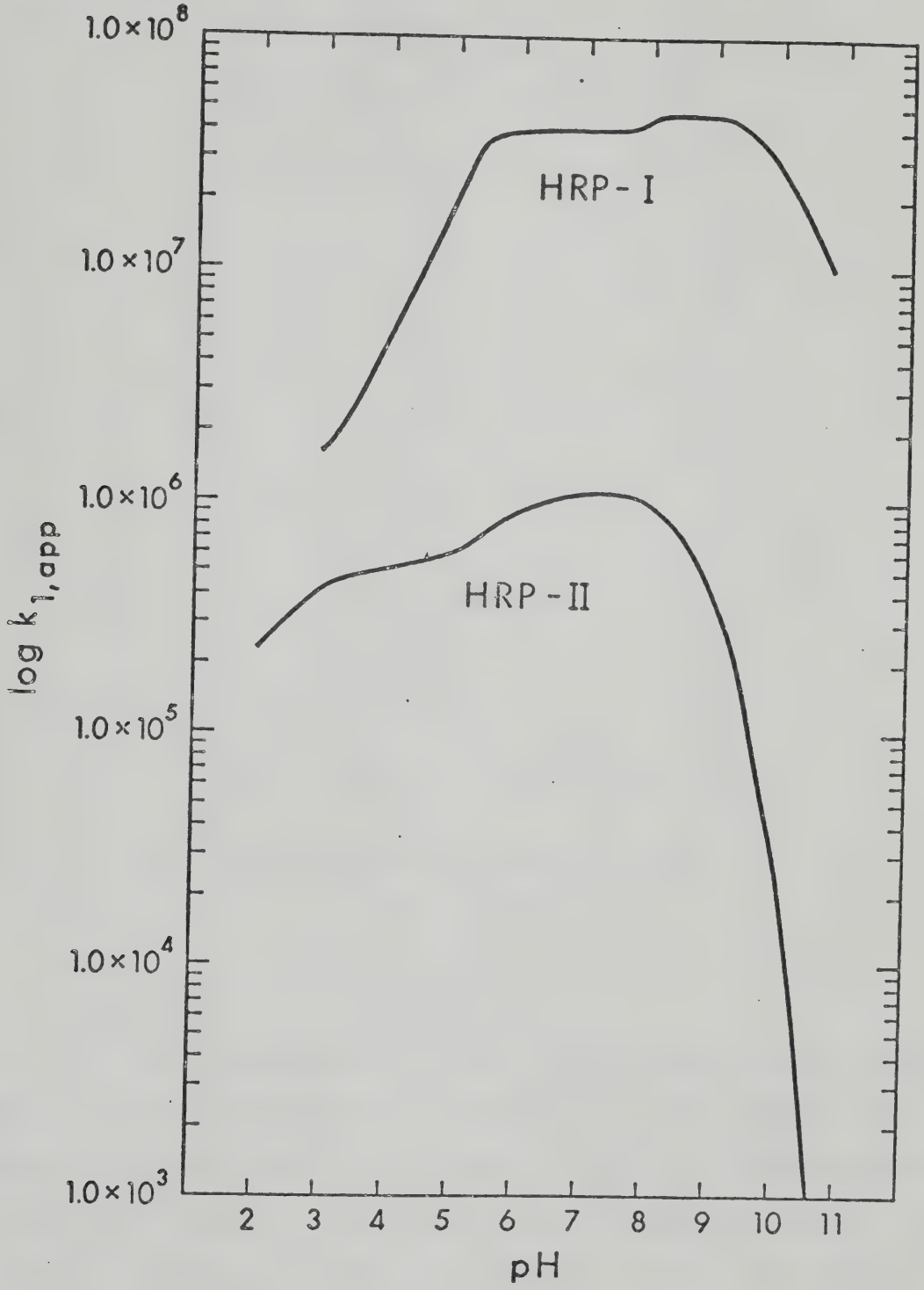

Fig. 3.2 Tne log (rate) *vs.* pH profiles for HRP-I and HRP-II with *p*-cresol as the substrate. Data for HRP-I, ref. 1; for HRP-II, ref. 29.

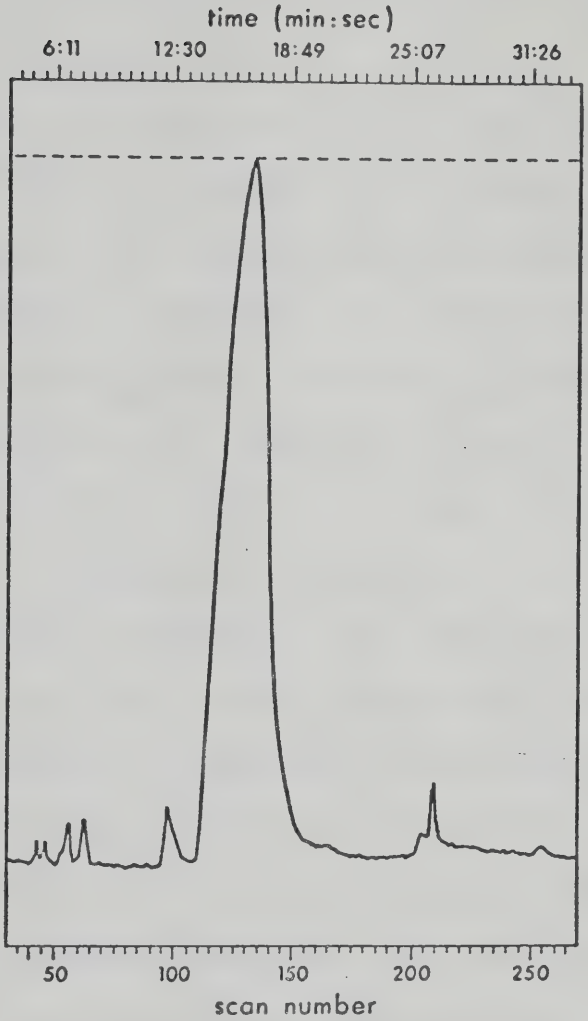

Fig. 3.3 Gas chromatogram of the volatile peroxidase steady state oxidation products of *p*-cresol from the coupled gas chromatograph and mass spectrometer. Note the preponderance of Pummerer's ketone, large peak at 17 minutes, compared to the other peroxidase oxidation products. The small peak at about 12 minutes corresponds to 2,2'-dihydroxy-5,5'-dimethyl-biphenyl.

Brown and Bocks (38) from the oxidation of *p*-cresol with a plant phenol oxidase.

The validity of Equation [11] is indicated by the many product identification studies for the steady state oxidation of *p*-cresol which reveal mostly dimeric products. More evidence in support of Equation [11] comes from the likelihood that this dimerization occurs very quickly, perhaps approaching the diffusion controlled limit for bimolecular reactions in solution. The rate of coupling of *p*-methylphenoxy radicals produced by irradiation of *p*-cresol in unbuffered aqueous solution has been measured to be 5.6×10^9 $M^{-1}s^{-1}$ (39). This rate should not be much different for the same radical produced by enzymatic dehydrogenation provided that the radical is not bound to the enzyme. Shiga and Imaizumi (9) have shown that the hyperfine lines of the EPR spectra of this radical are sharp and well averaged and the observed coupling constants of the hyperfine lines agree well with calculated values for an unbound and therefore electronically unperturbed free radical.

Equilibrium and Kinetic Studies on Pummerer's Ketone

The behavior of the major steady state oxidation product, Pummerer's ketone, was extensively characterized by kinetic and equilibrium studies. If Pummerer's ketone is also the major reaction product in the single turnover experiments, then its reactivity as a bifunctional substrate according to Equations [12] and [14] can be tested experimentally.

The results of the experimental tests to ascertain the reactivity of Pummerer's ketone and its reaction stoichiometry with HRP-I are summarized in Fig. 3.4. Spectrum A is the native enzyme at pH 10.51, and spectrum B is HRP-I prepared by adding one molar equivalent of hydrogen peroxide, Equation [1]. Spectrum C was recorded immediately after adding a half molar equivalent of Pummerer's ketone to the HRP-I, and D and E were recorded after 4 and 8 minutes. Therefore Pummerer's ketone does react quantitatively and with a 2:1 stoichiometry. The clearly defined isosbestic point at 398 nm proves that conversion of HRP-I to HRP-II is the only reaction occurring and no HRP-II is reduced to HRP. The lack of reactivity of HRP-II with Pummerer's ketone at high pH is an important point in later discussion.

The same experiment performed to obtain the data in Fig. 3.4 was repeated at pH 7.06 with the results shown in Fig. 3.5. Most of the small change in the spectra B to D is due to the spontaneous reduction of HRP-I and little due to the reaction of HRP-I with Pummerer's ketone as shown by a control experiment. It would appear that enolization, facilitated by an alkaline medium, is the cause of the reactivity of Pummerer's ketone at high pH and its relative unreactivity at neutral or low pH. By recording the absorption spectrum of Pummerer's ketone from 380 to 250 nm over a pH range of 7.10 to 14.30 it was shown that three spectroscopically distinct species were formed. The shape of the spectrum changed as the pH changed. An isosbestic

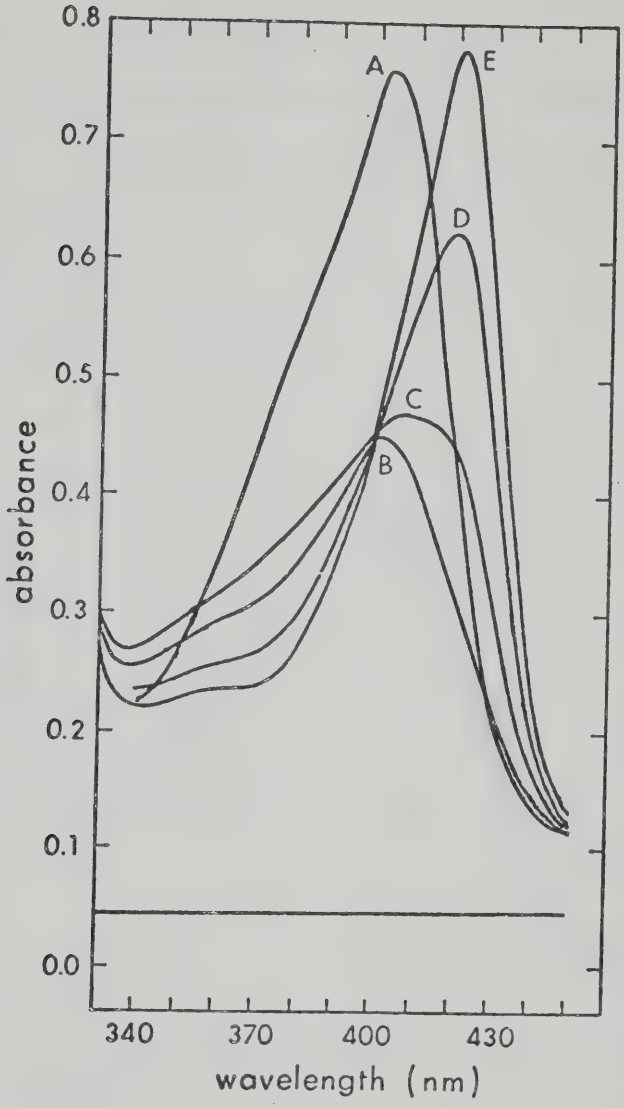

Fig. 3.4 The spectra A of HRP and B of HRP-I at pH 10.51 in carbonate buffer. Immediately after the addition of a half molar equivalent of Pummerer's ketone to HRP-I spectrum C was recorded. Spectra D and E were recorded 4 and 8 minutes later. The quantitative conversion of HRP-I with no further reaction of HRP-II is indicated by spectrum E and the isosbestic point at 398 nm. The H_2O baseline is included.

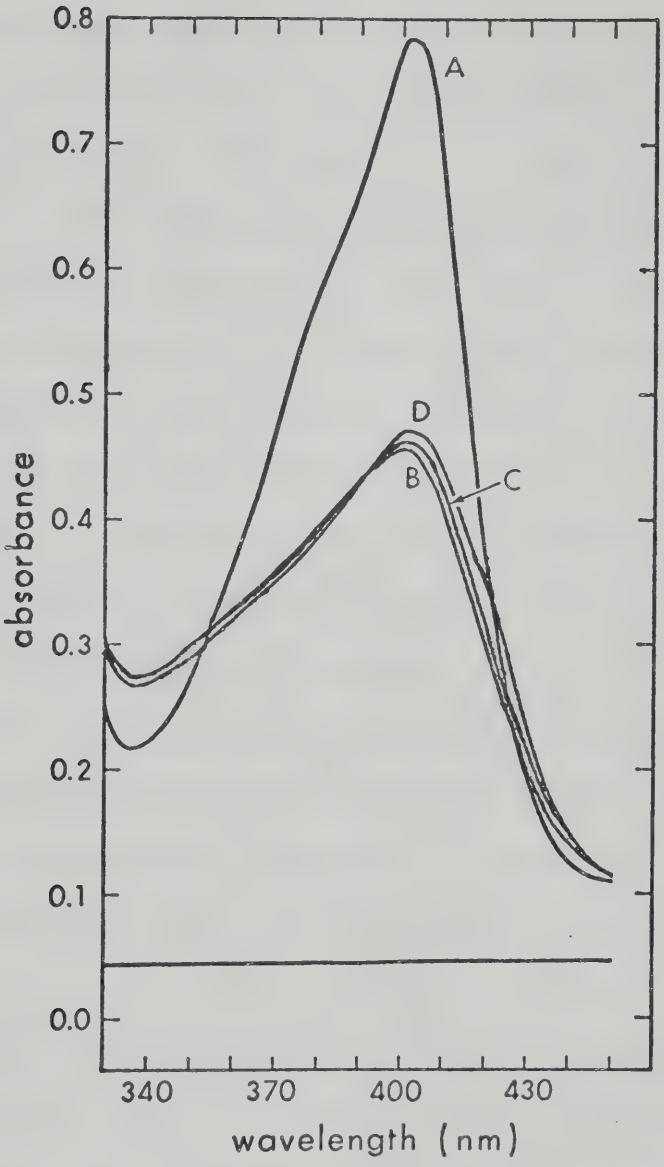

Fig. 3.5 The same experiment described in Fig. 3.4 except at pH 7.06 in phosphate buffer. Pummerer's ketone is unreactive at this pH because very little HRP-II was formed after 8 minutes, spectrum D.

wavelength of 272 nm was found from pH 7.10 to about 11.5 indicating tne interconversion of only two forms (assuming that there is no third species with a spectrum identical to one of the other two). From pH 11.5 to 14.3 the isosbestic point at 272 nm was lost as another distinct species appeared, and a new isosbestic wavelength occurred at 334 nm representing the interconversion of the second and a third form of Pummerer's ketone. The maximum absorption difference among all three forms occurred at 295 nm. Fig. 3.6 shows two spectrophotometric titration curves at different wavelengths. Curve A corresponds to the absorbance at 295 nm, A_{295}, and curve B corresponds to the absorbance at 272 nm, A_{272}, the isosbestic wavelength between the first and second species, so that it corresponds to the formation of the third species. A scheme to explain these results is illustrated in Fig. 3.7. The first inflection with increasing pH in curve A probably corresponds to the ionization of a proton from the carbon atom at position 4 of Pummerer's ketone (I) which yields the enolate anion (III). Structure III is written as a resonance hybrid of the canonical forms (IV), a carbanion, and (V), an oxyanion. The enolic form of Pummerer's ketone (II) is also in equilibrium with III. The second inflection in curve A corresponds to either the addition of hydroxide ion to III or the ionization of another proton from III. The β-addition of hydroxide ion to carbon at position 1 is more plausible since the protons on III are probably not sufficiently acidic to be removed in aqueous solution. The

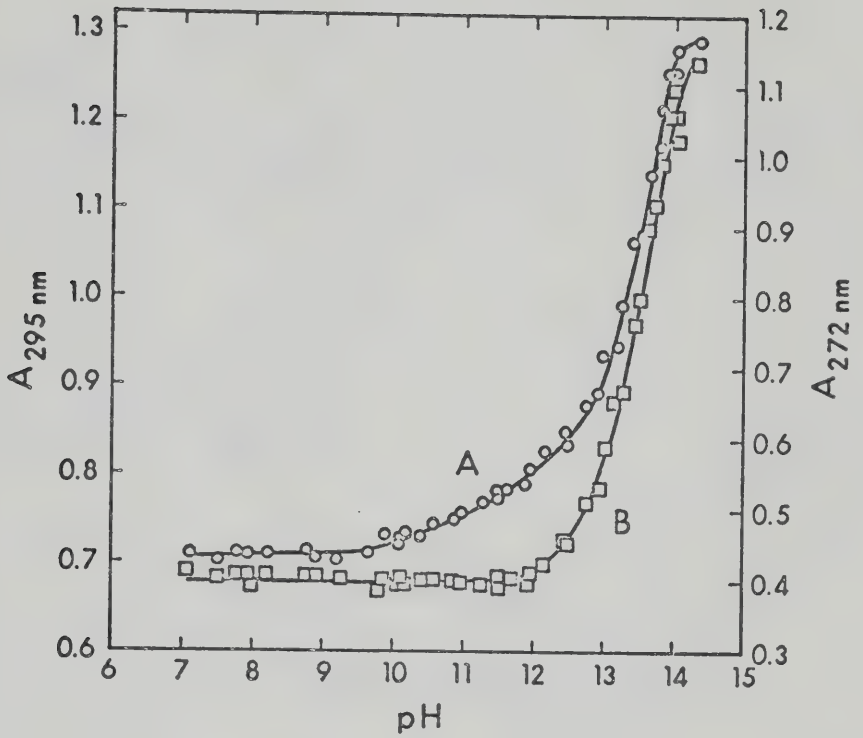

Fig. 3.6 Two spectrophotometric titration curves at different wavelengths: curve A, 295 nm and curve B, 272 nm. Curve B is at the isosbestic wavelength between Pummerer's ketone and the enolate anion, hence the absorbance change shows only the appearance of a third species at high pH. Curve A shows two inflections. The smooth lines were calculated using Equation [16], and the best fit parameters (Table 3.1) were obtained by nonlinear least squares analysis. The total concentration of all forms of Pummerer's ketone, $[I]_{total}$, is 0.266 mM.

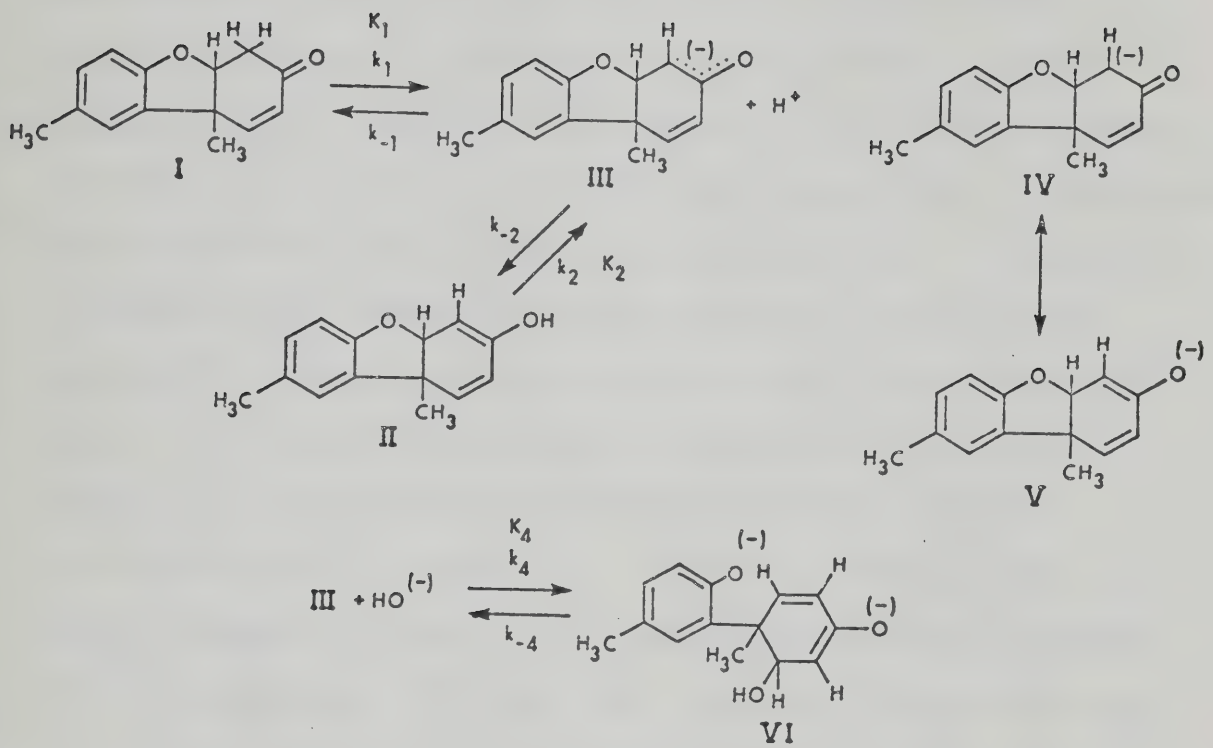

Fig. 3.7 A possible scheme for the ionization of Pummerer's ketone and enol formation. Pummerer's ketone (I) ionizes to give its enolate anion (III) which is written as a resonance hybrid of the canonical forms (IV), a carbanion, and (V), an oxyanion. III is also in equilibrium with the enol form (II). K_1 and K_2 are acid dissociation constants. β-Addition of hydroxide ion to III can form species VI. K_4 is the equilibrium constant for the formation of VI.

three α-carbonyl protons of Pummerer's ketone were exchanged with deuterium by dissolving the ketone in a solution of sodium deuteroxide in deuterium oxide. These protons can also be exchanged in deuterated methanol with a trace of alkoxide (33). However, the exchange of the proton on carbon at position 2 need not occur through ionization. A β-addition of deuteroxide ion to carbon at position 1 can be followed by exchange and then elimination thereby deuterating at position 2. Therefore the species at high pH is formulated as VI. The yellow sodium salt of Pummerer's ketone was shown to be a monosodium salt by titrating the sodium hydroxide which is formed as a hydrolysis product when the salt is added to water. The reversibility of the formation of VI was affirmed by dissolving Pummerer's ketone in warm 1.0 M NaOH, which gives a bright yellow solution, and titrating with 1.0 M HCl to obtain a precipitate which was identified by NMR to be unchanged Pummerer's ketone. The two inflections in the plot of A_{295} *vs.* pH cannot be explained solely in terms of I, II, and III as it can be shown that this scheme would exhibit one inflection. It is necessary to include the formation of VI. Considering the concentration of the enol (II) to be relatively small (large K_2), then Equation [16]

$$[16] \qquad A_{295} = \frac{[I]_{total}\left(\frac{\varepsilon_I[H^+]}{K_1} + \frac{\varepsilon_{VI}K_4K_w}{[H^+]} + \varepsilon_{III}\right)}{\frac{[H^+]}{K_1} + \frac{K_4K_w}{[H^+]} + 1}$$

can be derived using the conservation relations for the total absorbance, A_{295}, and the total concentration of all forms of Pummerer's ketone, $[I]_{total}$. The molar absorptivities at 295 nm for Pummerer's ketone (I), the enolate anion (III), and VI are ε_I, ε_{III}, and ε_{VI}. K_1 is the acid dissociation constant for Pummerer's ketone and K_4K_w is the product of the equilibrium constant of the formation of VI and the autoprotolysis constant of water. The data in curve A of Fig 3.6 and Equation [16] were used in a nonlinear least squares analysis to evaluate the constants. When the data in curve B are fit to Equation [16] the same values for the equilibrium constants are obtained within their standard deviations. The best fit values of the constants are compiled in Table 3.1 and were used to calculate the smooth lines through the data in Fig. 3.6.

It has been shown that the ionized form of *p*-cresol, the *p*-cresolate anion, does not react with HRP-I (1) or HRP-II (29). A phenol is a completely enolized compound, and since a wide variety of un-ionized phenols can reduce HRP-I (23) it is reasonable to expect the enol and not the enolate anion to be the reactive form of Pummerer's ketone. The slow reaction rate at pH 10.51 might be caused by the low concentration of the enol. In the experiment described in Fig 3.4, 8 minutes were required to complete the reduction of HRP-I by a half mole of Pummerer's ketone.

A simple stopped-flow experiment proved that the formation of the oxidizable form of Pummerer's ketone as

Table 3.1 The best fit values of the parameters in Equation [16] obtained from a nonlinear least squares analysis of the data in curve A of Fig. 3.6

Parameter	Best Value[a]
ε_I ($M^{-1}cm^{-1}$)	$(3.14\pm0.01)\times10^3$
ε_{III} ($M^{-1}cm^{-1}$)	$(3.50\pm0.02)\times10^3$
ε_{VI} ($M^{-1}cm^{-1}$)	$(6.29\pm0.08)\times10^3$
pK_1	10.7 ± 0.1
$p(K_4K_w)$	13.52 ± 0.03

[a]Errors represent standard deviations computed in the analysis

depicted in Fig 3.7 is relatively slow. With a concentration of 1.0 μM HRP-I and a total concentration of 135 μM Pummerer's ketone in all its forms in the observation cuvette at pH 9.64, the observed exponential trace on the oscilloscope was not that of a first-order reaction. The curve was biphasic showing a relatively fast reduction of HRP-I followed by a much slower one. At time zero the solution contained HRP-I, the ketone, enol, and enolate anion. The concentration of VI is negligible at this pH. The relative proportions of these forms of Pummerer's ketone is pH dependent, and the biphasic reaction can be explained from these relative proportions. Using the value of K_1 from Table 3.1 the concentration of the enolate anion can be calculated to be about 11 μM which is more than a tenfold excess with respect to the concentration of HRP-I. If the enolate anion were the reactive form, pseudo first-order kinetics, not biphasic kinetics, would be obtained. At pH 9.64 the concentration of the reactive form of Pummerer's ketone was apparently less than 1.0 μM. The fast reduction of a fraction of the HRP-I corresponds to the immediately available reactive species, and was followed by a slow reduction corresponding to a rate limiting formation of the reactive species. The data from the reaction trace were plotted as $\ln [(V_o-V_\infty)/(V_t-V_\infty)]$ *vs.* time, and the plot is shown in Fig. 3.8. The nonlinearity illustrates the biphasic reaction. The second section of the plot is linear for more than two half-lives and can be used to determined the ob-

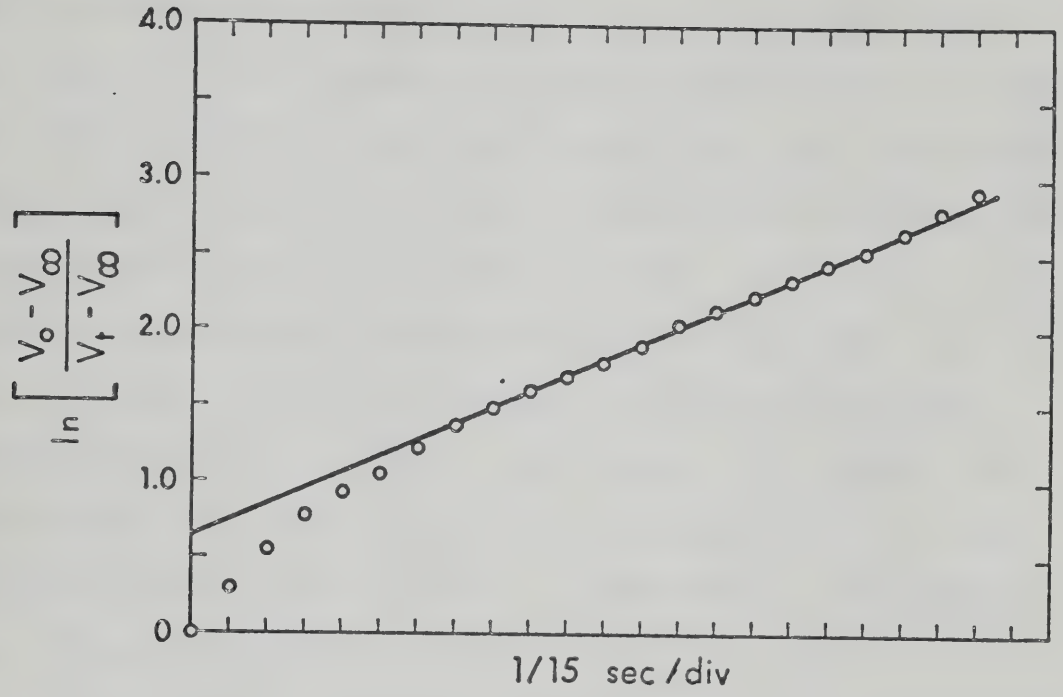

Fig. 3.8 Logarithmic plot for the reaction of HRP-I (1.0 μM) with Pummerer's ketone (135 μM) at pH 9.64. The fast initial rate corresponds to the reaction of HRP-I with less than one mole equivalent of the reactive form of Pummerer's ketone present at time zero. The slower reaction corresponds to the rate limiting removal of hydrogen ion from carbon at position 4 necessary to form the reactive enol or the rate limiting protonation of the enolate anion to form the enol. A k_{obs} value of 1.6 s^{-1} can be determined from the linear part of the slope which extends for more than two half-lives.

served first-order rate constant, k_{obs}, which is about 1.6 s^{-1}. The formation of the enol (II) via the enolate anion (III) involves ionization of hydrogen from carbon. In contrast with the dissociation of many weak acids the proton on carbon is removed relatively slowly, and the equilibrium between the ketone and the enol is therefore not established rapidly (40) which is typical of pseudo acids (41). Enol formation by protonation of the enolate anion may also be rate limiting. The rate constants of recombination for hydrogen ions and anions are very large (42), however the velocity of recombination may be relatively small at high pH values due to the very small concentration of hydrogen ion. From the scheme in Fig. 3.7, k_{obs} is a pseudo first-order rate constant for the protonation of the enolate anion and equals $k_{-2}[H^+]$ ($[H^+]$ is buffered).

The concentration of the enol as the reactive form can be calculated at time zero from the intercept of the extrapolated linear section of the plot in Fig. 3.8 to be about 0.53 μM. This permits a calculation of K_2 since the pH, the concentration of the enolate anion, and the concentration of the enol are known. With the equilibrium data the rate of the reverse reaction can be calculated. The values are recorded in Table 3.2.

Pummerer's ketone can only be oxidized in its enolic form and consequently is more readily oxidized at high pH. This might appear to provide an explanation of the events in the single turnover experiments depicted in Equations [4],

Table 3.2 The calculated values of some equilibrium and rate constants from Fig. 3.7

Constant	Calculated Value [a]
pK_2	8.3±0.1
k_{-2} ($M^{-1}s^{-1}$)	$(7\pm2)\times10^{9}$
k_2 (s^{-1})	$(3\pm2)\times10^{1}$

[a] Errors were calculated from these estimated errors, pH ±0.03, [enol] = 0.5±0.1 μM, and k_{obs} 1.6±0.2 s^{-1}; and from the standard deviations for the constants evaluated by nonlinear least squares analysis.

[11], [14], and [15] where only HRP-I is reacting. However, the reaction between Pummerer's ketone and HRP-I or HRP-II proceeds very slowly at other than high values of pH due to the relatively small concentration of the enolate anion and hence of the enol. Fig. 3.5 shows that the keto form which is predominantly present at neutral pH is unreactive, and at the high pH necessary for a significant amount of enolization a catalytically important acid group on HRP-II is ionized thus rendering it unreactive. The ionized form of HRP-II above pH 8.6 has been shown to be unreactive with several substrates (13,29,32). The reactivity of HRP-II with the enol at pH 10.51 was tested by adding a tenfold excess of Pummerer's ketone to a solution of HRP-II and observing the spectral changes. After 15 minutes there were no changes in the spectrum of HRP-II. An experiment at pH 9.51 showed that very little of the reactive form of Pummerer's ketone was present making reaction with HRP-I or HRP-II slow. There is no pH where both HRP-II and Pummerer's ketone can exist predominantly in their reactive forms.

Comparison of Transient State and Steady State Results

The similarities and differences of the *p*-cresol oxidation products obtained from HRP in the steady state and in the single turnover experiments will now be examined. The single turnover of one mole of HRP-I to HRP-II to HRP by one mole of *p*-cresol occurs from pH 3.5 to 10.2. Hence, HRP-II must react with $(PC)_2$ over this pH range. The unreactivity of HRP-II with Pummerer's ketone at high pH and

the extreme slowness of the reaction at neutral pH indicates that the free radical product represented by $(PC)_2$ in Equations [11], [12], and [14] is not Pummerer's ketone. A more suitable possibility for $(PC)_2$ is 2,2'-dihydroxy-5,5'-dimethylbiphenyl which, as shown in Fig. 3.3, was formed in the steady state reaction in small amount. This biphenol would very likely be reactive with HRP-II over a wide pH range; it would satisfy the 2:1 stoichiometry requirement of Equations [12] and [14]; and it would explain the following rate anomaly. Spectrum B of Fig. 3.1 was recorded as soon as possible after the addition of a half mole of *p*-cresol at pH 10.51. The reduction of HRP-I to HRP-II was complete within the time of less than 20 s to reach 420 nm. It is evident from Fig 3.4 that about 8 minutes are required for Pummerer's ketone to reduce HRP-I to HRP-II at pH 10.51 and therefore that Pummerer's ketone could not be responsible for reducing the second molar equivalent of HRP-I in spectrum B of Fig. 3.1. However, if $(PC)_2$ is the biphenol product, reduction could be complete within 20 s since phenols are facile substrates for peroxidase.

Therefore the biphenol and not Pummerer's ketone is the major oxidation product of *p*-cresol in the single turnover experiments. Since Pummerer's ketone is the chief steady state oxidation product of *p*-cresol, the assumption that the steady state and single turnover products are the same cannot be valid. There are reasonable arguments to support this assertion. Although Shiga and Imaizumi (9) have used

EPR to show that the free radical produced by the reaction of peroxidase and *p*-cresol is a *p*-methylphenoxy radical it may have significant *para* radical character since this would be a relatively stable tertiary radical. This electrophilic radical will react with the most available electron source which may differ greatly between the steady state and single turnover experiments. The greatest difference between the two experiments is the concentration of *p*-cresol. In the steady state experiment Pummerer's ketone may be formed via electrophilic attack of *p*-cresol by the *p*-methylphenoxy radical. Oxidative dimerizations can occur by the substitution of one radical into a neutral *p*-cresol molecule followed by further oxidation (21). Even if the rate constant of this electrophilic attack is relativly small compared to the rate constants of other possible radical reactions, the velocity of the reaction would be large due to the high concentration of *p*-cresol (0.11 M) in the steady state experiment. Pummerer's ketone might be formed as shown in Equation [17]. Electrophilic attack of *p*-cresol occurs in accord with the generalization that hydroxy groups are *ortho* directors when a methyl group blocks the *para* position. VIII might be oxidized by another *p*-methylphenoxy radical to give IX. To complete the formation of Pummerer's ketone a β-addition occurs (21).

In contrast the single turnover experiments contain no excess *p*-cresol. The formation of the *p*-methylphenoxy radical is fast (1), and without the scavenging effect of

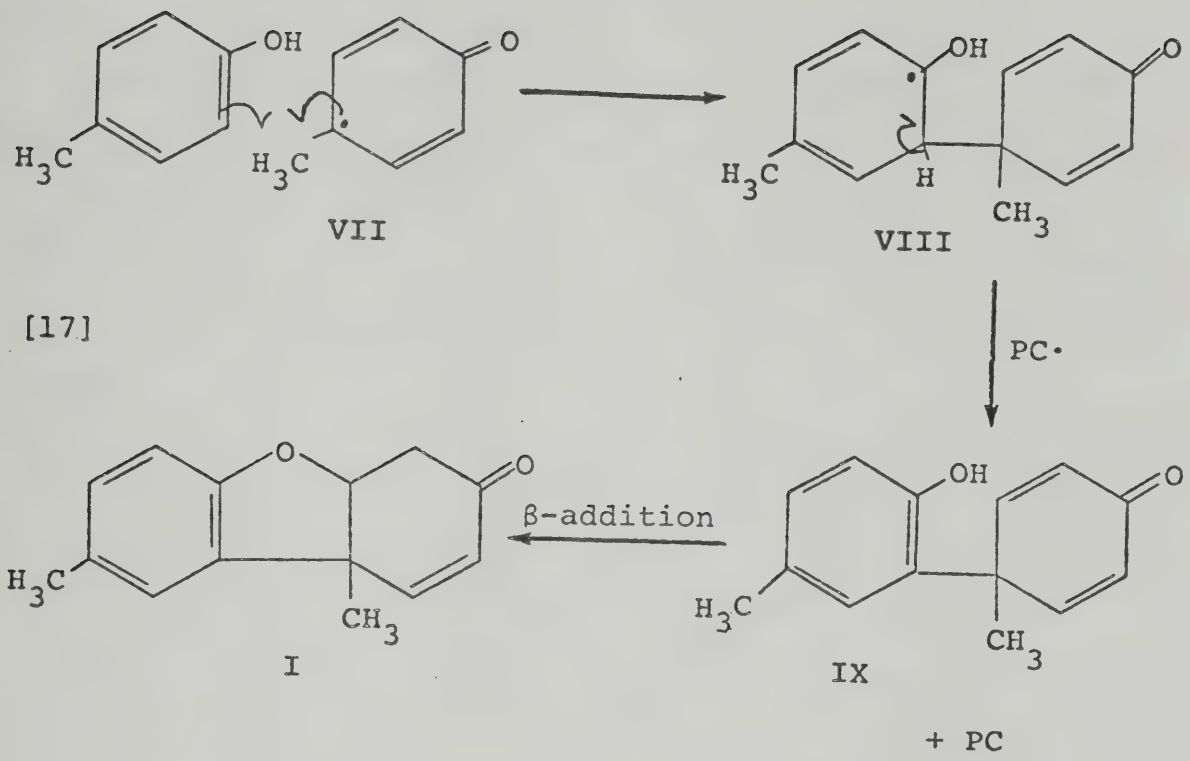

p-cresol two radicals may dimerize. The unpaired electron resides on the oxygen atom (9), but dimerization to form *p*-methylphenyl peroxide is unlikely since it would tend to dissociate reforming the two radicals. It is possible that the *p*-methylphenoxy radical also has significant *ortho* radical character (X), and 2,2'-dihydroxy-5,5'-dimethyl-biphenyl (XII) may be formed as in Equation [18]. Even if some of the terphenyl analogous to XII was formed by the free radicals in the single turnover experiments, it would also be capable of reducing HRP-II.

Although the reactivity of Pummerer's ketone with HRP-I at high pH might explain the quantitative yield of HRP-II in Fig. 3.1 spectrum B, this is better explained by the biphenol (XII) as it was a single turnover experiment. It also

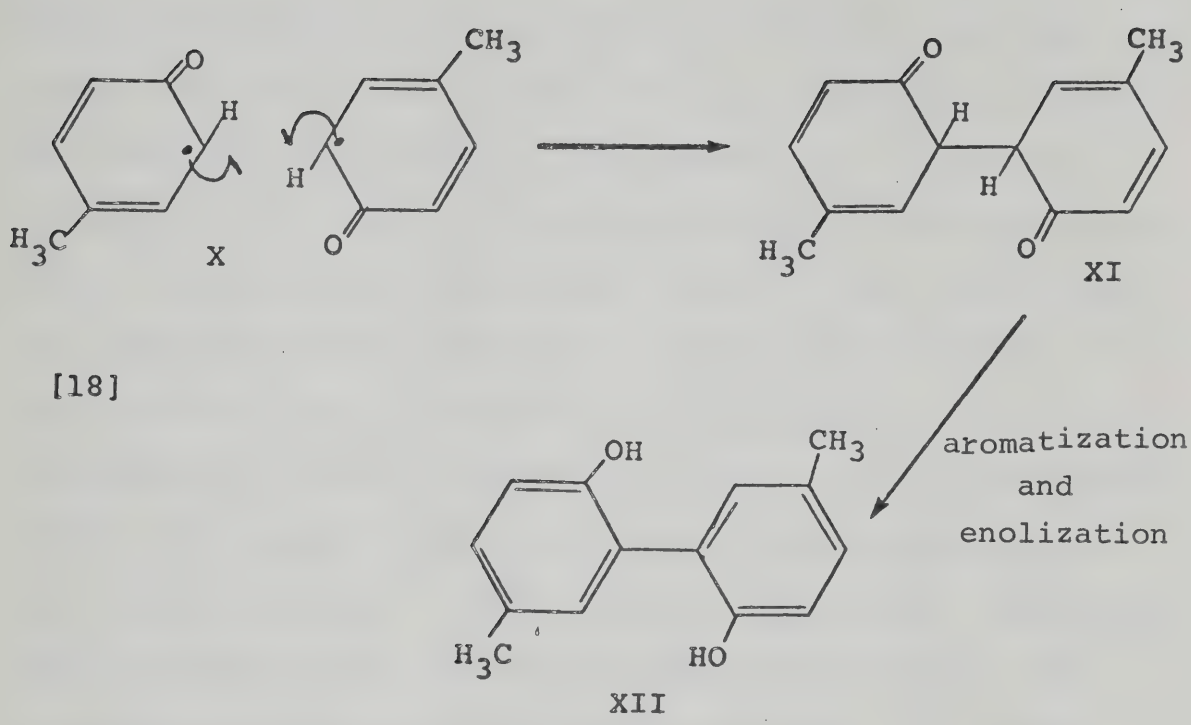

explains the rate anomaly.

It was disconcerting to realize that the complete single turnover in which HRP-I is converted quantitatively to HRP by the donation of two molar equivalents of electrons from one molar equivalent of *p*-cresol may involve a step, Equation [12], which also proceeds with a 2:1 stoichiometry. The same is true for the addition of a half molar equivalent of *p*-cresol to HRP-I (Equation [14]). An investigation of one stoichiometry problem immediately presented another stoichiometry problem. The first step in the solution of this second problem should be to identify the oxidation products of Pummerer's ketone and the biphenol in the single turnover experiments. This would be difficult for the following reasons. A single turnover of 100 mg of HRP with

Pummerer's ketone or the biphenol as the substrate would yield less than 0.4 mg of the oxidation product if it could be isolated quantitatively. HRP cannot be cycled in the steady state at high pH to oxidize Pummerer's ketone because HRP-II cannot react in its basic form. A very large excess of Pummerer's ketone relative to the enzyme is difficult to obtain due to the low solubility of the ketone in water. Although the biphenol could be oxidized by HRP in the steady state, the probable oxidation product is the corresponding 2,2'-diphenoquinone. Unless heavily substituted, especially with methoxy groups, 2,2'-diphenoquinone derivatives are extremely unstable and consequently difficult to isolate (43-45). Also, as this chapter has indicated, analysis of steady state products may have severe limitations in defining products from single turnover experiments.

To identify the oxidation product of Pummerer's ketone the only alternative is to rely on a model system. Potassium ferricyanide was initially chosen as a model oxidant because it oxidizes *p*-cresol by dehydrogenation as does HRP, and both oxidants give essentially the same products (46). Several unsuccessful attempts, with varying conditions of solvent and pH to promote enolization, were made to oxidize Pummerer's ketone with potassium ferricyanide. Coupled gas chromatography and mass spectometry consistently showed the reaction mixture extracts to cantain only unchanged Pummerer's ketone.

Another possibility for a model oxidant involves the

deuterohemin-H_2O_2 complex. Portsmouth and Beal (47) have shown this complex to behave like peroxidase with a variety of substrates. This complex can mimic HRP-I in several respects, and it has no intermediate analogous to HRP-II to prevent the steady state cycle. However, their results showed that oxidative breakdown of deuterohemin was a problem which was accelerated by excess hydrogen peroxide. Hence, this model system is of dubious value because the deuterohemin would have to be cycled in the steady state with excess hydrogen peroxide in order to produce an amount of the Pummerer's ketone oxidation product necessary for identification.

A possible product of the peroxidation of Pummerer's ketone is shown in structure XV and perhaps formed as shown in Equation [19]

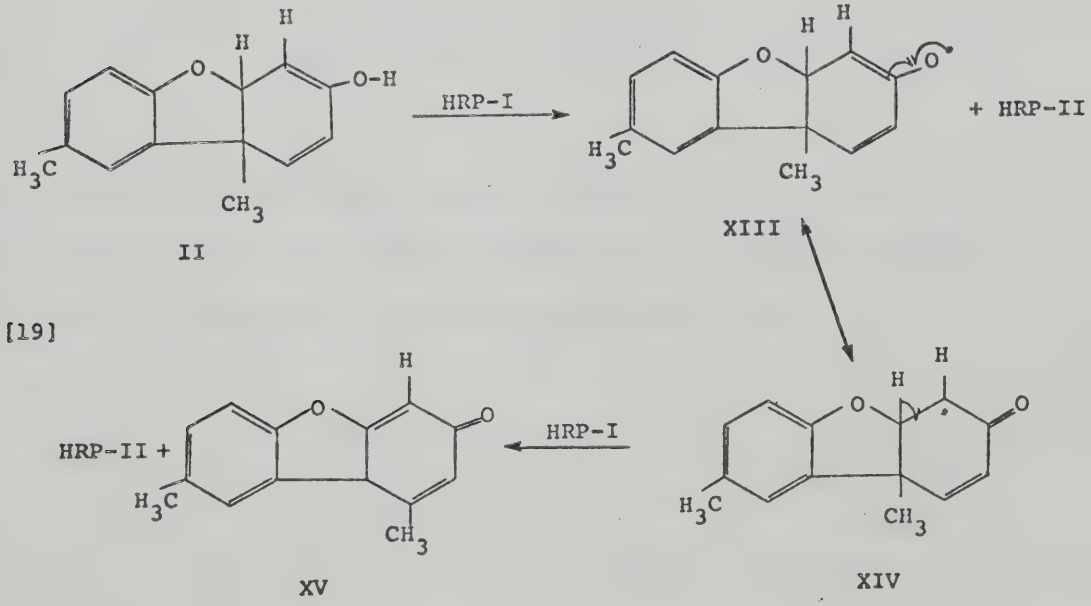

[19]

According to this scheme, the reactive enol (II) is dehydrogenated by one mole of HRP-I to yield HRP-II and the enol radical represented by the two canonical structures XIII and XIV. The second mole of HRP-I dehydrogenates the methine hydrogen (position 4a) to give XV. The required 2:1 stoichiometry, Equation [14], for the reduction of HRP-I to HRP-II is met by this scheme.

The 2:1 stoichiometry for the oxidation of guaiacol by HRP found by Santimone (25) might be best explained with a mechanism similar to that used for *p*-cresol. The *o*-methoxyphenoxy radical, G·, dimerizes to yield 2,2'-dihydroxy-5,5'-dimethoxybiphenyl, $(G)_2$, which has been isolated as a product of the peroxidase oxidation of guaiacol (8).

[7] $\text{HRP-I} + \text{G} \longrightarrow \text{HRP-II} + \text{G}\cdot$

[20] $\text{G}\cdot \longrightarrow \tfrac{1}{2}(\text{G})_2$

[21] $\text{HRP-II} + \tfrac{1}{2}(\text{G})_2 \longrightarrow \text{HRP} + \text{Products}$

---

[22] $\text{HRP-I} + \text{G} \longrightarrow \text{HRP} + \text{Products}$

This biphenol can very likely undergo further oxidation and reduce HRP-II to HRP. A probable oxidation product of $(G)_2$ is a 2,2'-diphenoquinone derivative (XVI).

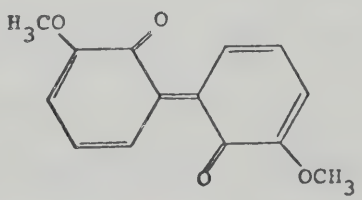

XVI

Derivatives of 4,4'-diphenoquinones are well known, and those of 2,2'-diphenoquinone although much less common are known to exist especially when substituted with methoxy groups (43-45). The tetrameric product formed by the peroxidase oxidation of guaiacol (8,48) may be a oxidized dimer of 2,2'-dihydroxy-5,5'-dimethoxybiphenyl.

Acknowledgments

Thanks are due to R. O'Donnell for assistance with the chromatographic techniques, and are due to Profs. W.A. Ayer, J. Hooz, K.R. Kopecky, and H.J. Liu for helpful discussions.

3.5 References

1. Hewson, W.D., and Dunford, H.B. (1976) *J. Biol. Chem.* 'in press'
2. Hassinoff, B.B, and Dunford, H.B. (1970) *Biochemistry* 9, 4930-4939
3. Chance, B. (1952) *Arch. Biochem. Biophys.* 41, 416-430
4. George, P. (1952) *Nature* 169, 612-613
5. George, P. (1953) *Biochem. J.* 54, 267-276
6. Elliott, K.A.C. (1932) *Biochem. J.* 26, 1281-1290
7. Westerfeld, W.W., and Lowe, C. (1942) *J. Biol. Chem.* 145, 463-470
8. Bootn, H., and Saunders, B.C. (1956) *J. Chem. Soc. (London)* 940-948
9. Shiga, T., and Imaizumi, K. (1975) *Arch. Biochem. Biophys.* 167, 469-479

10. Pummerer, R., Melamed, D., and Puttfarcken, H. (1922) *Ber.* 55, 3116-3132

11. Hubbard, C.D., Dunford, H.B., and Hewson W.D. (1975) *Can. J. Chem.* 53, 1563-1569

12. Schonbaum, G.R., and Lo, S. (1972) *J. Biol. Chem.* 247, 3353-3360

13. Cotton, M.L., and Dunford, H.B. (1973) *Can. J. Chem.* 51, 582-587

14. Herington, E.F.G., and Kynatson, W. (1957) *Trans. Faraday Soc.* 53, 138-142

15. Loev, B., and Goodman, M.M. (1970) in Progress in Separation and Purification (Perry, E.S., and Van Oss, C.J., eds) Vol. 3, pp. 73-95, Wiley-Interscience, Toronto

16. Chance, B. (1952) *Arch. Biochem. Biophys.* 37, 235-237

17. Roman, R., and Dunford, H.B. (1973) *Can. J. Chem.* 51, 588-596

18. Roman, R., and Dunford, H.B. (1972) *Biochemistry* 11, 2076-2082

19. Ohnishi, T., Yamazaki, H., Iyanagi, T., Nakamura, T., and Yamazaki, I. (1969) *Biochim. Biophys. Acta* 172, 357-369

20. Pummerer, R., Puttfarcken, H., and Schopflocher, P. (1925) *Ber.* 58, 1808-1820

21. Barton, D.H.R., Deflorin, A.M., and Edwards, O.E. (1956) *J. Chem. Soc. (London)* 530-534

22. Arkley, V., Dean, F.M., Robertson, A., and Sudisunthorn, P. (1956) *J. Chem. Soc. (London)* 2322-2328

23. Job, D., and Dunford, H.B. (1976) *Eur. J. Biochem.* 66, 607-614

24. Danner, D.J., Brignac, Jr., P.J., Arceneaux, D., and Patel, V. (1973) *Arch. Biochem. Biophys.* 156, 759-763

25. Santimone, M. (1975) *Can. J. Biochem.* 53, 649-657

26. Bielski, B.H.J., and Gebicki, J.M. (1974) *Biochim. Biophys. Acta* 364, 233-235

27. Bielski, B.H.J., Comstock, D.A., Haber, A., and Chan, P.C. (1974) *Biochim. Biophys. Acta* 350, 113-120

28. Chen, C.-L., Conners, W.J., and Shinker, W.M. (1969) *J. Org. Chem.* 34, 2966-2971

29. Critchlow, J.E., and Dunford, H.B. (1972) *J. Biol. Chem.* 247, 3703-3713

30. Knoblauch, O. (1898) *Z. Physik. Chem.* 26, 96-108

31. Frost, A.A., and Schwemer, W.C. (1952) *J. Am. Chem. Soc.* 74, 1268-1273

32. Dunford, H.B., and Cotton, M.L. (1975) *J. Biol. Chem.* 250, 2920-2932

33. Kirby, G.W., and Tiwari, H.P. (1964) *J. Chem. Soc. (London)* 4655-4657

34. Bowden, K., and Reece, C.H. (1950) *J. Chem. Soc. (London)* 2249

35. Kaeding, W.W. (1963) *J. Org. Chem.* 28, 1063-1067

36. Sugita, J. (1966) *Nippon Kagaku Zasshi* 87, 603-607

37. Kametani, T., Ohkubo, K., and Takano, S. (1968) *Chem. Pharm. Bull. (Tokyo)* 16, 1095-1097

38. Brown, B.R., and Bocks, S.M. (1963) in Enzyme Chemistry of Phenolic Compounds, Proceedings of the Plant Phenolics Group Symposium (Pridham, J.B., ed) pp. 129-138, Pergamon Press, New York

39. Dobson, G., and Grossweiner, L.I. (1965) *Trans. Faraday Soc.* 61, 708-714

40. Hantzsch, A. (1899) *Ber.* 32, 575-600

41. Bell, R.P. (1959) in The Proton in Chemistry pp. 13-16, Cornell University Press, New York

42. Eigen, M., Kruse, W., Maass, G., and De Maeyer, L. (1964) in Progress in Reaction Kinetics (Porter, G., ed) Vol. 2, pp. 285-318, MacMillan, New York

43. Schulte-Frohlinde, D., and Erhardt, F. (1964) *Ann.* 671, 92-97

44. Hewgill, F.R., and Hewitt, D.G. (1967) *J. Chem. Soc. (C)* 723-725

45. Adderly, C.J.R., and Hewgill, F.R. (1968) *J. Chem. Soc. (C)* 1434-1438

46. Scott, A.I. (1965) *Quart. Rev. (London)* XIX, 1

47. Portsmouth, D., and Beal, E.A. (1971) *Eur. J. Biochem.* 19, 479-487

48. Santimone, M., and Dou, H.M.M. (1974) *C.R. Acad. Sci. Paris (Series C)* 278, 1469-1471

CHAPTER IV. ARRHENIUS ACTIVATION ENERGY FOR THE FORMATION OF HORSERADISH PEROXIDASE COMPOUND I

4.1 Summary

The rate of formation of Compound I from the reaction of native horseradish peroxidase with hydrogen peroxide was studied from 3.7 to 70.0°. The second-order rate constants were used to construct an Arrhenius plot from which the activation energy of this reaction was calculated to be 3.5±1.0 kcal/mole. The irreversibility of the reaction at 25° was confirmed by comparing the absolute absorbance changes as recorded by the stopped-flow apparatus with the known spectra of the native enzyme and Compound I.

4.2 Introduction

The stoichiometric reaction for the formation of Compound I from HRP is

[1] $$HRP + H_2O_2 \longrightarrow \text{Compound I}$$

and is known to be second order over a range of substrate concentrations (1). The first temperature dependence of the rate of this reaction was undertaken in 1947, at which time there appeared to be no significantly measurable increase in rate with temperature (2,3). The reverse rate of reaction 1 has been considered to be very small, approximately seven orders of magnitude smaller than the forward rate (1). The

present paper describes experiments performed to obtain the temperature dependence of the reaction from which the activation energy for the formation of Compound I can be calculated. Also, changes in absorbance measurements have been used to verify the essential irreversibility of this reaction.

4.3 Experimental

Materials

Horseradish peroxidase (Lot No. 7024524) was purchased from Boehringer-Mannheim Corp. as an ammonium sulfate precipitate and was prepared for use by extensive dialysis aganst multiply distilled water followed by Millipore filtration. Isozyme C, using the notation of Shannon *et al.* (4) and of Paul and Stigbrand (5) has been determined to be the major component of HRP obtained from Boehringer-Mannheim Corp. (6). Despite some fairly complicated kinetics, there has never been any valid kinetic evidence for a detectable amount of a second isozyme component (7). Enzyme purity and concentration were determined from absorbance measurements at 280 and 403 nm. A purity number of 3.54 was obtained. Published values usually lie between 2.8 and 3.2. It was found that extensive dialysis tends to increase PN values. Multiply distilled water was used throughout and buffers were made from reagent grade materials.

Apparatus

Kinetic runs were carried out on a Gibson-Durrum stopped-flow spectrophotometer model D-110 in the absorbance mode at 403 nm with a 2 cm cuvette. Steady-state spectra and absorbance measurements were made on a Cary 14 spectrophotometer, pH was measured with an Orion 801 pH meter outfitted with a Fisher combination electrode calibrated with fresh standard buffers, and solution temperatures were maintained to ±0.3° by circulating thermostated water. The upper limit of the temperature range was 70.0° because at any higher temperature a significant amount of HRP denatured during the incubation period. A check for decomposition of hydrogen peroxide and/or enzyme was carried out by incubating the solutions in the drive syringes for a period of time approximately equal to the time necessary to perform a kinetic experiment. Then the solutions were quickly cooled to 25° and a kinetic experiment performed in order to compare the absorbance change accompanying the reaction after incubation with the absorbance change expected without the incubation period. Because the enzyme absorption at 403 nm decreases with denaturation, the lack of a significant decrease in the absorbance change indicated no destruction of either reactant.

Methods

Stopped-flow kinetics were performed under second-order conditions where the initial concentrations of HRP and hydrogen peroxide are equal. The concentration of hydrogen

peroxide was determined as previously described (8). One drive syringe contained 2.0 μM HRP and the other contained 2.0 μM hydrogen peroxide, resulting in an initial reactant concentration of 1.0 μM for both reactants in the 2 cm cuvette. Both drive syringe solutions had phosphate buffer (pH 7.10±0.02 and ionic strength 0.01) and 0.1 M potassium nitrate as common components for a total ionic strength of 0.11. The reaction resulted in a decrease in absorbance as a function of time because the molar absorptivity at 403 nm for Compound I is less than for HRP (ε_{HRP}= 1.02×10^5 $M^{-1}cm^{-1}$ (9) and $\varepsilon_{Compound\ I}$= 5.31×10^4 $M^{-1}cm^{-1}$ (10, 11)). Checks of the absorbance changes recorded by both instruments should be the same. In the experiments performed on a Cary 14 spectrophotometer, initiation of the formation of Compound I was accomplished using a few microliters of hydrogen peroxide (equimolar with respect to HRP) on the end of a Teflon plumper.

Steady-state spectra, initiated in the same fashion, were recorded with [HRP] = 2.0 μM, $[I^-]$ = 10.0 μM, and $[H_2O_2]$ = 4.0 μM. The steady-state spectrum of such a reaction mixture is known to be that of Compound I (11). To achieve the steady state for a sufficiently long period of time to record the spectrum (about 50 s), the enzyme must cycle many times, the period of the cycle depending on the rate constant of the Compound I reaction with iodide ion and the concentration of iodide which govern the rate-controlling step. Iodide ion was in excess of the hydrogen peroxide so

that should the steady state end before the spectrum was scanned the enzyme would revert to the native form and no longer exist as Compound I which would facilitate detection of the end of the steady state.

The integrated rate expression for the reaction of HRP with H_2O_2 where the reactants are in equal initial concentration and combine in a 1:1 stoichiometry is

$$[2] \qquad 1/[HRP]_t = kt + 1/[HRP]_o$$

The concentration of HRP at time t was determined by

$$[3] \qquad [HRP]_t = [HRP]_o(V_t - V_\infty)/(V_o - V_\infty)$$

where V is the stopped-flow apparatus photomultiplier voltage and V_o, V_t, and V_∞ are voltages at times 0, t, and ∞. V_∞ values were determined by retriggering the data collection system (12) about 8 s after the reaction data had been recorded. Rate constants were determined from linear least-squares analyses of plots of $1/[HRP]_t$ *vs.* t. These plots were linear for 3 to 5 half-lives.

A near neutral pH of 7.10 was chosen because the rate of formation of Compound I has been shown to be virtually pH independent from pH 5 to 9 (13). Preparing solutions at this pH at room temperature served to minimize any change in rate that might be a consequence of the change in pH of the solution with temperature.

4.4 Results and Discussion

The Arrhenius plot shown in Fig. 4.1 was constructed from the rate constants recorded in Table 4.1 and yields an activation energy of 3.5±1.0 kcal/mole. The activation energy error was estimated by raising the value of the rate constant of the highest temperature and lowering the value of the rate constant at the lowest temperature by half of the experimental error in the average rate constant determination; a new slope was calculated using these two points and gave a new activation energy different by 1.0 kcal/mole. The value of the activation energy corresponds to isozyme C. The activation energy of Compound I formation with hydrogen peroxide has recently been determined for isozymes A2 and C to be 4.0 and 2.2 kcal/mole, respectively. These values were obtained from measurements at three temperatures over the range of 10 to 40° (14). If the experimental error of ±1.0 kcal/mole can also be applied to their measurements (14), then all three values are identical within experimental error. A small value for the activation energy is necessary if HRP is to be an efficient enzyme.

The transition state theory interprets the Arrhenius preexponential factor A as

$$[4] \qquad A = \frac{\kappa k T}{h} \exp\left(\Delta S^{\ddagger}/R\right)$$

where κ, k, h, and $S^{\ddagger}$ are, respectively, the transmission coefficient (usually assumed to be unity), Boltzmann's

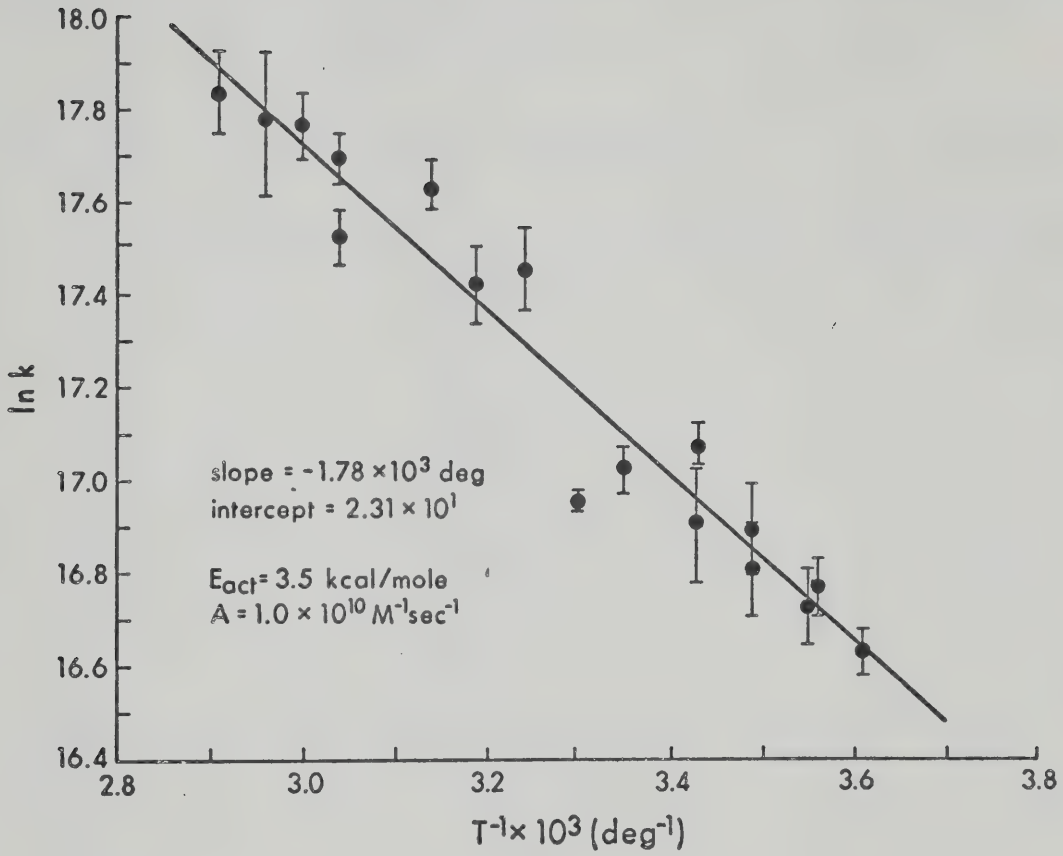

Fig. 4.1 Arrhenius plot of ln k *vs.* T^{-1}.

Table 4.1 Second-Order Rate Constants for the Formation of Compound I from Native HRP at pH 7.10.

T (°C)	$kx10^{-7}$ $(M^{-1}s^{-1})^a$	No. of Determinations
3.7	1.7±0.1	8
7.4	1.9±0.1	5
8.6	1.8±0.2	5
13.0	2.0±0.2	5
13.5	2.2±0.2	5
18.1	2.6±0.1	8
18.7	2.2±0.1	6
25.0	2.5±0.1	5
30.0	2.3±0.1	7
35.0	3.8±0.4	4
40.0	3.7±0.3	6
45.0	4.6±0.3	6
55.4	4.1±0.3	5
55.6	4.8±0.3	7
60.0	5.2±0.4	7
65.0	5.3±0.8	6
70.0	5.6±0.6	7

[a] Errors are the average deviation from the mean.

constant, Planck's constant, and the entropy of activation. The entropy of activation obtained from Equation [4] is -12.8±0.1 cal/mole-deg. The negative value can be explained in part by a reaction where the activated complex is more ordered than the two reactants (15). However, the negative entropy also correlates with a small steric factor according to collision theory, and this is to be expected for reaction at the active site of an enzyme, as discussed below.

The literature on diffusion controlled reactions is not always consistent since different assumptions and boundary conditions have been used to derive different equations (16,17). Thus the existence of any steric factor has been assumed to preclude diffusion control (18,19). However, spheres with a uniform surface were assumed to be the reactants. Such a model is not particularly satisfactory for an enzymatic reaction where the active site is localized on one portion of a large sphere or perhaps is buried in a cleft of the sphere (20,21). In an interesting publication by Schmitz and Schurr (22) it is pointed out that moderate angular constraints imposed on reactants that orient by rotational diffusion can lead to a rather drastic decrease in the maximum diffusion-controlled rate from about 10^{10} to values of 10^6 to 5×10^5 $M^{-1}s^{-1}$. They contend that it is plausible that reactions thought to be far removed from the diffusion-controlled rate might in fact be strongly viscosity dependent. The model used by these workers is a rotating sphere diffusing to a localized site on a plane. This appears

to be an accurate model for the planar ferriprotoporphyrin IX which is the active site of HRP. When a reaction rate is strongly viscosity dependent, the activation energy can in large part be determined by the temperature variation of the diffusion coefficients of the reactants as the viscosity of of the water changes and not solely determined by the fraction of reactant molecules with sufficient energy to form products. Other collisions between the enzyme's protein moiety and hydrogen peroxide may be ineffective. Since coefficients of viscosity and diffusion are inversely proportional, the criterion of a dependence on fluidity of solvent (the inverse of viscosity) as an indication of diffusion control is used here and in the following chapter (17).

Although indisputable proof that the reaction rate between HRP and hydrogen peroxide is diffusion-controlled is lacking, the conjecture is worth consideration. Since superoxide dismutase is known to react with the oxygen radical anion ($O_2^{\cdot-}$) at a rate of $(1.5\pm0.1)\times10^9$ $M^{-1}s^{-1}$ (23), it might be inferred that 10^7 $M^{-1}s^{-1}$ does not represent a diffusion-controlled rate limit. However, no entropy of activation (or steric factor) has been measured for the superoxide dismutase reaction.

When the Naperian logarithm of the fluidity of water is plotted against $T^{-1}(°K^{-1})$ over the same temperature range as the Arrhenius plot, a slope of $(-1.92\pm0.03)\times10^3$ deg is obtained (24), which when multiplied by the gas constant, R, gives the activation energy of the fluidity of water as 3.89±0.04 kcal/mole (fluidity is the reciprocal of viscosity).

This is the theoretical minimum activation energy for reactions in aqueous solution (17) and is the same as the Arrhenius activation energy for Compound I formation within experimental error.

The percentage error in the measurement of a second-order rate constant can be calculated according to the method of Benson (25). Percentage errors calculated with this method at several temperatures gave an average of 37±5%.

The study conducted in 1947 (2) quotes rate constants of 8, 9, and 9, all times 10^6 $M^{-1}s^{-1}$ at 3, 25, and 42°, respectively, which are consistently lower than the rate constants in Table 4.1 measured at comparable temperatures. Dolman *et al.* (13) have measured the rate of Compound I formation at pH 7.07 and 25° to be 1.84×10^7 $M^{-1}s^{-1}$. This value agrees more favorably with the present work.

It is interesting to compare briefly the combining rates of other heme systems with oxygen containing substrates. The rate of lactoperoxidase Compound I formation has been measured at pH 7.17 and 25° by Maguire *et al.* (26) to be 1.2×10^7 $M^{-1}s^{-1}$, and by Chance (27) at pH 7.0 to be 2×10^7 $M^{-1}s^{-1}$. The rate of formation of HRP Compound I has been measured with methyl, ethyl (1), and hydroxymethyl (28) hydroperoxides and gave the respective rate constants 1.5, 3.6, and 0.5 all times 10^6 $M^{-1}s^{-1}$ which are much slower than for hydrogen peroxide. Bonnischsen *et al.* (2) have measured the rate of hydrogen peroxide and horse blood catalase combination at 25° to be 3.5×10^7 $M^{-1}s^{-1}$.

Much of the work on the kinetics of the reaction of hemoglobin and myoglobin with oxygen has been compiled by Antonini and Brunori (29). Ilgenfritz and Schuster recently used the temperature-jump technique to measure the rate of oxygen binding to hemoglobin (30). At low oxygen saturations a fast binding step with a rate constant of 4×10^7 $M^{-1}s^{-1}$ was found and at high oxygen saturation two steps were found, a fast and a slow step with respective rate constants of 4×10^7 and 5×10^6 $M^{-1}s^{-1}$. They concluded that the first binding step occurred as fast as the last step and the low affinity of deoxyhemoglobin for oxygen arises from the fast dissociation rate of Hb_4O_2, 10^3 s^{-1}. The two hemoproteins show many similarities in their kinetics. However, electric field jump measurements have shown a time constant of 10^{-7} s for hemoglobin, but a correspondingly short time constant could not be found for myoglobin, which in the oxidized state, gave time constants of 10^{-6} s (31). The rate of reaction of horse blood catalase with hydrogen peroxide has been measured at two different temperatures and, assuming the validity of the Arrhenius equation, the activation energy was calculated to be 1.7 kcal/mole (2). This value is well below the minimum activation energy for the fluidity of water and is therefore of interesting origin.

To test whether reaction 1 was going to completion in the stopped-flow apparatus, the absorbance change, ΔA, at 25° was determined several times with an average of 0.095±0.003. The theoretical ΔA at this temperature for the same cuvette

and solution specifications is 0.0978. Steady-state spectra of Compound I reacting with iodide ion, where more than 99% of the enzyme should be in the form of Compound I, gave ΔA = 0.100 within the reading precision of the recorded spectra. These absorbance measurements substantiate the claim that reaction 1 is essentially irreversible (1).

Steady-state spectra were attempted at higher temperatures; but the much accelerated spontaneous decay of Compound I to Compound II, Which is a one electron reduction of the Compound I, interfered with the steady state. For pH values slightly greater than 7, Compound I is known to react with iodide ion approximately 10^3 times faster than Compound II (11,12). This means that any spontaneously formed Compound II will react much less readily with iodide ion and therefore accumulate in the system if it is formed spontaneously. Accumulation of some Compound II occurred at 40° thereby making accurate absorbance measurements impossible for steady-state experiments. The ΔA for steady-state spectra at 40 and 55° agreed reasonably well with the ΔA as measured at the corresponding temperature in the stopped-flow apparatus, but because of the problem of Compound I spontaneously forming Compound II, these results should probably not be relied upon to confirm the irreversibility of reaction 1 at these temperatures.

4.5 References

1. Chance, B. (1949) *Arch. Biochem. Biophys.* 22, 224-252

2. Bonnischsen, R.K., Chance, B., and Theorell, H. (1947) *Acta Chem. Scand.* 1, 685-709

3. Laidler, K.J., and Bunting, P.S. (1973) in The Chemical Kinetics of Enzyme Action 2nd Ed. pp. 199-216, Claredon Press, Oxford

4. Shannon, L.M., Kay, E., and Lew, J.Y. (1966) *J. Biol. Chem.* 241, 2166-2172

5. Paul, K.-G., and Stigbrand, T. (1970) *Acta Chem. Scand.* 24, 3607-3617

6. Phelps, C., and Antonini, E. (1969) *Biochem. J.* 114, 719-724

7. Dunford, H.B., and Cotton, M.L. (1975) *J. Biol. Chem.* 250, 2920-2932

8. Cotton, M.L., and Dunford, H.B. (1973) *Can. J. Chem.* 51, 582-587

9. Schonbaum, G.R., and Lo, S. (1971) *J. Biol. Chem.* 247, 3353-3360

10. Brill, A.S., and Sandberg, H.E. (1968) *Biochemistry* 7, 4254-4260

11. Roman, R., and Dunford, H.B. (1972) *Biochemistry* 11, 2076-2082

12. Roman, R., Dunford, H.B., and Evett, M. (1971) *Can. J. Chem.* 49, 3059-3063

13. Dolman, D., Newell, G.A., Thurlow, M.D., and Dunford, H.B. (1975) *Can. J. Biochem.* 53, 495-501.

14. Marklund, S., Ohlsson, P.J., Opara, A., and Paul, K.-G. (1974) *Biochim. Biophys. Acta* 350, 304-313

15. Dunford, H.B. (1974) *Physiol. Vég.* 12, 13-23

16. Smoluchowski, M.V. (1917) *Z. Phys. Chem.* 92, 129-168

17. Caldin, E.F. (1964) in Fast Reactions in Solution p. 12, Wiley and Sons, New York

18. Collins, F.C., and Kimball, G.E. (1949) *J. Collid. Sci.* 4, 425-437

19. Logan, S.R. (1967) *Trans. Faraday. Soc.* 63, 1712-1719

20. Hammes, G.G. (1968) in Advances in Protein Chemistry (Anfinsen, Jr., C.B., Anson, M.L., Edsall, J.T., and Richards, F.M., eds) Vol. 23, p. 17, Academic Press, New York

21. Hearno, J.Z., Bernhard, S.A., Friess, S.L., Botts, D.J., and Morales, M.F. (1959) in The Enzymes (Boyer, P.D., Lardy, H., and Myrbäck, K., eds) Vol 1, pp. 60-62, Academic Press, New York

22. Schmitz, K.S., and Schurr, J.M. (1972) *J. Phys. Chem.* 76, 534-545

23. Pich, M., Rabani, J., Yost, F., and Fridovich, J. (1974) *J. Am. Chem. Soc.* 96, 7329-7333

24. Hodgman, C.D. (ed) (1960) in The Handbook of Chemistry and Physics 41st Ed. p. 2181, Chemical Rubber Publishing Company, Cleveland

25. Benson, S.W. (1969) in The Foundations of Chemical Kinetics pp. 86-89, McGraw-Hill, Toronto

26. Maguire, R.J., Dunford, H.B., and Morrison, M. (1971) *Can. J. Biochem.* 49, 1165-1171

27. Chance, B. (1949) *Science* 109, 204-208

28. Marklund, S. (1972) *Acta Chem. Scand.* 26, 2128-2130

29. Antonini, E., and Brunori, M. (1971) Hemoglobin and Myoglobin in Their Reactions with Ligands North Holland, Amsterdam

30. Ilgenfritz, G., and Schuster, T.M. (1974) *J. Biol. Chem.* 249, 2959-2973

31. Ilgenfritz, G. (1968) *Biochem. Saurest. Colloq. Ges. Biol. Chem.* 19, 53-62

CHAPTER V. EFFECT OF GLYCEROL AND ETHANOL ON THE REACTIVITY OF HORSERADISH PEROXIDASE WITH HYDROGEN PEROXIDE AND CYANIDE

5.1 Summary

Pseudo first-order kinetics was used to show that the rate limiting step of Compound I formation of horseradish peroxidase is second order from pH 3.19 to 9.76, first order in horseradish peroxidase and first order in hydrogen peroxide. The rate is pH independent from pH 5.96 to 9.76, and at pH 7.04 it is independent of ionic strength from I=0.01 to 0.11. At pH 7.04 (measured at 25°) and 40° the rate is viscosity independent as tested in aqueous glycerol solutions, thus demonstrating that the rate is not diffusion controlled. The presence of ethanol decreases both the rate of Compound I formation and cyanide binding to the native enzyme. Since Compound I formation and cyanide binding involve ligation at the sixth coordination position of the heme moiety, the inhibition has been interpreted in terms of the binding of ethanol, probably to the sixth position. Evidence of an enzyme-ethanol complex was obtained by difference absorption and circular dichroic spectroscopy. The circular dichroic spectrum of horseradish peroxidase was studied as a function of temperature. An evaluation is made of the peroxidase reactions carried out in aqueous methanol or ethanol in which rate changes have been interpreted in terms of the dielectric constant of the solvent medium.

5.2 Introduction

The rate of Compound I formation of HRP from the reaction of the native enzyme with hydrogen peroxide has been studied over a wide range of pH (1,2). The rate is independent of pH between 5 and 9. The rate of Compound I formation at one pH value in this pH independent region has been measured as a function of temperature. On the basis of an activation energy value of 3.5 kcal/mole it was postulated that this reaction may be diffusion controlled, albeit with stringent steric requirements (3). The rate of a diffusion controlled reaction is inversely proportional to the viscosity of the medium in which it occurs. The rate of Compound I formation displayed a threefold increase from 4° to 70°; while the viscosity of water displays a 3.8-fold decrease over the same temperature range. Aqueous glycerol solutions have been used previously to study the effect of viscosity on the rate of diffusion controlled bimolecular reactions (4-6). Glycerol is particularly suitable for this application due to its high viscosity, high dielectric constant, and because it forms nearly ideal solutions with water (7,8).

Aqueous solutions of other organic solvents have also been used to study the effect of dielectric constant upon reaction rates (9,10), and this theory has been applied to enzyme reactions (11-13). The reaction between catalase and hydrogen peroxide has been shown to decrease with increasing concentrations of ethanol (14,15). Increasing amounts of ethanol slow the peroxidation of guaiacol by peroxidase

(from Japanese radish) and hydrogen peroxide (16). The rate of this same reaction, but catalyzed by three isozymes of turnip peroxidase, decreases with increasing amounts of ethanol (17). An expression for the reaction between dipolar molecules was used to interpret these results. The steady state rate of oxidation of guaiacol by HRP and hydrogen peroxide is inhibited by methanol (18). This was explained in terms of competitive inhibition where two moles of methanol bind to one mole of HRP. It has been noted previously that the rate of Compound I formation for HRP isozymes A and C is affected by ethanol, and this was interpreted in terms of the hydrophobicity of the heme pocket (19).

This chapter presents the results of studying Compound I formation in glycerol in order to evaluate the postulate of a diffusion-controlled rate. The rate was also measured in the presence of ethanol in order to compare this solvent system with glycerol. An analogy which has evolved between Compound I formation and cyanide binding is further developed (1,2,20).

5.3 Experimental

Materials

Horseradish peroxidase (E.C. 1.11.1.7 donor-H_2O_2-oxidoreductase) was purchased from Sigma as a lyophilized salt-free powder (Type VI, lot 25C-9570), and it was also purchased from Boehringer Mannheim GmbH as a purified ammonium sulfate

suspension (Lot 7315529). The Sigma preparation after vacuum dialysis against multiply distilled water (21) had a PN of 3.1. The Boehringer Mannhiem preparation had a PN of 3.3 after extensive dialysis against multiply distilled water. Isozyme C (22,23) has been determined to be the major component of many commercial preparations (24-26). Glycerol from Fisher was vacuum distilled (140°, 1.5 torr) to remove trace impurities which caused a reaction with native HRP. All other materials were reagent grade.

Methods

Absorbance spectra and measurements were obtained with a Cary 14 spectrophotometer equipped with a 0-1-2 and 0-.1-.2 absorbance slidewire. The cell compartment temperature was maintained by circulating thermostated water. Difference spectra were obtained by first recording the baseline with 2 ml of the aqueous-organic solution in the sample cell and 2 ml of aqueous solution in the reference cell. Both cells contained buffer. An identical amount of enzyme was pipetted into each cell, and the solutions were thoroughly mixed with a Teflon plumper before recording the spectrum. CD spectra were recorded with a Jasco model ORD/UV-5 spectrometer which had been specially modified for sensitive CD measurements. The cells used to obtain the CD spectra were jacketed and could be thermostated with circulating water for precise temperature control. A rapid flow of anhydrous nitrogen through the cell compartment prevented condensation of water

on the cell windows during the low temperature measurements. From 600 to 250 nm in a 2 cm cell the concentration of HRP or Compound I was 9 μM in phosphate buffer pH 7.04 with I=0.005. Below 250 nm a 1 mm cell was used with a 1.93 μM concentration of Compound I and HRP in the same buffer.

The rate measurements were obtained with a Gibson-Durrum stopped-flow apparatus model D-110 using a least a tenfold excess of hydrogen peroxide or cyanide compared to the enzyme to ensure pseudo first-order conditions. The concentration of HRP was 0.6 μM. The rate of reaction of HRP with hydrogen peroxide or cyanide was followed at 403 or 420 nm, respectively. Both drive syringes contained 0.1 M potassium nitrate and buffer of I=0.01 for a total ionic strength of 0.11. For the stopped-flow experiments in aqueous-organic solutions, equal amounts of glycerol or ethanol were added to the enzyme and substrate solutions. For each set of conditions eight individual determinations of the rate constant were averaged for the best value. The nonlinear least squares method of computing first-order rate constants has been described (27). The kinetic curves were first order and followed Equation [1]

$$[1] \qquad \frac{-d[HRP]}{dt} = k_{obs}[HRP]$$

where k_{obs} is a pseudo first-order rate constant. Errors given for the rate constants are the larger of either the average standard deviations or the average deviation from

the mean value.

The concentration of HRP was determined spectrophotometrically at 403 nm using a molar absorptivity of 1.02×10^5 $M^{-1}cm^{-1}$ (28). The concentration of hydrogen peroxide was checked weekly using the HRP assay (29). Potassium cyanide solutions were prepared immediately prior to use and were not used longer than a few hours. The pH was measured with an Orion 801 pH meter equipped with a Fisher combination electrode calibrated to ±0.03 pH units with commercial standard buffers. The pH of the phosphate buffer was measured to be 7.04 at 25° in the absence of organic solvent. The addition of glycerol or ethanol (30) alters the pH significantly; and therefore, as the quantity of these organic solvents was varied the pH also changed. The change in pH was not a problem because both the rate of Compound I formation (1) and the rate of cyanide binding (31) are pH independent near pH 7. For the same reason the change in pH as a function of temperature does not affect the rate of Compound I formation or cyanide binding. The ethanol concentrations were corrected to account for using 95% v/v stock solutions.

An Ostwald viscometer thermostated at 40° was used to determine relative viscosities. The flow time of a solution of 0.6 μM HRP in 0.1 M potassium nitrate and phosphate buffer pH 7.04, I=0.01, at 40° was assigned unit relative viscosity, $\eta_{rel}^{40°}$. Flow times were determined in triplicate and were reproducible within 0.2 s with times ranging from 72 to 180 s.

The dielectric constant of the aqueous-organic solutions at 40° were interpolated from published data (32) and were then corrected for the effect of 0.11 M electrolyte (33). The electrolyte correction required that the dielectric constant be diminished by 2 units.

5.4 Results

Compound I Formation in H_2O

The value of k_{obs} for the formation of Compound I was determined at 25° for several concentrations of H_2O_2 and in several buffers from pH 3.19 to 9.76. These data are plotted as k_{obs} *vs.* $[H_2O_2]$ in Fig. 5.1. Fig. 5.1A shows the data at pH 7.04 in phosphate buffer, and the data for Fig. 5.1B encompass a wide range of pH. These plots are linear and have zero intercepts indicating the rate limiting step of Compound I formation for this $[H_2O_2]$ concentration range is overall second order, first order in horseradish peroxidase and first order in hydrogen peroxide. The slope is the second-order apparent rate constant $k_{1,app}$. Equation [2]

$$[2] \qquad \frac{-d[HRP]}{dt} = k_{1,app}[HRP]_{total}[H_2O_2]_{total}$$

defines $k_{1,app}$. The values of $k_{1,app}$ from the data in Fig. 5.1 are recorded in Table 5.1. Between pH 5.96 and 9.76 the rate is essentially pH independent, whereas at pH 4.38 and 3.19 this rate is much slower. This trend agrees with the work

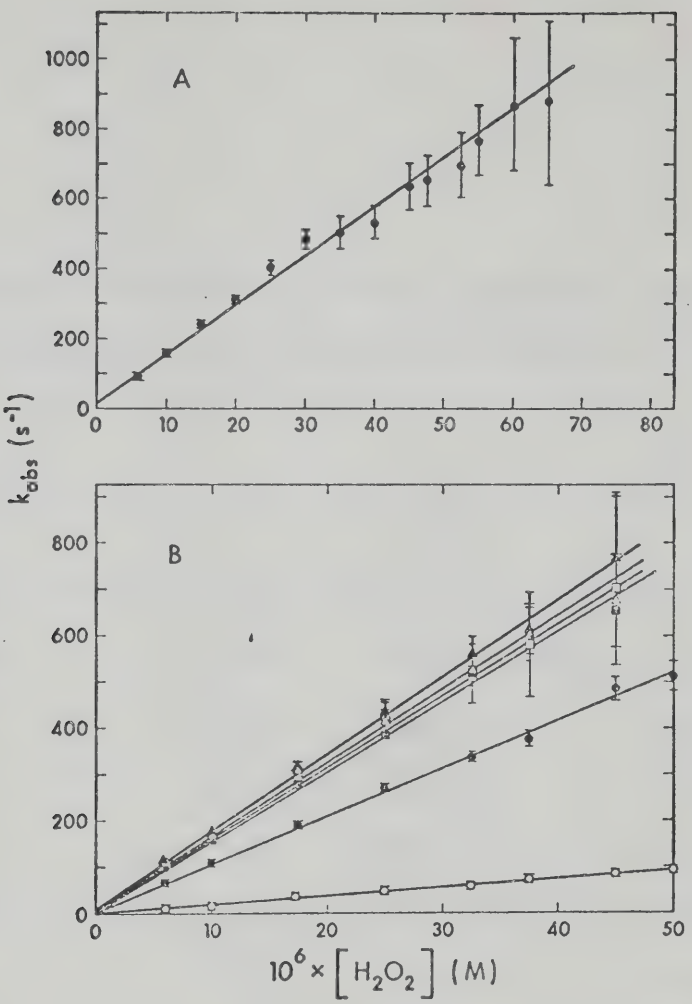

Fig. 5.1 Linear plots of k_{obs} *vs.* $[H_2O_2]$ for Compound I formation at 25° and several pH values. A. Phosphate pH 7.04. B. ○ Glycine-HNO_3 pH 3.19; ● Acetate pH 4.38; ■ Phosphate pH 5.96; ▲ Tris-HNO_3 pH 8.09; Δ Carbonate pH 9.22; □ Carbonate pH 9.76. When the symbols are bigger than the error, there are no error bars. The slopes, which were calculated by a linear least squares analysis, are the values of $k_{1,app}$ (See Table 5.1).

Table 5.1 Apparent Second-Order Rate Constants for the Formation of Compound I as a Function of pH at 25°.

$10^{-7} \times k_{1,app}$ $(M^{-1}s^{-1})$ [a]	pH	Buffer	$10^{6} \times [H_2O_2]$ range
0.185±0.008	3.19	Glycine-HNO_3	6-50
1.04±0.01	4.38	Acetate	6-50
1.55±0.03	5.96	Phosphate	6-45
1.42±0.03	7.04	Phosphate	6-65
1.67±0.02	8.09	Tris-HNO_3	6-45
1.59±0.02	9.22	Carbonate	6-45
1.52±0.03	9.76	Carbonate	6-45

[a] The errors are standard deviations computed by the linear least squares analysis.

of Dolman *et al.* (1).

The rate of Compound I formation was studied as a function of ionic strength to evaluate the primary salt effect. The rate measurements were obtained at 40° in phosphate buffer pH 7 with $[H_2O_2]$=15 μM. Since Fig. 5.1A is linear, $k_{1,app}$ could be obtained by dividing k_{obs} by 15 μM. The Brønsted-Debye limiting rate equation predicts that a plot of log $k_{1,app}$ *vs.* the square root of ionic strength should be linear with a slope of zero if the net charge on one of the reactants is zero. The ionic strength of the buffer was maintained at 0.01 while that of KNO_3 was varied. The values of $k_{1,app}$ as a function of ionic strength are recorded in Table 5.2. There is no significant variation in rate which is in agreement with $Z_{H_2O_2}$=0 at pH 7.04. Thus, H_2O_2 and not HO_2^- is the reactive species in agreement with the results of Dolman *et al.* (1).

Compound I Formation in Glycerol

The rate of Compound I formation was studied in the presence of increasing amounts of glycerol to determine the effect of viscosity on the rate. The rate measurements were made in phosphate buffer near pH 7 at a temperature of 40° with $[H_2O_2]$=15 μM. The dielectric constant of the solutions, as well as the viscosity, is changed by the addition of glycerol. The values of $k_{1,app}$, the concentration of glycerol, the relative viscosity, and the dielectric constant (corrected for the presence of electrolyte) are recorded in Table 5.3.

Table 5.2 Apparent Second-Order Rate Constants for Compound I Formation as a Function of Total Ionic Strength in Phosphate Buffer pH 7.04 at 40°.

$10^{-7} \times k_{1,app}$ ($M^{-1}s^{-1}$)	Total Ionic Strength
1.99±0.05	0.01
1.96±0.05	0.02
2.04±0.06	0.03
2.00±0.07	0.04
1.94±0.07	0.05
1.93±0.07	0.06
2.02±0.07	0.07
2.04±0.07	0.08
2.00±0.10	0.09
1.99±0.06	0.10
2.03±0.10	0.11

Table 5.3 Apparent Second-Order Rate Constants for the Formation of Compound I as a Function of the Concentration of Glycerol in Phosphate Buffer near pH 7 at 40°.

$10^{-7} \times k_{1,app}$ ($M^{-1}s^{-1}$)	[Glycerol] (M)	$\eta_{rel}^{40°}$	$\epsilon_{corr}^{40°}$ [a]
1.88±0.06	0.0	1.00	71.4
1.92±0.07	0.342	1.07	70.6
1.93±0.06	0.685	1.13	69.7
1.98±0.08	1.03	1.20	68.9
1.99±0.09	1.37	1.27	68.1
1.85±0.08	1.57	1.32	67.6
1.94±0.07	1.71	1.37	67.3
1.84±0.07	2.05	1.46	66.6
1.92±0.07	2.40	1.58	65.7
1.89±0.07	2.74	1.71	64.9
1.81±0.06	2.88	1.78	64.6
1.82±0.07	3.08	1.86	64.1
1.86±0.08	3.42	1.95	63.3
2.05±0.09	3.77	2.19	62.5
1.80±0.06	4.11	2.42	61.7

[a] Dielectric data from Akerlof ref. 32 is corrected for the presence of electrolyte by the method of Hasted *et al.* ref. 33.

The rate of Compound I formation is independent of viscosity and dielectric constant of the solvent.

Compound I Formation in Ethanol

The rate of Compound I formation was studied in the presence of increasing amounts of ethanol in phosphate buffer near pH 7 at 40° with $[H_2O_2]$=15 μM. The values of $k_{1,app}$, the concentration of ethanol, and the dielectric constant corrected for the effect of electrolyte are recorded in Table 5.4. A significant decrease in $k_{1,app}$ occurs with increasing ethanol concentration. This result can be interpreted in terms of competitive inhibition, Equation [3],

[3]

$$\begin{array}{ccc} \text{HRP} + H_2O_2 & \xrightarrow{k_a} & \text{Compound I} \\ K \uparrow\downarrow & & \\ \text{HRP-EtOH} & & \end{array}$$

where the enzyme is in equilibrium with an enzyme-ethanol complex. This complex is considered to be unreactive or at least not significantly reactive compared to uncomplexed HRP. Defining K as the dissociation constant for the HRP-EtOH complex, and using the expression for the reaction velocity; Equation [4] can be derived.

[4]

$$\frac{1}{k_{1,app}} = \frac{[EtOH]}{k_a K} + \frac{1}{k_a}$$

Table 5.4 Apparent Second-Order Rate Constants for the Formation of Compound I as a Function of the Concentration of Ethanol in Phosphate Buffer near pH 7 at 40°

$10^{-7} \times k_{1,app}$ ($M^{-1}s^{-1}$)	[EtOH] (M)	$\epsilon^{40°}_{corr}$ [a]
2.03±0.1	0.0	71.4
1.83±0.09	0.0	71.4
1.72±0.07	0.811	69.5
1.62±0.06	1.22	68.7
1.48±0.1	2.03	66.5
1.42±0.04	2.43	65.4
1.36±0.05	2.84	64.2
1.28±0.05	3.25	63.2
1.22±0.03	3.65	62.4
1.21±0.04	4.06	61.4
1.19±0.04	4.46	60.1
1.14±0.04	4.87	58.8

[a] See footnote *a* of Table 5.3.

If Equations [3] and [4] apply, a plot of the reciprocal of $k_{1,app}$ *vs.* [EtOH] should be linear. Fig 5.2 shows that this plot is linear, and K=7.2±0.4 M can be calculated from the slope and ordinate intercept or from the negative abscissa intercept. The value of K and k_a are recorded in Table 5.6.

Cyanide Binding to HRP in Ethanol

The rate of formation of the cyanide complex of native HRP is also inhibited by ethanol. The rate measurements were obtained in phosphate buffer near pH 7 at 40° with [KCN]=50 μM. With this large excess of KCN compared to HRP the binding can be considered to be almost irreversible. The values of $k_{2,app}$ (the second-order apparent rate constant for cyanide binding) are recorded in Table 5.5. The decrease in $k_{2,app}$ with increasing ethanol concentration can be interpreted by the same inhibition scheme that was used for Compound I formation, Equation [5].

[5]

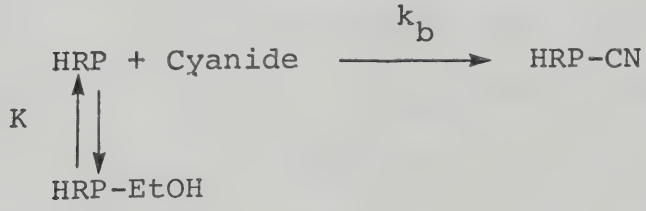

Fig. 5.3 shows the linear plot of the reciprocal of $k_{2,app}$ *vs.* [EtOH] which yields the same value of K within its standard deviation (6.9±0.8 M) as did the results for Compound I formation. See Table 5.6.

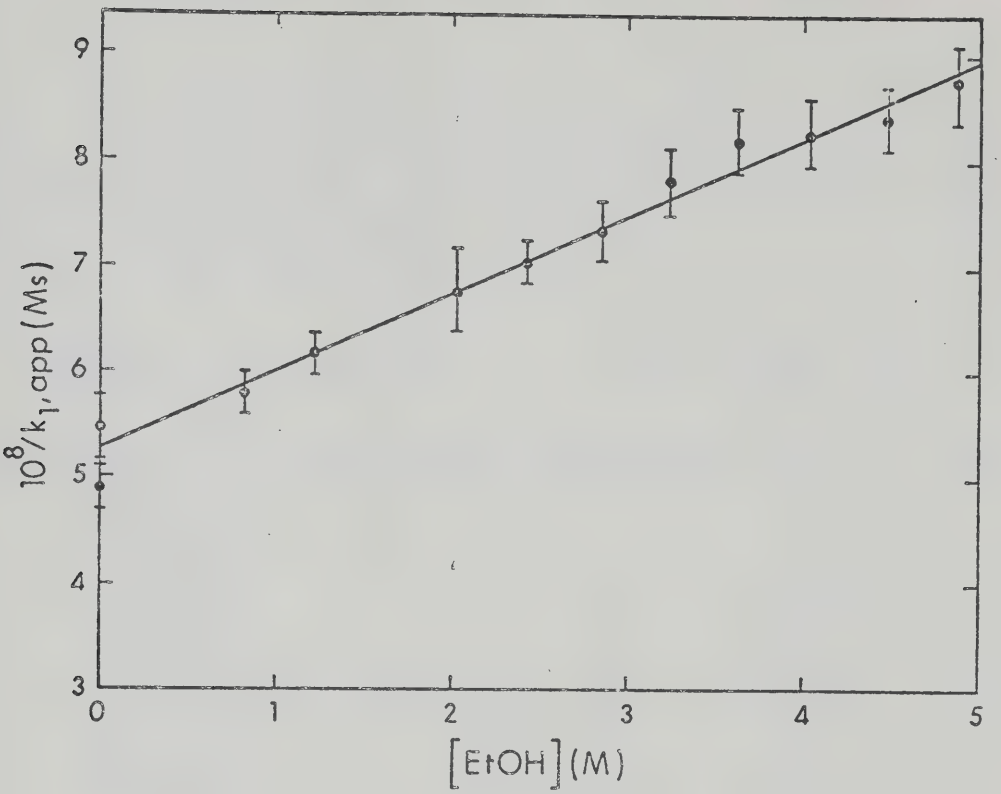

Fig. 5.2 Linear plot according to Equation [4] of the reciprocal of $k_{1,app}$ *vs.* the concentration of ethanol in phosphate buffer pH 7 at 40°. $k_{1,app}$ was determined from k_{obs} at $[H_2O_2]$ = 15 μM. The values of k_a and K were calculated from the ordinate intercept and slope which were determined by a linear least squares analysis (See Table 5.6).

Table 5.5 Apparent Second-Order Rate Constants for the Binding of Cyanide as a Function of the Concentration of Ethanol in Phosphate Buffer near pH 7 at 40°.

$10^{-5} \times k_{2,app}$ ($M^{-1}s^{-1}$)	[EtOH] (M)
1.81±0.06	0.0
1.76±0.04	0.406
1.72±0.02	0.811
1.56±0.04	1.23
1.59±0.05	1.62
1.49±0.10	2.03
1.46±0.04	2.43
1.47±0.03	2.84
1.36±0.09	3.25
1.31±0.06	3.65
1.32±0.03	4.06
1.14±0.08	4.46
1.07±0.10	4.87

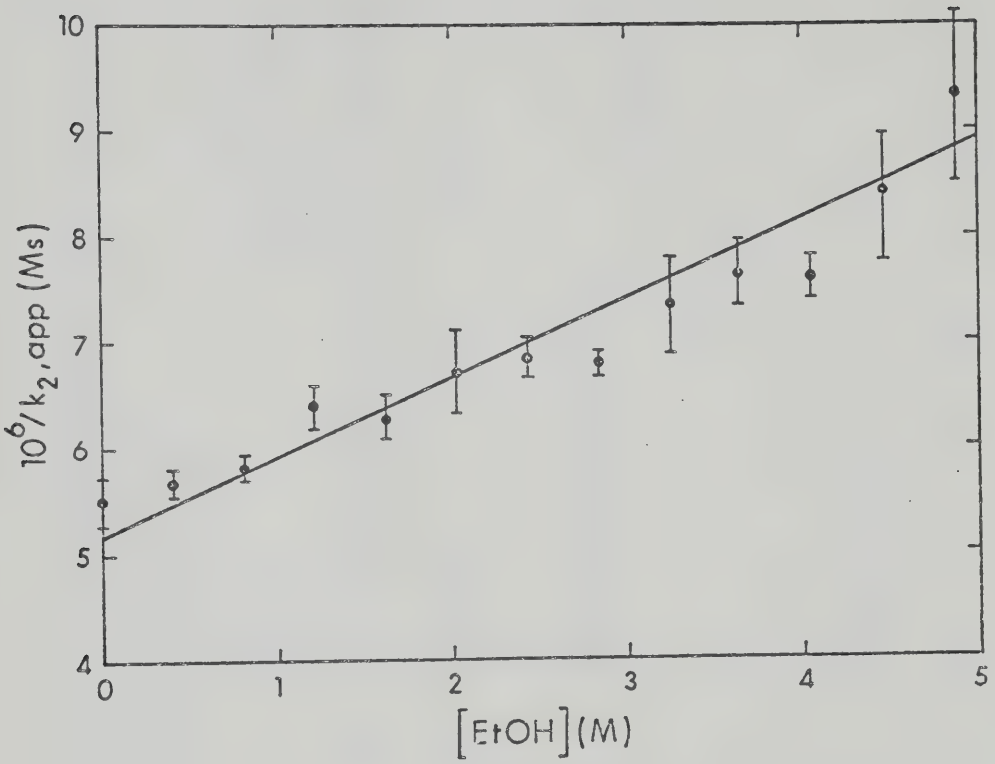

Fig. 5.3 Linear plot of the reciprocal of $k_{2,app}$ *vs.* the concentration of ethanol according to Equation [4] but applied to cyanide binding in phosphate buffer at pH 7 at 40°. $k_{2,app}$ was determined from k_{obs} at [KCN] = 50 μM. The values of k_b and K were calculated from the ordinate intercept and slope which were determined by a linear least squares analysis (See Table 5.6).

Table 5.6 Kinetic and Equilibrium Parameters for the Reaction of HRP with Hydrogen Peroxide and Cyanide in the Presence of Ethanol.

Parameter [a]	Compound I Formation	Cyanide Binding	Difference Spectroscopy
K (M)	7.2±0.4	6.9±0.8	4±1
k_a ($M^{-1}s^{-1}$)	$(1.89\pm0.03)\times10^{7}$		
k_b ($M^{-1}s^{-1}$)		$(1.92\pm0.07)\times10^{5}$	
$\varepsilon^{409}_{HRP-EtOH}$ ($M^{-1}cm^{-1}$)			9.9×10^{4} [b]

[a] At 40° in phosphate buffer pH near 7.

[b] Based on an estimated value of $\varepsilon^{409}_{HRP} = 9.4\times10^{4}\ M^{-1}cm^{-1}$.

Spectrophotometric Detection of the HRP-EtOH Complex

Difference absorption spectroscopy was used to detect the complex between ethanol and native HRP. A difference spectrum was recorded as a function of time and is shown in Fig. 5.4. Positive extrema are located at 409 and 386 nm, and negative extrema are located at 480 and 255 nm. A pair of isosbestic wavelengths on the baseline (452 and 263 nm) indicated the interconversion of only two species. After 60 minutes the spectrum ceased to change. The maximum difference in absorbance at 409 nm represents less than 3% of the total absorbanced based on an estimated molar absorptivity of 9.4×10^4 $M^{-1}cm^{-1}$ for HRP at 409 nm. Difference spectroscopy was used to make a determination of the HRP-EtOH dissociation constant, K, as defined in Equations [3] to [5]. The reciprocal of the absorbance change at 409 nm, ΔA^{409}, was plotted against the reciprocal of the concentration of ethanol according to Equation [6]

$$[6] \quad \frac{1}{\Delta A^{409}} = \frac{K}{\Delta\varepsilon^{409}[HRP]_{total}[EtOH]} + \frac{1}{\Delta\varepsilon^{409}[HRP]_{total}}$$

where $[HRP]_{total} = [HRP] + [HRP\text{-}EtOH]$ and $\Delta\varepsilon^{409} = \varepsilon^{409}_{HRP\text{-}EtOH} - \varepsilon^{409}_{HRP}$. The plot is shown in Fig. 5.5. The linear slope and ordinate intercept or the negative abscissa intercept can be used to calculate K=4±1 M.

Circular dichroic spectroscopy was also used to detect the ethanol complex of HRP. The CD spectrum of native HRP

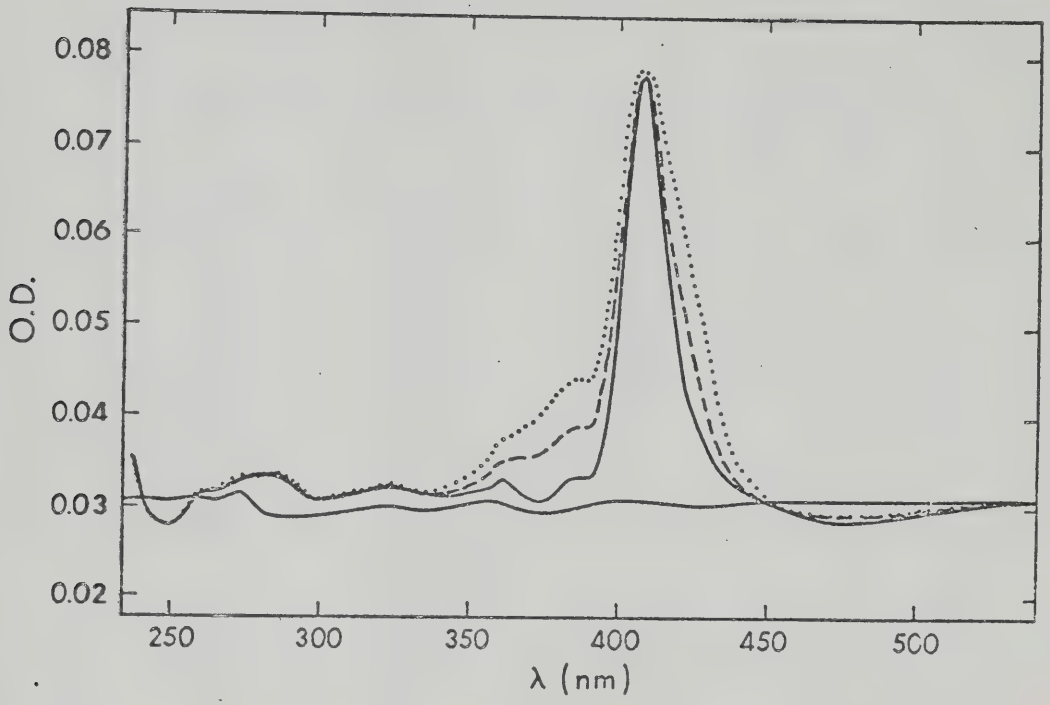

Fig. 5.4 The difference absorption spectra in 1 cm cells of HRP (17.5 μM) in ethanol (2.6 M) and phosphate buffer pH 7 (ionic strength .005) at 40°. The reference cell contained equal quantities of everything in the sample cell but ethanol. The first spectrum (——) was recorded within 1 minute of mixing, and the second (----) and third (····) at 25 minutes and 60 minutes. Isosbestic points occur at 452 and 263 nm. HRP (0.7 ml of 67.4 μM) was pipetted into the reference then sample cell each containing 2 ml of solution. The 0-0.1 slidewire was used.

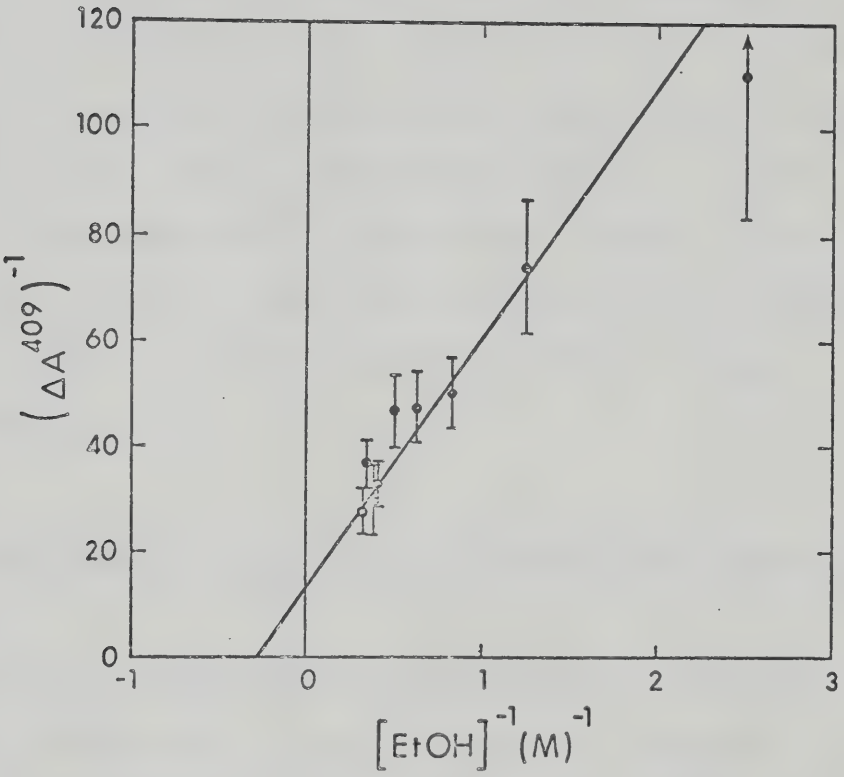

Fig. 5.5 Double reciprocal plot of the absorbance change ΔA *vs.* the concentration of ethanol in phosphate buffer pH 7 (ionic strength 0.005) at 40°. ΔA was determined by difference spectroscopy. The straight line was calculated using a linear least squares analysis weighted by the reciprocal of the estimated percent error in each data point. The value of K (See Table 5.6) was obtained from the ordinate intercept and slope or from the negative absicissa intercept.

in Fig. 5.6 is identical to that already published for HRP isozyme C (34,35). In 3.5 M ethanol there are slight reproducible differences in the CD spectrum, presumably due to the HRP-EtOH complex. The ellipticity of the positive band in the Soret region is increased slightly and is shifted from 407 to 410 nm. Also, the negative bands at 372 and 340 nm have slightly smaller ellipticities. Other regions of the CD spectrum, including the large negative band at 208 nm (not shown) which correlates with the α-helical content, remain unchanged.

Spectrophotometric Detection of Interactions between HRP and Glycerol

Difference absorption spectroscopy was used to detect a change in native HRP in the presence of glycerol. The spectrum is shown in Fig. 5.7, and there was little change with time. Broad absorbance maxima occur at 407 and 385 nm, and a minimum occurs at about 290 nm. The absorbance change at 407 nm represents approximately 1.5% of the total absorbance. The CD spectra of HRP in water and in glycerol are identical from 600 to 190 nm within instrumental sensitivity.

Temperature Dependence of the CD Spectrum of HRP

The temperature dependence of the CD spectrum of HRP, Fig. 5.8, was investigated to see if there are thermally induced structural changes. Increasing the temperature from 4° to 67° decreased the ellipticity of the positive Soret

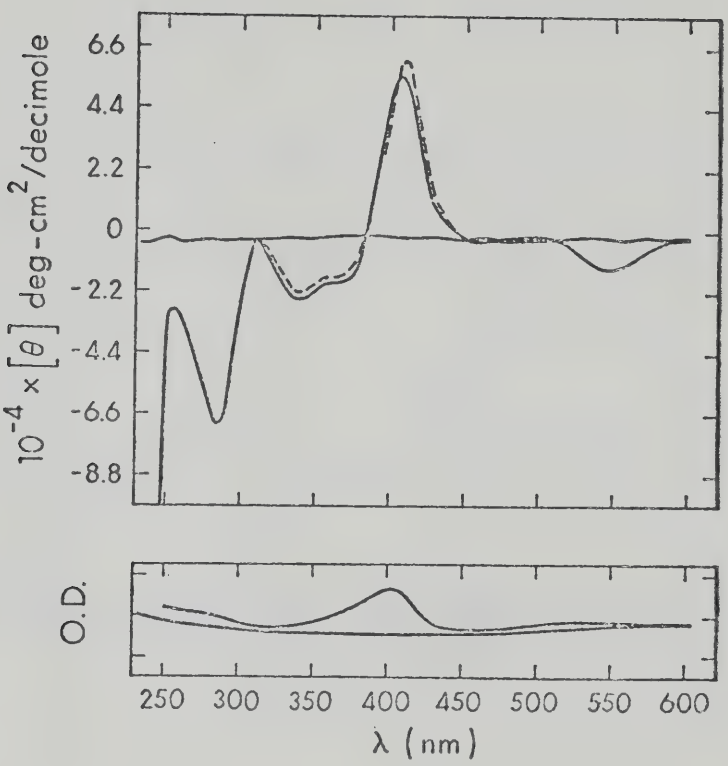

Fig. 5.6 Circular dichroic spectra of HRP (——) and its ethanol complex (----). The enzyme concentration was 9.0 μM with phosphate buffer pH 7 (ionic strength 0.005) at 40 in a 2 cm cell. The ethanol concentration was 3.5 M. The absorption spectra at the bottom of the figure were recorded simultaneously with the CD spectra. The baselines for each solution were coincident.

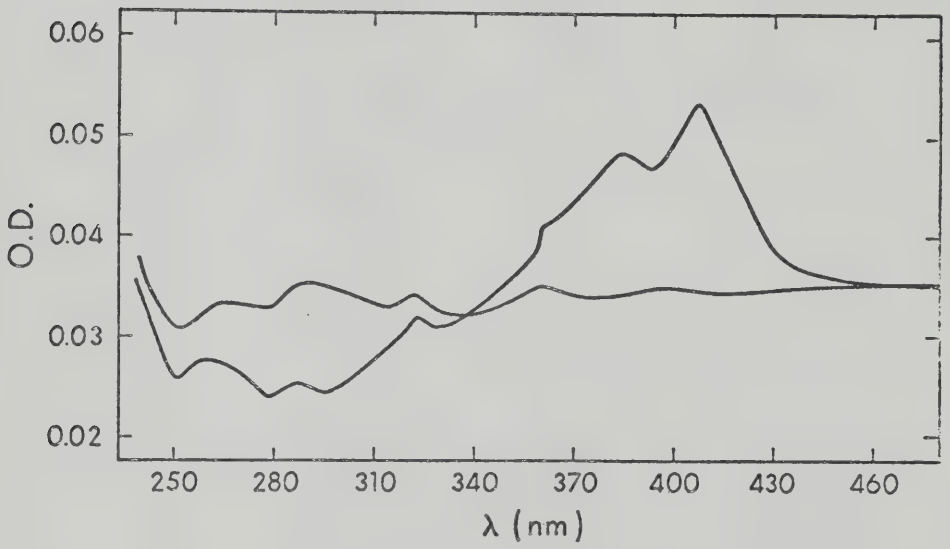

Fig. 5.7 The difference absorption spectrum in 1 cm cells of HRP (13.5 μM) in glycerol (2.8 M) and phosphate buffer pH 7 (ionic strength 0.005) at 40°. The reference cell contained everything in the sample cell but glycerol. The spectrum was recorded within 1 minute of mixing and did not change significantly with time. HRP (0.5 ml of 67.4 μM) was pipetted into the reference then sample cell each containing 2 ml of solution. The 0-0.1 slidewire was used.

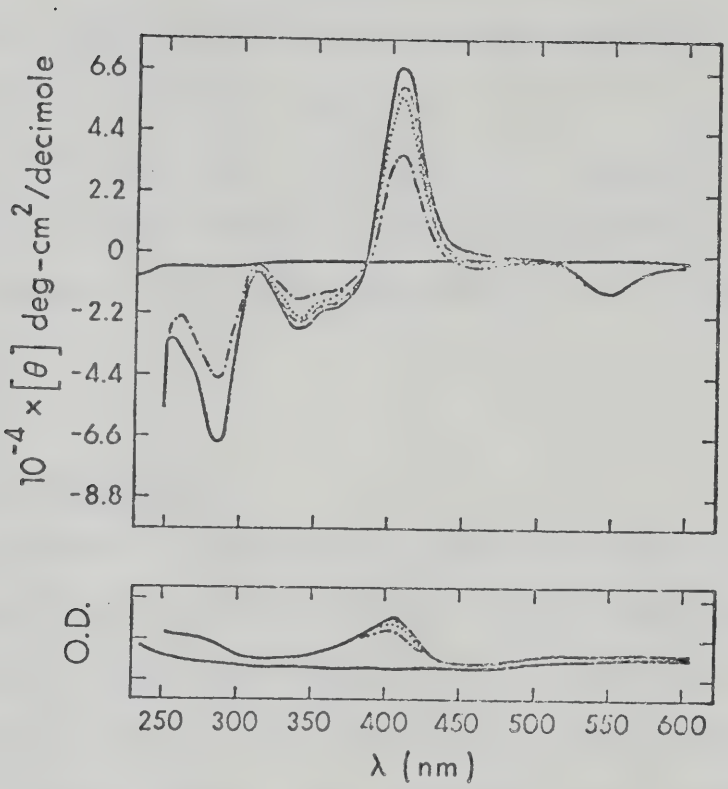

Fig. 5.8 Circular dichroic spectra of HRP at several temperatures (—— 4°; --- 27°; ··· 48°; and -·-· 67°). The concentration of HRP was 9 μM with phosphate buffer pH 7 (ionic strength 0.005) in a 2 cm cell. The same solution was used for all temperatures. The absorption spectra at the bottom of the figure were recorded simultaneously with the CD spectra. When the sample at 67° had been cooled to 26° it produced CD and absorption spectra identical to those at 27° indicating reversibility. Both baselines were temperature independent.

band. From 300 to 250 nm only the spectrum at 67° was detectably different. After the sample was held at 67° for 30 minutes (the time required to record the spectrum), it was quickly cooled in ice-water and the allowed to return to 26°. Its spectrum was identical to that of the unheated sample at 27°. Therefore, these thermally induced changes are reversible. The changes in the absorption spectrum are also reversible.

CD Spectrum of Compound I

The CD spectrum of Compound I, Fig. 5.9, was recorded at 20° and is very different from that of HRP. The negative band at 544 nm of HRP has disappeared in Compound I. The ellipicity of the positive Soret band has decreased and has shifted from 407 to 423 nm. The negative band at 208 nm (not shown) remained unchanged. The stability of the Compound I preparation was verified by observing that there was no detectable change in its absorption spectrum at 400 nm after the time required to record the spectrum.

5.5 Discussion

The linear plots of k_{obs} *vs.* $[H_2O_2]$ for Compound I formation in H_2O demonstrate a second-order rate limiting step. This result does not eliminate the possibility of a transient enzyme-substrate complex, but it places limits on the pertinent rate constants. If a complex were present under the conditions of Fig. 5.1A, then the unimolecular rate

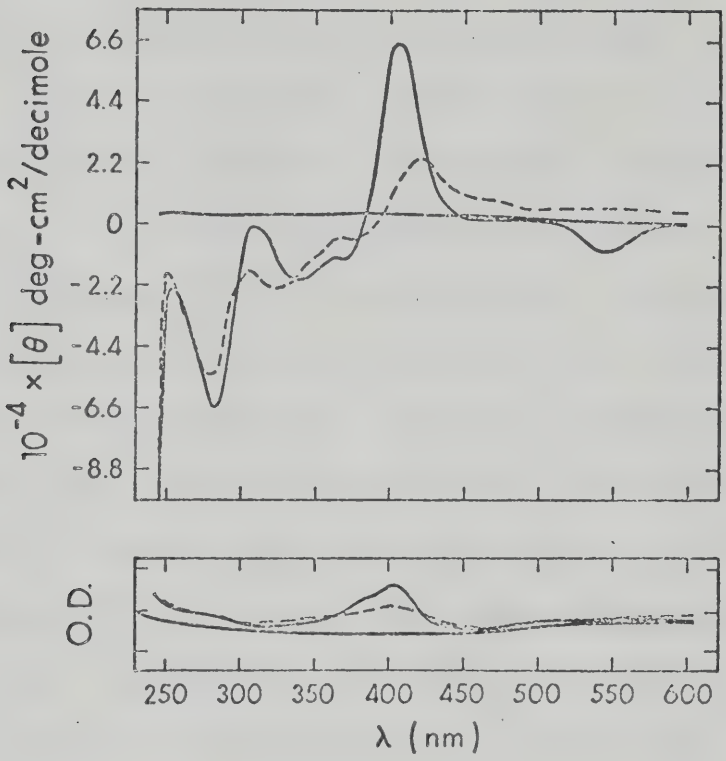

Fig. 5.9 Circular dichroic spectra of HRP (——) and Compound I (---). The enzyme concentration was 9 μM with pH 7 phosphate buffer (ionic strength 0.005) at 20° in a 2 cm cell. Compound I was prepared by adding 1 molar equivalent of H_2O_2 contained in 20 μl of solution. The absorption spectra at the bottom of the figure were recorded simultaneously with the CD spectra. After recording the spectrum of Compound I, a check of the absorbance at 400 nm showed that virtually none of the Compound I spontaneously decayed.

constant for the dissociation of the complex to form Compound I must be greater than 900 s^{-1}. At this value of k_{obs} a second-order step would still be rate limiting. This same argument applies to the data in Fig 5.1B. A rate limiting first-order step for Compound I formation has been detected above pH 10.5 (2). The independence of the rate of Compound I formation from pH 5.96 to 9.76 and from ionic strength 0.01 to 0.11 is an important result because this indicates that the un-ionized form of H_2O_2 is the reactive species. The addition of large quantities of ethanol or glycerol significantly alters the activity coefficients of the ions. This produces changes in pH. Since the rate of Compound I formation near pH 7 is independent of pH, any change in rate must be attributed to other causes. This is also true for cyanide binding, since the rate of binding is pH independent from 6 to 8 (31).

Measurements of the rate of Compound I formation as a function of the concentration of glycerol show that this rate is independent of viscosity and dielectric constant (Table 5.3). The existence of a compensatory effect where a possible viscosity effect is offset by a dielectric effect, which results in no net change in rate, is not possible since both a decrease in dielectric constant and an increase in viscosity are expected to cause a decrease in the rate of Compound I formation. The concentration range of glycerol used at 40° was chosen to simulate the viscosity changes of water from 40° to 2°. The rate of Compound I formation is not limited

by the rate of diffusion of the reactants; and therefore, the measured activation energy must correspond to a step which occurs after HRP encounters a molecule of hydrogen peroxide. Also, it has recently been shown that several substituted perbenzoic acids form Compound I at a significantly faster rate than hydrogen peroxide (36).

Although Fig. 5.7 shows that HRP is not in its native state in the presence of glycerol, this may be due only to the binding of glycerol to the protein through the formation of stable hydrophobic bonds between glycerol and hydrophobic amino acid side chains (37-39). For glycerol and ethanol at equal concentrations, the absorbance changes induced by glycerol are smaller than those induced by ethanol by a factor of about two. This binding of glycerol in combination with viscosity and dielectric effects causes no net change in the rate of Compound I formation.

The presence of ethanol decreases both the rate of Compound I formation and the rate of cyanide binding. This result has been interpreted as ethanol behaving as an inhibitor where one molecule of HRP binds one molecule of ethanol. The rate decrease of Compound I formation with increasing ethanol concentration cannot be due to the change in dielectric constant of the medium since there was no rate decrease in glycerol solutions. The inhibition of cyanide binding strongly implies that ethanol is bound to the sixth coordination position of the heme. This is also consistent with the ethanol inhibition of Compound I formation which, by analogy

with chloroperoxidase, also involves ligation at the sixth position (40). Further evidence that ethanol binds to the sixth coordination position is supplied by the close agreement of the two kinetically determined HRP-EtOH dissociation constants, Table 5.6. The agreement between the kinetically and spectrophotometrically determined dissociation constant seems only fair, but the errors in the spectrophotometric determination are large due to the very small absorbance changes. The kinetically and spectrophotometrically determined dissociation constants almost certainly refer to the same equilibrium. The binding of ethanol is also indicated by comparing the CD spectrum of HRP in the presence and absence of ethanol.

Evidence is accumulating that ethanol can act as a ligand for ferrihemoproteins. Indications of ethanol binding to ferrihemoglobin and ferrihemoglobin hydroxide have been obtained by magnetic susceptibility measurements (41). The ferrihemoglobin-EtOH complex formation leads to an increase in high spin character at pH 6.5. The predominently low spin ferrihemoglobin hydroxide is converted into a high spin complex in 20% v/v of ethanol. These workers also concluded that ethanol probably binds to the heme iron (41), and they estimated a dissociation constant for the ethanol complex of about 0.4 M. Their interpretation is also based on the bind- of only one molecule of ethanol per heme. Very recently the binding of ethanol to ferrihemoglobin at pH 6.3 has been demonstrated with difference absorption and electron para-

magnetic resonance spectroscopy (42). The binding stoichiometry was one ethanol molecule per heme group, and the dissociation constant of ferrihemoglobin-EtOH was 0.2 M at pH 6.3. Ethanol also produced spectral changes in the hemoproteins ferrimyoglobin and catalase, but these absorbance changes were deemed too small for quantification.

The spectral changes observed in the presence of ethanol, displayed in Fig. 5.4, did not occur at the same rate. The sharp maximum at 409 nm is fully developed and can be recorded within the 60 s required to mix the samples and scan the spectrum. However, the maximum at 386 nm requires about 60 minutes to develope its full absorbance. This slow step may represent a sluggish conformational change which occurs subsequent to ethanol binding. Following the formation of the alkaline form of HRP and turnip peroxidase P_1, two slow absorbance changes have been noted (2), which also may be a manifestation of conformational changes.

Many results concerning the decrease in rate of peroxidase reactions in the presence of ethanol and methanol have been interpreted in terms of the change in the dielectric constant of the medium, although the possibility of other important factors was realized (14,16,17). The mathematical expression for a reaction rate as a function of dielectric constant (13) is based on a model involving simple ions or dipolar molecules. An enzyme in solution may have catalytically important ionizable groups; and thus, the dielectric constant may alter the reaction rate. However, in view of

the mounting evidence for the binding of ethanol and methanol to hemoproteins these kinetic studies might be best interpreted in terms of competitive inhibition.

The thermally induced reversible changes in the CD spectrum of HRP indicate that the asymmetric environment of the heme changes due to a temperature dependent enzyme conformation or that the heme group itself is changing. The CD bands may have changed as a consequence of the thermal equilibrium betweem the high and low spin states of ferric HRP (43) since HRP at pH 7 and 40° is only about 80% high spin (44). CD studies of ferricytochrome c at pH 5 have shown that the presence of ethanol almost doubles the Soret band ellipticity and shifts its peak from 402 to 405 nm (45). This result was interpreted in terms of the ethanol exposing the buried heme to the solvent. If this change in conformation causes the removal of one or both of the fifth or sixth position ligands of the heme, the normally low spin ferricytochrome c at pH 5 (46) will become high spin (47). Since these axial positions are open to the solvent (48), ethanol binding might occur and contribute further to a high spin form.

5.6 References

1. Dolman, D., Newell, G.A., Thurlow, M.D., and Dunford, H.B. (1975) *Can. J. Biochem.* 53, 495-501
2. Job, D., and Dunford, H.B. (1976) 'submitted for publication'

3. Hewson, W.D., and Dunford, H.B. (1975) *Can. J. Chem.* 53, 1928-1932

4. Strother, G.K., and Ackerman, E. (1961) *Biochim. Biophys. Acta* 47, 317-326

5. Warrick, P., Jr., Auborn, J.J., and Eyring, E.M. (1972) *J. Phys. Chem.* 76, 1184-1191

6. Cerjan, C., and Barnett, R.E. (1972) *J. Phys. Chem.* 76, 1192-1195

7. Robinson, R.A., and Stokes, R.H. (1959) in Electrolyte Solutions 2nd Edition, pp. 241-245, Butterworths, London

8. Stokes, R.H., and Robinson, R.A. (1966) *J. Phys. Chem.* 70, 2126-2130

9. Laidler, K.J., and Eyring, H. (1940) *Ann. N.Y. Acad. Sci.* 39, 303-339

10. Hiromi, K. (1960) *Bull. Chem. Soc. Japan* 33, 1251-1264

11. Barnard, M.L., and Laidler, K.J. (1952) *J. Am. Chem. Soc.* 74, 6099-6101

12. Laidler, K.J., and Eithier, M.C. (1953) *Arch. Biochem. Biophys.* 44, 338-345

13. Hiromi, K. (1960) *Bull. Chem. Soc. Japan* 33, 1264-1269

14. Ogura, Y., Hattori, A., Tonomura, Y., and Hino, S. (1950) in Symposium on Enzyme Chemistry 5, 28-45

15. Kremer, M.L. (1970) *Biochim. Biophys. Acta* 198, 199-209

16. Tonomura, Y. (1953) *J. Japan Biochem. Soc. (Seikagaku)* 25, 175-183

17. Hosoya, T. (1960) *J. Biochem.* 48, 803-811

18. Maurel, P., and Travers, F. (1973) *C.R. Acad. Sci. Paris (Series D)* 276, 3057-3060

19. Marklund, S., Ohlsson, P.-I., Opara, A., and Paul, K.-G. (1974) *Biochim. Biophys. Acta* 350, 304-313

20. Cotton, M.L., Dunford, H.B., and Raycheba, J.M.T. (1973) *Can. J. Biochem.* 51, 627-631

21. Hewson, W.D., and Dunford, H.B. (1976) *J. Biol. Chem.* 'in press'

22. Shannon, L.M., Kay, E., and Lew, J.Y. (1966) *J. Biol. Chem.* 241, 2166-2172

23. Paul, K.-G., and Stigbrand, T. (1970) *Acta Chem. Scand.* 24, 3607-3617

24. Delincée, H., and Radola, B.J. (1970) *Biochim. Biophys. Acta* 200, 404-407

25. Hollenberg, P.F., Rand-Meir, T., and Hager, L.P. (1974) *J. Biol. Chem.* 249, 5816-5825

26. Santimone, M. (1973) Doctoral Thesis Université D'Aix-Marseille, France, pp. 66-72

27. Roman, R., Dunford, H.B., and Evett, M. (1971) *Can. J. Chem.* 49, 3059-3063

28. Schonbaum, G.R., and Lo. S. (1972) *J. Biol. Chem.* 247, 3353-3360

29. Cotton, M.L., and Dunford, H.B. (1973) *Can. J. Chem.* 51, 582-587

30. Bates, R.G., Paabo, M., and Robinson, R.A. (1963) *J. Phys. Chem.* 67, 1833-1838

31. Ellis, W.D., and Dunford, H.B. (1968) *Biochemistry* 7, 2054-2062

32. Åkerlöf, G. (1932) *J. Am. Chem. Soc.* 54, 4125-4139

33. Hasted, J.B., Ritson, D.M., and Collie C.H. (1948) *J. Chem. Phys.* 16, 1-21

34. Strickland, E.H. (1968) *Biochim. Biophys. Acta* 151, 70-75

35. Strickland, E.H., Kay, E., Shannon, L.M. and Horwitz, J. (1968) *J. Biol. Chem.* 243, 3560-3565

36. Davies, D.M., Jones, P., and Mantle, D. (1976) *Biochem. J.* 157, 247-253

37. Kaminsky, L.S., and Davidson, A.J. (1969) *Biochemistry* 8, 4631-4637

38. Herskovits, T.T., Gadegbeku, B., and Jaillet, H. (1970) *J. Biol. Chem.* 245, 2588-2598

39. Jacobson, A.L., and Krueger, P.J. (1975) *Biochim. Biophys. Acta* 393, 274-283

40. Hager, L.P., Doubek, D.L., Silverstein, R.M., Hargis, J.H., and Martin, J.C. (1972) *J. Am. Chem. Soc.* 94, 4364-4366

41. Coryell, C.D., and Stitt, F. (1940) *J. Am. Chem. Soc.* 62, 2942-2951

42. Brill, A.S., Castleman, B.W., and McKnight, M.E. (1976) *Biochemistry* 15, 2309-2316

43. Tamura, M. (1971) *Biochim. Biophys. Acta* 243, 249-258

44. Hartree, E.F. (1946) *Ann. Rept. Progr. Chem. (Chem. Soc. London)* 43, 287-296

45. Kaminsky, L.S., Yong, F.C., and King, T.E. (1972) *J. Biol. Chem.* 247, 1354-1359

46. Theorell, H. (1941) *J. Am. Chem. Soc.* 63, 1820-1827

47. Theorell, H., and Åkesson, Å. (1941) *J. Am. Chem. Soc.* 63, 1812-1818

48. Lanir, A., and Aviram, I. (1975) *Arch. Biochem. Biophys.* 166, 439-445

CHAPTER VI. CONCLUSIONS

6.1 Concluding Remarks

Although HRP is one of the most extensively characterized enzymes, its biological role has been obscured by the large number and variety of substrates it can oxidize. Facile catalysis of a certain reaction is one criterion for assigning a biological role to an enzyme. It is reasoned that a substrate with a higher turnover rate is more apt to be the enzyme's natural substrate than a slowly reacting substrate. This criterion is somewhat moot, but it does provide a basis for initial comparisons. The HRP catalyzed oxidation of *p*-cresol by H_2O_2 exhibits one of the fastest turnover rates with the exception of a few other phenols which are oxidized at only a slightly faster rate (1). The importance of phenolic compounds in plant physiology, the presence of peroxidase in plants, and the knowledge that many phenolic compounds are oxidized by peroxidase (1) all suggest the possible involvement of peroxidase in the oxidative biosynthesis of plant natural products. The low substrate specificity of peroxidase could be an indication of the enzyme's ability to oxidize a variety of precursor compounds.

A study of the biosynthesis of natural products via the oxidation of phenolic precursors requires a knowledge of free radical reactions. The subsequent reactions of an enzymatically formed free radical of a phenolic precursor

can be complex. Products can be formed by the dimerization of two free radicals, by the substitution of a free radical into other molecules present, or by the free radical oxidation of other molecules. These mechanisms provide the possibility of a variety of products. The HRP catalyzed oxidation of *p*-cresol exemplifies the variety of products which can be derived from the oxidation of a single precursor. Also, the relative amount of each product is highly dependent upon the reaction conditions. When all of the *p*-cresol is rapidly oxidized to form the free radical with no excess *p*-cresol present, the predominant reaction is free radical dimerization. However, when the free radicals are formed in the presence of a large excess of *p*-cresol, the free radicals react preferentially with *p*-cresol. These two different free radical reactions lead to different products.

The mechanism of Compound I formation from HRP and H_2O_2 is of interest in peroxidase chemistry because it is the oxidized form of the enzyme that is active. If HRP is to be an efficient catalyst, the formation of its first reactive intermediate, Compound I, should be fast. The finding that the activation energy of Compound I formation is similar in magnitude to the activation energy of diffusion led to the possibility that the rate of this reaction is limited by the rate of diffusion of the reactants. This possibility was discounted, however, because at a single temperature the rate is independent of viscosity. The

occurrence of an activation energy approximately equal to the activation energy of diffusion, might be explained in terms of an initial complex between HRP and H_2O_2 (2), as shown in Equation [1].

[1] $$HRP + H_2O_2 \underset{}{\overset{K}{\rightleftharpoons}} HRP\text{-}H_2O_2 \xrightarrow{k} \text{Compound I}$$

By assuming a fast equilibrium between the reactants and the complex, it can be shown that the apparent activation energy of Compound I formation, $E_{a,app}$, is the sum of the enthalpy of complex formation, ΔH, and the activation energy of the unimolecular formation of Compound I from the complex, E_a.

[2] $$E_{a,app} = \Delta H + E_a$$

If ΔH is sufficiently negative, values of $E_{a,app}$ can be less than the activation energy of diffusion or even negative (3). The small value for the apparent activation energy for Compound I formation could be explained by the exothermic formation of an intermediate complex.

Possible future work on Compound I formation could involve a study of the reaction rate in deuterium oxide. This technique could detect a rate limiting proton transfer through a primary isotope effect. The occurrence of a rate limiting proton transfer would provide further evidence that diffusion does not limit the rate of Compound I formation.

6.2 References

1. Job, D., and Dunford, H.B. (1976) *Eur. J. Biochem.* 66, 607-614

2. Jones, P., and Dunford, H.B. (1976) 'paper in preparation'

3. Marcus, R.A., and Sutin, N. (1975) *Inorg. Chem.* 14, 213-216

B30175